Conformal Field Theory and Numerical Techniques in the Fractional Quantum Hall Effect

Greg James Henderson

St John's College

University of Oxford

A thesis submitted for the degree of

Doctor of Philosophy in Theoretical Physics

Trinity Term 2023

To my father, James R. Henderson

Abstract

This thesis presents the development of Conformal Field Theory (CFT) methods to analyse the topological properties of fractional quantum Hall effect (FQHE) wave functions, and numerical techniques to find accurate FQHE trial ground state wave functions.

In Chapter 2, we argue that the real-space entanglement spectra (RSES) of generic chiral FQHE ground states have a scaling property, discussed in previous works, where the RSES is given as the spectrum of an operator that is an integral of local operators along the real-space cut that can be expanded in negative powers of the real-space cut length. This is directly tested for the bosonic Composite Fermion (CF) wave functions on the sphere at filling fraction 2/3.

In Chapter 3, it is shown that all chiral Parton-type FQHE ground and edge state trial wave functions, in the planar geometry, can be expressed as CFT correlation functions. A field-theoretic generalisation of Laughlin's plasma analogy, known as the generalised screening hypothesis, is then formulated for these states, where the implications for inner products of edge state trial wave functions are discussed. These implications of generalised screening are then numerically tested in two specific cases.

In Chapter 4, a method for the energy minimisation of paired CF trial wave functions is discussed, with the goal of producing accurate ground state trial wave functions for electrons, with Coulomb interactions, at filling fraction 5/2. The resulting energetics are then presented for the optimised paired CF versions of the Pfaffian, anti-Pfaffian and particle-hole (PH) symmetric Pfaffian topological orders and are compared to their zero-parameter trial wave function counterparts. It is found that the effective CF pairing in the Pfaffian and anti-Pfaffian wave functions is well approximated by a weak-pairing BCS-type description, and certain pathologies are found for the PH-Pfaffian wave functions.

Acknowledgements

First and foremost, I am extremely grateful to my supervisor Prof. Steve H. Simon both for the opportunity to pursue a DPhil and for his careful guidance, tutelage and patience over the last few years. I am truly thankful for the time and many deep ideas he has shared with me, and for teaching me to be a better researcher. I am also grateful to Dr. G. J. Sreejith with whom I have collaborated on much of the work of this thesis. I have immensely benefitted from our countless discussions throughout my studies. A special thanks also goes to Dr. Gunnar Möller who I have also collaborated on some of the work presented here. Gunnar has taught me many valuable practical skills, for which I am very appreciative.

Throughout my time in Oxford, I have benefitted greatly through the interactions of many of my colleagues. In particular, I would like to thank Tobias Swann, Krishnendu Ray, Dr. Yves Kwann, Dr. Joe Huxford, Saraswat Bhattacharyya, Minghao Li and Jovan Jovanovic. I am also grateful to Prof. Zohar Nussinov for taking the time to listen and give useful comments on my work.

I would also like to give a special thanks to Prof. Yang Bo and his research group at Nanyang Technological University Singapore, both for many insightful discussions and for their kind hospitality during my visit. In particular, I would like to thank Dr. Yoshiki Fukusumi, Dr. Wang Yuzhu and Dr. Ji Guangyue.

I am also very much grateful to my parents, Fiona E. Henderson and John D. Lindley, for their love, care and support throughout my studies.

Finally, my endless gratitude and love go to my partner, Dr. Aili Shao, for all her inspiration, love and support.

The work presented in Chapter 2 of this thesis is based on the publication of Ref. [1]. My collaborator, Dr. G. J. Sreejith, has provided the numerically calculated real-space entanglement spectra for Chapter 2 and the unprocessed Monte Carlo estimated inner-product data required for the numerical tests of Chapter 3. Code from the package DiagHam has been used for Chapter 4.

Contents

Chapter 1

Introduction

A system composed of many interacting particles, in close proximity to each other, can exhibit collective properties that are primarily determined by how the constituent particles are organised rather than their individual properties[2]. The broad area of study concerned with such systems and their emergent collective properties is known as *condensed matter physics*, which is the field that this thesis belongs.

Within this field, a distinct way the constituents of a system can be organised is often referred to as a *phase of matter*. It was first pointed out by Landau [3] that many possible distinct phases of a system could be understood through the concept of *symmetry breaking*, where each phase is characterised by its various symmetries (or lack thereof). In fact, for many years after Landau's work, there were no known phases of matter that could not be characterised this way[1].

That was until the discovery of the *integer* [4] and *fractional* [5] *quantum Hall effect*, which we abbreviate IQHE and FQHE respectively. These effects are when a system composed of a large number of electrons confined to move in two dimensions, near absolute zero temperature and under the influence of a large perpendicular magnetic field has a measured Hall resistance of the form $\frac{h}{e^2\nu}$, where e is the electric charge of an electron, h is Plank's constant and ν is quantised such that it takes an integer or

[1]Within this framework of phases of matter one does not distinguish between liquids and gases as the phase boundary between liquid and gas has an endpoint, which allows one to continuously move a system from a liquid to a gas.

fractional value in the integer or fractional quantum Hall effect respectively. It was clear from the outset of the discovery of these effects that the various ν's corresponded to different phases of matter, however, it eventually became apparent that any two such phases could not be distinguished by their symmetry properties[6, 7].

These phases of matter then represented a fundamentally new way that the constituent particles of a system can be organised at absolute zero temperature, and are now referred to as *topological phases of matter* [7–9]. A system in such a phase is said to exhibit *topological order*. Rather than symmetry, topological order is characterised at a macroscopic level by certain collective phenomena that are completely quantum mechanical in nature. Firstly, a system in a topological phase has a bulk gap, which is to say any localised excitations inside the system cost a finite amount of energy to create. Secondly, these phases can have low-energy quasi-particles that can be "fractionalised" compared with the constituent particles and are, in general, neither fermions nor bosons but are in fact anyons, with different phases hosting different types of anyons [10–16]. Also, on closed manifolds, a system in a topological phase can have a ground state degeneracy that only depends on the topology of the manifold [6]. Furthermore, a system in a topological phase can have low-energy effective degrees of freedom at its edge that are described by a *conformal field theory* (CFT) [17–20]. These macroscopic characterisations are often referred to as the *universal* or *topological* properties of a given phase. Such properties can be summarised by saying that the low energy effective theory of a topologically ordered system is a *topological quantum field theory* (TQFT), which is the origin of the word "topological" in the name "topological order"[9, 21–24]. At a microscopic level, topological order can be characterised by so-called "patterns of long-range entanglement", where the local degrees of freedom of a system are quantum-mechanically entangled in such a way that they cannot be disentangled without crossing a phase transition[25].

The existence of anyons within these phases of matter has sparked particular interest

over the past few decades. From a purely theoretical point of view, anyons are a fundamentally different kind of particle [26, 27]. They can be split into two classes: *abelian* and *non-abelian* anyons. Abelian anyons simply change their wave function by a phase factor when exchanged whereas for non-abelian anyons there exists a degenerate space of states, for given anyon positions, that transform onto each other when the anyons are exchanged. These properties of non-abelian anyons became of practical interest after it was realised they could potentially be used for fault-tolerant universal quantum computation [9, 24].

In the endeavour to understand what phases of matter can occur in theory and in particular experiments, the FQHE stands out from many other subfields of condensed matter physics through its use of *zero-parameter trial wave functions*[28]. This approach was initiated in Laughlin's explanation of the FQHE at filling fractions $\nu = \frac{1}{m}$ with $m \in 2\mathbb{N} + 1$, where zero-parameter trial wave functions were used as accurate approximations of the actual ground states of the systems under consideration [10]. In a more modern interpretation of this approach, a trial wave function is proposed in the hope that it is not necessarily a very accurate approximation to the ground state of a particular system, but is in fact adiabatically connected to the exact ground state. That is, it is hoped that there exists a way to deform the system's Hamiltonian such that we can, in theory, adiabatically evolve the system from the exact ground state to the trial ground state without passing a phase transition. If this can be done, then the exact and trial ground states are in the same phase of matter and, thus, the universal properties of the exact ground state can be predicted by calculating those of the trial ground state. One can then think of a trial wave function as being a representative wave function for a particular topological phase of matter. In practice, however, extracting the topological properties of a given trial wave function is highly non-trivial, and establishing the adiabatic connection to the exact ground state of a real system is even more so.

One method that has proved particularly useful both generally in condensed matter physics and, more specifically, for determining the topological phase of a given ground state is to spatially bipartition the system and study the *quantum entanglement* between the two subsystems[29]. The full information regarding the entanglement between the two subsystems is contained in the *entanglement spectrum* (ES) (to be detailed later), which was originally proposed by Li and Haldane [30]. When the system is spatially bipartitioned this is called a *real-space entanglement spectrum* RSES. In their pioneering work, Li and Haldane, using an approximation to the RSES[2], numerically demonstrated for some particular cases that the ES resembled, in structure, the energy spectrum of the edge degrees of freedom of the given system. Many works have subsequently shown this to occur in many other cases [31–34]. Other works have also given arguments as to why this occurs [35–37]. Of particular interest here are the arguments of Dubail, Read and Rezayi (DRR) [35] and Qi, Katsura and Ludwig (QKL) [36]. In the work of QKL, it is argued that the RSES can be modelled as the ES of the interacting edges of the two subsystems, which allowed them to understand the structure of the RSES in the *thermodynamic limit*. DRR showed that the RSES of many FQHE trial wave functions have a *scaling property*, which allowed the RSES of large but finite systems to be understood.

The particular class of trial wave functions considered in DRR's work are those that can be written as a correlation function of a two-dimensional conformal field theory (CFT). From the point of view of condensed matter physics, 2d CFT has its beginnings in the description of systems near second-order phase transitions [38, 39]. Roughly speaking, the "holomorphic parts" of the correlation functions of these CFTs are certain functions called *conformal blocks*. The so-called "monodromy properties" of these conformal blocks form certain representations of the braid group [40–42] and, as shown by Witten [43], have a deep connection to $(2+1)$d TQFT. In other words, the

[2]More precisely they used the "orbital" ES

monodromy properties of these conformal blocks could be used to describe anyons. It was first shown by Fubini [44] that Laughlin ground and quasi-hole trial wave functions could be expressed as CFT conformal blocks. Around the same time, in a now-famous work, Moore and Read showed that a variety of other FQHE ground state trial wave functions could be expressed as the correlation functions of CFT and used a certain CFT to generate a new trial wave function now termed the Moore-Read Pfaffian. They also proposed that quasi-particle trial wave functions could be expressed using CFT conformal blocks, where they conjectured that adiabatic exchange of these quasi-particles corresponded to the monodromy of these conformal blocks and that the edge degrees of freedom of the system are described by (a Wick rotated version of) the same CFT used to generate the ground state, with this being known as the Moore-Read (MR) conjecture. If true, it would imply the Moore-Read Pfaffian state could host non-abelian anyons, which was later verified by Monte Carlo methods [45]. Not long after Moore and Read's work it was also realised that this formalism could also be used to generate trial wave functions for edge excitations, or *edge states* [46], where this would give a linear map from the (dual) Hilbert space of the CFT to the space of wave functions.

In the case of Laughlin's trial wave functions the adiabatic exchange statistics of quasi-holes can be calculated using Laughlin's *plasma analogy* [10, 11], where the norm-square of the trial wave function can be expressed as the partition function of a classical 2d plasma. If this plasma is in a screening phase, then the exchange statistics correspond to the monodromy of the conformal blocks that can be used to express the quasi-hole trial wave functions. This was later generalised by Read to wave functions that are expressed as CFT correlation functions [47], in what is termed the *generalised screening hypothesis*, where it was argued that if this holds the adiabatic exchange of quasi-particles is given by the monodromy of the corresponding conformal block wave functions. It was also shown by DRR that if the generalised screening hypothesis holds

then the linear map from the (dual) Hilbert space of the CFT to the space of trial edge states preserves the inner product of the two Hilbert spaces in the thermodynamic limit (i.e. becomes an isometric isomorphism in the technical langauge). In other words, if the generalised screening hypothesis holds the edge degrees of freedom could indeed be described by the same CFT used to generate the wave function. From this, DRR were also able to show that the RSES of these wave functions had a scaling property, so long as generalised screening holds. This scaling property is that the RSES, at large but finite system sizes, can be expressed as the spectrum of a CFT operator which is a sum of integrals of local operators of the CFT. Each term in this sum is weighted in such a way that at larger system sizes it can be well approximated by only a small number of terms.

Combining the results of Read and DRR, one can then see that the MR conjecture can be reformulated as the generalised screening hypothesis, which can be seen as a natural generalisation of Laughlin's plasma analogy. Roughly speaking, if generalised screening holds the topological properties of the trial wave function can be simply "read off" from the CFT used to generate the wave function.

Another set of trial wave functions, outside those considered by Read and DRR, are the, very successful, *Composite Fermion* trial wave functions, originally proposed by Jain [48, 49]. These trial wave functions are motivated by the Composite Fermion (CF) theory of FQHE, where it is argued that it is energetically favourable for electrons to bind to an even number of wave function vortices to form CF quasi-particles. Within a certain mean-field approximation, these vortices screen the magnetic field so that the CFs are in a lower effective magnetic field, wherein they can form IQH states. The corresponding trial wave function is a product of an IQH ground state and a "flux-attaching" Jastrow factor. These CF wave functions have been shown to be expressible as *anti-symmetrised* CFT correlation functions [50, 51], although this anti-symmetrisation procedure meant that it has not been obvious if the arguments of

Read and DRR can be extended to these states [52].

An even wider class of trial wave functions, which include the CF wave functions, are the *Parton* wave functions. These are motivated by a microscopic theory of the FQHE where the electrons are split into several fictitious Partons that are strongly bound to move in clusters (i.e. so that they form full electrons). Each individual Parton species experiences a lower effective magnetic field, as they have a fraction of the charge of an electron, and can then form IQH states. The corresponding trial wave functions are products of several IQH ground state wave functions (one for each Parton species). Parton wave functions have seen renewed interest recently as being possible representative wave functions for particular phases of matter occurring in GaAs heterostructures [53, 54] and in graphene systems [55].

Assuming this microscopic Parton theory, Wen derived the effective low energy field theories for certain Parton states termed the *symmetric* states. Importantly, these effective field theories indicated that such states are likely to host non-abelian anyons. More recently, the quasi-particle exchange statistics of two particular Parton wave functions have been directly shown, under certain assumptions, to be non-abelian where these wave functions were also shown to be the exact densest zero-energy ground states of certain model Hamiltonians[56, 57]. Although previous works have made some progress[58, 59], it is still not known if the CFT methods described above can be applied to the Parton wave functions.

The wave function proposed in the work of Moore and Read, known as the Moore-Read Pfaffian state, is one of the simplest FQH states that can host non-abelian anyons, and early numerical studies suggested that it could be likely to occur at $\nu = 5/2$ in GaAs heterostructures [60, 61]. Later studies, however, showed there are other possible phases that can occur at $\nu = 5/2$: the anti-Pfaffian [62–64] and the particle-hole symmetric Pfaffian (PH-Pfaffian) [65]. All numerical studies to date have pointed to the Moore-Read Pfaffian or anti-Pfaffian as being the most energetically favourable

phases in this setting [60, 61, 66, 67]. On the contrary, experimental measurements of the heat conductivity at the edge of this system are consistent with the PH-Pfaffian phase [68]. The precise nature of the $\nu = \frac{5}{2}$ FQHE in GaAs still remains elusive at the time of writing.

All three of these phases can be understood as *paired* CFs, with each phase corresponding to a different pairing channel [69–71]. Using this picture, Möller and Simon (MS) proposed a *multi-parameter* trial wave function for the Moore-Read Pfaffian phase, where the pairing wave function of the CFs can be adjusted by these parameters [72]. As discussed by MS, varying the pairing parameters of a given MS wave function to minimise its energy, would give a wave function which is a better approximation of the actual ground state, which was the main motivation for proposing such wave functions given the relatively low overlap of the Moore-Read wave function with the exact ground state (at small system sizes), in comparison to other known trial states such as Laughlin's. The Möller-Simon wave functions have been extended by Yutushui and Mross (YM) to give trial wave functions for the anti-Pfaffian and PH-Pfaffian phases, where the corresponding wave functions have been studied for a given set of *fixed* parameters [73]. These paired CF wave functions offer alternative forms of the existing trial wave functions for the PH-Pfaffian and anti-Pfaffian phases, which are numerically tractable at larger system sizes. The energetics of the fixed parameter paired CF wave functions proposed by YM and the energy minimisation of their corresponding MS versions have not yet been studied. As for the MS version of the Moore-Read state, minimising the energy of these wave functions could allow for more accurate trial wave functions compared with the fixed parameter version proposed by YM, which could ultimately be crucial for determining what phase of matter actually forms at $\nu = \frac{5}{2}$ in GaAs heterostructures.

This thesis presents contributions to the development of CFT methods to understand the structure of real-space entanglement spectra and to identify the topological

properties of trial wave functions using the generalised screening hypothesis, and to the development of numerical methods to optimise and analyse paired CF wave functions.

In Chapter 2 we argue, by starting from QKL's approach, and numerically substantiate that, DRR's scaling property should be a generic feature of the RSES of many FQH states,

In Chapter 3 we show that both the Parton and CF trial wave functions can be expressed as CFT correlation functions without explicit anti-symmetrisation. A generalised screening hypothesis for these wave functions is formulated, where it is then demonstrated how the various topological properties can be extracted. Some of the predictions of the screening hypothesis are numerically tested in two specific examples.

In Chapter 4 we discuss the energy minimisation of paired CF wave functions. The results of the energy minimisation of the paired CF wave functions for the Pfaffian, anti-Pfaffian and PH-Pfaffian phases are presented and compared to their fixed parameter counter-parts in the case of the pure Coulomb interaction in the second Landau level. The resulting pairing functions are analysed and found to be well approximated by a weak-pairing BCS-type description for the Pfaffian and anti-Pfaffian cases. Certain pathologies are found for the paired CF versions of the PH-Pfaffian state.

For the remainder of this chapter, we will briefly introduce the IQHE, FQHE and rational CFT, which set the scene for the rest of this thesis. In Sec. 1.1 we discuss the integer quantum Hall effect and introduce the concept of Landau levels and edge states. Then in Sec. 1.2 we go on to discuss the FQHE and Laughlin's plasma analogy. CF and Parton wave functions are covered in Sec. 1.2.3. Finally, in Sec. 1.3 we briefly discuss rational CFT which will lay the groundwork for Chap. 2 and Chap. 3.

1.1 The integer quantum Hall effect

It was first observed by Von Klitzing that a two-dimensional electron gas subject to a large magnetic field, near absolute zero temperatures, showed extremely flat plateaus

in the off-diagonal resistivity, ρ_{xy}, as a function of the electron density [4]. That is, the Hall resistance was measured to be quantised, with this quantisation being so precise it is now used as a resistance standard. Within these samples, the electrons are confined to move in two dimensions by a quantum well potential along one direction. When this quantum well is sufficiently strong and the temperature is sufficiently low, then the electron can, effectively, only move in a two-dimensional plane.

Ignoring any inter-electron interactions and assuming a perfectly clean sample, once the electrons confined to the plane are subjected to a strong magnetic field perpendicular to the plane, their single-particle energy levels become a discrete set called *Landau levels*. The number of states within a given Landau level (LL) is proportional to the area of the plane the electrons are confined within. If the electrons exactly fill n of these LLs the diagonal elements of the conductivity tensor must be zero as there is an energy gap to any unoccupied states, and it can be shown that the Hall resistance is $\frac{h}{e^2 n}$. If we only partially fill a LL in a clean sample then this is no longer the case, as there is no longer a gap to the unoccupied states.

The appearance of the plateaus seen in experiments is, in fact, a result of *disorder*. When a "weak" disorder potential is included a given Landau level is split into a band of energy levels, with the low and high energy states of a given band being *localised*. The states in the middle of the band are *extended*. These localised states do not contribute to the conduction properties of the system. Hence, as the chemical potential moves through the localised states the conduction properties of the system remain constant. This partly explains the plateaus in the Hall resistance, but does not explain why they take the same value as a completely clean sample with an integer number of LLs exactly filled. This final part of the story was explained by Laughlin using an argument based on gauge invariance [74]. Halperin later clarified this argument, where the importance of *edge states* was emphasised[75]. That is, the states near the edge of the sample, edge states, remained extended even in the presence of disorder.

1.1.1 Landau levels in the disk geometry

Now consider a single particle of mass m_e and charge e moving in the two-dimensional (x, y)-plane in the presence of a uniform magnetic field B perpendicular to the plane of motion. The Hamiltonian of the particle is written as,

$$H = \frac{(\mathbf{p} - e\mathbf{A})^2}{2m_e} \tag{1.1}$$

where $\mathbf{A} = (A_x, A_y)^T$ with $\partial_x A_y - \partial_y A_x = B$. We will work here in the *symmetric gauge* with $\mathbf{A} = \frac{B}{2}(-y, x)^T = \frac{Br}{2}\hat{\theta}$, where (r, θ) are the usual polar coordinates.

Let us now find all the eigenstates of this Hamiltonian along with their corresponding energies. First define the complex coordinates,

$$z = x + iy \qquad \bar{z} = x - iy \tag{1.2}$$

Thinking of this as a coordinate transformation in the usual sense and recalling that $\mathbf{A}$ is a contravariant vector, we can define $A_z = \frac{1}{2}(A_x - iA_y) = -i\frac{B\bar{z}}{4}$ and $A_{\bar{z}} = i\frac{Bz}{4}$. In these coordinates the metric tensor with raised indices is given by $g^{zz} = g^{\bar{z}\bar{z}} = 0$ and $g^{z\bar{z}} = g^{\bar{z}z} = 2$. In these coordinates the Hamiltonian takes the form,

$$\begin{aligned} H =& \frac{1}{m_e}\left[\left(-i\hbar\partial + i\frac{eB\bar{z}}{4}\right)\left(-i\hbar\overline{\partial} - i\frac{eBz}{4}\right) + \left(-i\hbar\overline{\partial} - i\frac{eBz}{4}\right)\left(-i\hbar\partial + i\frac{eB\bar{z}}{4}\right)\right] \\ =& \frac{\hbar\omega_c}{2}\left[\left(\frac{\bar{z}}{2l_B} - 2l_B\partial\right)\left(\frac{z}{2l_B} + 2l_B\overline{\partial}\right) + 1\right] \end{aligned} \tag{1.3}$$

where $\partial = \partial_z$, $\overline{\partial} = \partial_{\bar{z}}$, $\omega_c = \frac{eB}{m_e}$ is the cyclotron frequency and $l_B = \sqrt{\frac{\hbar}{eB}}$ is the magnetic length. We then define the operators,

$$\begin{aligned} b =& \frac{1}{\sqrt{2}}\left(\frac{\bar{z}}{2l_B} + 2l_B\partial\right) \qquad b^\dagger = \frac{1}{\sqrt{2}}\left(\frac{z}{2l_B} - 2l_B\overline{\partial}\right) \\ a =& \frac{1}{\sqrt{2}}\left(\frac{z}{2l_B} + 2l_B\overline{\partial}\right) \qquad a^\dagger = \frac{1}{\sqrt{2}}\left(\frac{\bar{z}}{2l_B} - 2l_B\partial\right) \end{aligned} \tag{1.4}$$

These operators have the following commutation relations,

$$[a, a^\dagger] = [b, b^\dagger] = 1 \qquad [a, b] = [a^\dagger, b] = 0 \tag{1.5}$$

which are the commutation relations for the ladder operators of two independent harmonic oscillators. We can then form an orthonormal basis of our single-particle Hilbert space with the states labelled by two natural numbers n and m and given by,

$$|n, m\rangle = \frac{(a^\dagger)^n (b^\dagger)^m}{\sqrt{n!m!}} |0\rangle \tag{1.6}$$

where $|0\rangle$ is the unique state such that $a|0\rangle = b|0\rangle = 0$ and is normalised $\langle 0|0\rangle = 1$.

The Hamiltonian can also be expressed as,

$$H = \hbar\omega_c \left(a^\dagger a + \frac{1}{2} \right) \tag{1.7}$$

which implies that $|n, m\rangle$ are eigenstates with energies that only depend on n: $H|n, m\rangle = E_n |n, m\rangle$, where $E_n = \hbar\omega_c(n + 1/2)$. The energy levels are referred to as *Landau levels*, where $n = 0$ is called the *lowest Landau level* (LLL).

The angular momentum operator (in units of $\hbar$) is defined as,

$$L_z = z\partial - \bar{z}\overline{\partial} = b^\dagger b - a^\dagger a \tag{1.8}$$

which then implies the state $|n, m\rangle$ is an angular momentum eigenstate (as expected given the rotational invariance of the Hamiltonian) with angular momentum $m - n$.

The states of the LLL must be such that $a|\psi\rangle = 0$. Expressing the wave function ψ as $\psi(x, y) = f(z, \bar{z}) e^{-\frac{|z|^2}{4l_B^2}}$, this condition to be in the LLL can then be expressed as $\overline{\partial} f(z, \bar{z}) = 0$. Thus, in the LLL f is analytic (holomorphic) over the entire plane. As $b|0\rangle = 0$ it follows that $\langle x, y|0\rangle \propto e^{-\frac{|z|^2}{4l_B^2}}$. We then have,

$$\psi_m(z) \equiv \langle x, y|0, m\rangle \propto z^m e^{-\frac{|z|^2}{4l_B^2}} \tag{1.9}$$

The probability density $|\psi_m(z)|^2$ is maximised on a ring centred at the origin of

radius $r_{\max} = l_B\sqrt{2m}$, where the probability density falls exponentially away from this ring with a decay length of order l_B. In other words, the orbital $\psi_m(z)$ is localised to a ring centred at the origin with radius $l_B\sqrt{2m}$ and a thickness on the order of l_B. Suppose we confined this single particle such that it can only occupy the orbitals with $m < M$ (for some M). The single particle can then only move in a disk roughly of radius $l_B\sqrt{2M}$, with the magnetic flux through this disk being $\Phi = M\Phi_0$ where $\Phi_0 = \frac{h}{e}$ is known as the *magnetic flux quantum*. If we have N of these particles all confined to move on this disk then we can define the *filling fraction*, ν, as $\nu = \frac{N}{M}$, which is the ratio of the number of particles to the number of orbitals they can occupy.

Let us now consider the case when these N particles are non-interacting fermions. Let $c_m^\dagger$ be the fermion creation operator for the orbital $\psi_m(z)$. If $N = M$ then we are at the filling fraction $\nu = 1$ and the ground state of the system is,

$$|\Psi\rangle = c_{N-1}^\dagger c_{N-2}^\dagger \dots c_1^\dagger c_0^\dagger |0\rangle \tag{1.10}$$

where $|0\rangle$ is now the zero-particle vacuum. The real-space representation of this state (i.e. the wave function) is a *Slater determinant* of the form,

$$\begin{aligned}\Psi(\mathbf{z}) &\propto \det[z_1^{N-1}, z_2^{N-2}, \dots, z_N^0] \exp\left(\sum_{i=1}^N -\frac{|z_i|^2}{4l_B^2}\right) \\ &= \prod_{i<j}^N (z_i - z_j) \exp\left(\sum_{i=1}^N -\frac{|z_i|^2}{4l_B^2}\right)\end{aligned} \tag{1.11}$$

where we use $\mathbf{z}$ as a shorthand notation for all the particle coordinates, $\mathbf{z} = z_1, z_2, \dots, z_N$ and for a set of N orbitals $\phi_i(z)$ we define $\det[\phi_1(z_1), \phi_2(z_2), \dots, \phi_N(z_N)] \equiv \sum_{\sigma\in S_N} \mathrm{sgn}\sigma\ \phi_{\sigma(1)}(z_1)\phi_{\sigma(2)}(z_2)\dots\phi_{\sigma(N)}(z_N)$ with S_N being the set of permutation of the set $\{1, 2, \dots, N\}$.

The density of this state is $\langle\rho(z)\rangle = \sum_{m=0}^{N-1} \frac{1}{2\pi l_B^2}\frac{1}{m!}\left(\frac{|z|^2}{2l_B^2}\right)^m e^{-\frac{|z|^2}{2l_B^2}} = \frac{1}{2\pi l_B^2}\big[1 - \sum_{m=N}^\infty \left(\frac{|z|^2}{2l_B^2}\right)^m \frac{1}{m!} e^{-\frac{|z|^2}{2l_B^2}}\big]$. The terms in this sum with $m \geq N$ will only have exponentially small contributions when z is inside the disk. Hence, the density is uniform inside the disk

with a value $\frac{1}{2\pi l_B^2}$ and falls essentially to zero outside the disk with a decay length of order l_B.

Notice that if we wanted to excite the system inside the disk we must move at least one fermion from the $\psi_m(z)$ orbitals to an orbital in a higher LL, which would cost at least $\hbar\omega_c$ in energy to do. We then say that there is a *bulk gap* of $\hbar\omega_c$. One can also say that this state is *incompressible* as increasing the density of the system amounts to creating excitations.

By applying $a^\dagger$ repeatedly n times to $\psi_m(z)$ we can see that the n^{th} LL single particle orbitals take the form $\psi_{n,m}(z) = f_{n,m}(z,\bar{z})e^{-\frac{|z|^2}{4l_B^2}}$, where $f_{n,m}(z,\bar{z})$ is a polynomial with the highest power of z being m and highest power of $\bar{z}$ being n. Now let $f(z,\bar{z})$ be a generic polynomial in z and $\bar{z}$ with the corresponding wave function $\psi(z) = f(z,\bar{z})e^{-\frac{|z|^2}{4l_B^2}}$. To project this wave function to the LLL, with the projection operator denoted by $\mathcal{P}_{LLL}$, we simply move all the $\bar{z}$'s in f to the left and then replace them with $2l_B^2\partial$, where this derivative does not act on the Gaussian factor [49]. For example, $\mathcal{P}_{LLL}z^3\bar{z}^2e^{-\frac{|z|^2}{4l_B^2}} = 24l_B^4 z e^{-\frac{|z|^2}{4l_B^2}}$.

A system composed of N identical particles in the n lowest LLs will have a wave function of the form $\Psi(\mathbf{z}) = f(z_1,\bar{z}_1,z_2,\bar{z}_2,\ldots,z_N,\bar{z}_N)\exp\left(\sum_{i=1}^N -\frac{|z_i|^2}{4l_B^2}\right)$, where f is a polynomial with the highest power in any $\bar{z}$'s is less than n. If the identical particles are fermions or bosons then f must be anti-symmetric or symmetric under swapping the particle coordinates respectively.

1.1.2 Edge states

Now let us consider the case of N fermions all within the LLL, with $N \gg 1$. We can define the $\nu = 1$ edge states to be the multi-particle states where all the $|0,m\rangle$ single-particle orbitals are occupied for $m \leq N-p$ and are unoccupied for $m \geq N+p$, for some chosen positive integer p such that $\frac{p}{N} \ll 1$. In other words, these are "excited" states of the $\nu = 1$ ground state where all the excitations are occurring at the edge of

the system.

Further, add to this system a rotationally symmetric confining potential Hamiltonian $H_{\text{confinement}} = \sum_j U(r_j)$, which is sufficiently weak that inter LL transitions can be ignored and such that $U(r) \approx (r - l_B\sqrt{2N})F$ near the edge of the system for some positive F. This perturbation merely alters the energy of the single particle orbitals, with the orbitals near the edge will have a change in energy of $\langle 0, N + \Delta m| U |0, N + \Delta m\rangle \approx \sqrt{2}l_B(\sqrt{N + \Delta m} - \sqrt{N})F \approx \frac{Fl_B\Delta m}{\sqrt{2N}}$. Thus, the energy of a given edge state is $E = \frac{Fl_B\Delta L_z}{\sqrt{2N}}$, where ΔL_z is the angular momentum relative to the ground state. In the thermodynamic limit for a fixed F, the gap in the energy spectrum of the edge states goes to zero. That is to say, they are *gapless*. Furthermore, as ΔL_z can only be positive, for a fixed number of particles N, the excitations on the edge can only move in the anti-clockwise direction (for positive electric charge of the fermions) and are said to be *chiral*. The effective field theory description of these edge states is that of a $(1 + 1)$d free complex chiral fermion theory, which is also a *conformal field theory*.

The importance of these edge states was first pointed out by Halperin [75] and they are of particular importance in experiments as it is very often only the edge of the system that can be directly probed.

1.1.3 Landau levels on the sphere

It is often theoretically convenient when considering the bulk properties of a particular phase of matter to place it on a closed manifold so as to remove edge effects. In the case of the quantum Hall effect, the *sphere* is the typical geometry of choice [76].

Consider a spherical shell of radius R with a *magnetic monopole* placed at its centre, such that the magnetic flux going through the sphere is $2Q$ in units of the magnetic flux quantum. We now wish to consider the quantum mechanical motion of a charged particle moving around on this spherical shell.

Let us first consider adiabatically moving this particle around the equator. The

Berry phase picked up by this particle will then be $\exp\left(i\frac{e}{\hbar}\oint_{\text{equator}}\mathbf{A}\cdot d\mathbf{r}\right)$. Applying Stoke's theorem on the upper or lower hemisphere gives this phase to be $e^{i2\pi Q}$ and $e^{-i2\pi Q}$ respectively. As these two answers must be the same we then have that $2Q$ must be an *integer*, which is the Dirac quantisation condition. In other words, there is exactly an integer number of flux quanta going through the sphere.

The Hamiltonian of the particle is,

$$H = \frac{|\mathbf{\Lambda}|^2}{2m_e R^2} \tag{1.12}$$

where $\mathbf{\Lambda} = \mathbf{r}\times[-i\hbar\nabla - e\mathbf{A}]$ is the dynamical angular momentum momentum. We will work in the gauge $\mathbf{A} = \frac{\hbar Q}{eR}\cot\theta\hat{\phi}$ (in spherical polar coordinates). Note that this has two singularities at the north and south poles, where each has a magnetic flux of Q (in units of the magnetic flux quantum). These singularities have no physical significance provided we impose a branch cut on the particle's wave function at $\phi = 0$ with the boundary condition, $\psi(\theta, 2\pi) = e^{-i2\pi Q}\psi(\theta, 0)$. The generators of rotation are given by,

$$\mathbf{L} = \mathbf{\Lambda}/\hbar + Q\mathbf{\Omega} \tag{1.13}$$

where $\mathbf{\Omega} = \mathbf{r}/R$. These have the usual $\mathfrak{su}(2)$ algebra $[L_a, L_b] = i\sum_c \epsilon_{abc}L_c$ and the Hamiltonian can now be expressed as,

$$H = \frac{\hbar^2}{2R^2 m_e}[L^2 - Q^2] \tag{1.14}$$

We can form a basis of the Hilbert space involving the simultaneous eigenstates of L^2 and L_z, $|l, m\rangle$ with eigenvalues $l(l+1)$ and m respectively. As the Hamiltonian is positive definite the allowed values of l are $l \geq Q$. Furthermore, the boundary condition across the branch cut implies $m - Q \in \mathbb{Z}$, which then implies that $l - Q$ must also be an integer. So $l = Q, Q+1, Q+2, \ldots$. For the given l, m can take value $-l, -l+1, \ldots, l$. It can be shown that the multiplicity of a given l is one [77]. Each l can then be thought of as a Landau level, with the usual LL index being $n = l - Q$.

The corresponding wave functions are called *monopole harmonics* and are denoted $Y_{Qlm}(\mathbf{\Omega})$ [77, 78]. Defining the spinor coordinates $u = \cos(\theta/2)e^{i\phi/2}$ and $v = \sin(\theta/2)e^{-i\phi/2}$, one can express the LLL wave functions as (for $Q > 0$),

$$Y_{QQm}(\mathbf{\Omega}) \propto v^{Q-m}u^{Q+m} \tag{1.15}$$

The monopole harmonics for $Q < 0$ are related to the $Q > 0$ monopole harmonics by $Y^*_{Qlm}(\mathbf{\Omega}) = (-1)^{Q+m}Y_{(-Q)l(-m)}(\mathbf{\Omega})$ defined by Eq. 1.13.

On the sphere, the $\nu = 1$ state can be formed by $N = 2Q + 1$ fermions filling the entire LLL. The filling factor on the sphere is defined to be $\nu = \lim_{N\to\infty} \frac{N}{2Q}$. At a finite system size $N = \nu(2Q + \mathcal{S})$ where $\mathcal{S}$ is called the shift and depends on the phase of matter present on the sphere.

1.2 The fractional quantum Hall effect

Not long after Von Klitzing's work, another plateau in the Hall resistance at $\frac{h}{(1/3)e^2}$ was found by Tsui, Stormer and Gossard [5], which was the discovery of the FQHE. Drawing an analogy with the IQHE, the occurrence of this plateau could be explained by the existence of a bulk gap, in the absence of disorder, when the system is precisely at the filling fraction $\nu = 1/3$. For a large magnetic field, however, all the electrons of the system must be in the LLL. Ignoring the interactions between the electrons would lead one to conclude the system has $\binom{3N}{N}$ possible orthogonal states all with the same energy. The occurrence of a bulk gap must then be purely a result of the inter-electron interactions. This would then be a strongly correlated gapped phase of matter.

Rather than trying to exactly solve this problem, Laughlin proposed a series of ground-state trial wave functions for completely clean systems at the filling fractions $\nu = 1/m$, with m being an odd positive integer, which were shown to be very good approximations to the exact ground states at small system sizes [79]. Laughlin further proposed trial wave functions for the elementary quasiparticle excitations, which were

shown to have charges of magnitude e/m by using a plasma analogy. Laughlin also suggested that plateaus of the Hall resistance were due to disorder pinning the quasiparticle excitations that are created as the filling fraction is slightly changed. As opposed to the IQHE, the effects of disorder in the FQHE are still an open area of research at the time of writing [80].

Many other plateaus have been observed since the discovery of the $\nu = \frac{1}{3}$ effect, with some being those predicted by Laughlin, such as $\nu = \frac{1}{5}$ [81], and many others beyond the $\nu = \frac{1}{m}$ series such at $\nu = \frac{2}{5}$ and $\nu = \frac{2}{7}$ [82, 83]. It was initially proposed that these additional filling fractions could be understood as a *hierarchy*, where states at one level of the hierarchy could be understood as occurring from the condensation of quasiparticles of a state at a lower level, with the Laughlin states being at the lowest level [76, 84]. Another explanation of these additional filling fractions later came from the development of Jain's *Composite Fermion* theory along with the corresponding trial wave functions [48, 49]. It was later argued that the CF states and hierarchy states are the same phases of matter [12], however, it was the CF theory that provided numerically tractable trial wave functions for these states. The CF trial wave functions were later generalised to the *Parton* trial wave functions [85, 86].

In the years since these early works, the FQHE has grown into a very large field of study with many active areas of research [28, 52, 87, 88]. In what follows we will discuss the Laughlin trial wave functions in Sec. 1.2.1, Laughlin's plasma analogy in Sec. 1.2.2, and the CF and Parton trial wave functions in Sec. 1.2.3.

1.2.1 Laughlin ground, quasihole and edge state trial wave functions

The Laughlin trial wave function at $\nu = \frac{1}{m}$ in the planar geometry with N particles is given by

$$\Psi_m(\mathbf{z}) = \prod_{i<j}^{N}(z_i - z_j)^m e^{-\sum_{i=1}^{N}\frac{|z_i|^2}{4l_B^2}} \tag{1.16}$$

It was argued by Laughlin that the elementary excitations could be created by adiabatic insertion of flux tubes, with the locations of the excitations coinciding with those of the flux tubes. The proposed trial wave function for p such *quasiholes* at the locations $\mathbf{w} = w_1, w_2, \ldots, w_p$ (using complex coordinates) is given by,

$$\Psi(\mathbf{w};\mathbf{z}) = \left[\prod_{i=1}^{p}\prod_{j=1}^{N}(w_i - z_j)\right]\Psi_m(\mathbf{z}) \tag{1.17}$$

It was first shown by Haldane, using the now termed *Haldane pseudo-potentials*, that $\Psi_m(\mathbf{z})$ is the exact "densest" ground state of a local two-body interaction within the lowest Landau level [76]. The states of two particles in the LLL can be labelled one-to-one with their total and relative angular momentum M and $\tilde{m}$ respectively, $|M, \tilde{m}\rangle$. Any rotationally invariant two-body interaction within the LLL, V, must commute with the total and relative angular momentum operators of two particles, which implies $V|M, \tilde{m}\rangle = V_{\tilde{m}}|M, \tilde{m}\rangle$, where $V_{\tilde{m}}$ is an eigenvalue that cannot depend on M as V only acts on the relative coordinates. The Haldane pseudo-potentials $\hat{V}_n$ are defined by $\hat{V}_n|M, \tilde{m}\rangle = \delta_{n,\tilde{m}}|M, \tilde{m}\rangle$. $\Psi_m(\mathbf{z})$ is an exact ground state of $H_m = \sum_{n=1}^{m-1}\hat{V}_n$ (which is positive semidefinite). The null space of H_m (i.e. states satisfying $H_m\Psi = 0$) is the space of states of the form $P(\mathbf{z})\Psi_m(\mathbf{z})$, where $P(\mathbf{z})$ is a symmetric polynomial. Amongst these null states $\Psi_m(\mathbf{z})$ is the unique state with the lowest angular momentum (i.e. the "densest" state).

Within the null space, we can define the *edge states* to be the wave functions where the highest power of any z, p, in their corresponding $P(\mathbf{z})$ polynomials are such that $\frac{p}{N} \ll 1$. Interstingly, such wave functions can also be expressed as $\Psi_{\nu=1,\text{edge}}(\mathbf{z})\Psi_{m-1}(\mathbf{z})$, where $\Psi_{\nu=1,\text{edge}}(\mathbf{z})$ is a $\nu = 1$ edge state. One can give the edge states some dynamics by adding to the model Hamiltonian H_m a weak quadratic confinement potential $U(r) = \frac{Fr^2}{2l_B\sqrt{2mN}}$ (assume $U \ll H_m$), which is normalised such that the force on the particles

near the edge of the system remains constant with increasing N. The energy of an edge state with angular momentum ΔL_z relative to $\Psi_m(\mathbf{z})$ given this confinement is $E = \frac{Fl_B\Delta L_z}{\sqrt{2mN}}$. From this simple model, we can then see that the edge excitations are gapless.

1.2.2 Laughlin's plasma analogy

The norm square of the Laughlin ground state trial wave function, at $\nu = 1/m$, is given by,

$$Z_N \equiv \langle \Psi_m | \Psi_m \rangle = \int \prod_{i=1}^{N} d^2 z_i \exp\left(\sum_{i<j}^{N} m \ln |z_i - z_j| - \sum_{k=1}^{N} \frac{|z_k|^2}{2l_B^2} \right) \tag{1.18}$$

which is the partition function of a one-component two-dimensional plasma where particles interact via the 2D coulomb interaction (i.e. $\ln r$ potential) in the presence of a background r^2 potential. it has been demonstrated numerically that this plasma is in a screening phase for $m \lesssim 70$ [89]. If we attribute a dimensionless charge 1 to the particles of this plasma then the background potential can be associated with a background charge density $\rho = -\frac{1}{2\pi m}\nabla^2 \frac{r^2}{2l_B^2} = -\frac{1}{2\pi m l_B^2}$. Assuming this plasma is in its screening phase, which we will take as given for the rest of this section, the particles of the plasma will form a disk of uniform density $\frac{1}{2\pi m l_B^2}$ so as to screen this background charge. Thus, the density profile of the Laughlin trial wave functions must be that of a uniform disk of charge density $\frac{1}{2\pi m l_B^2}$, which implies the system is indeed at a filling fraction $\nu = \frac{1}{m}$.

The norm square of any quasihole wave function can also be expressed as a partition function of this plasma, but now with static charges placed at the quasihole locations,

$$Z_N(\mathbf{w}) \equiv \langle \Psi_m(\mathbf{w}) | \Psi_m(\mathbf{w}) \rangle = \int \prod_{i=1}^{N} d^2 z_i \exp\Bigg(\sum_{a=1}^{p} \sum_{i=1}^{N} 2 \ln |w_a - z_i| + \sum_{i<j}^{N} 2m \ln |z_i - z_j| - \sum_{k=1}^{N} \frac{|z_k|^2}{2l_B^2} \Bigg) \tag{1.19}$$

where these static charges have charge $\frac{1}{m}$. Thus, to screen the background charge and these static charges, the particles will still have a uniform density of $\frac{1}{2\pi m l_B^2}$ at a location far away from any static charges, and near the static charges, the particle density will fall such that the average number of particles in the neighbourhood of a static charge is $1/m$ less than if the static charge had not been there. In other words, the quasiholes have fractional charge $-\frac{e}{m}$. One can also use this plasma analogy to calculate quasiparticle adiabatic exchange statistics [11] and the equal time electron propagator along the edge [90, 91].

1.2.3 Composite Fermion and Parton trial ground and edge state wave functions

Let us imagine we have a system of N electrons confined to an area with N_ϕ flux quanta passing through it. We now assume that at low energies each electron becomes bound to p wave function vortices to form CFs (with p even). Within a mean-field approximation, the effective number of flux quanta experienced by the CFs is $N_\phi^* = N_\phi - pN$ (for large N). Keeping within this mean-field picture, if the effective filling fraction $\nu^* = \frac{N}{N_\phi^*}$ is an integer, $\nu^* = n$, then one expects that the CFs will form an IQH state and we would, in principle, have an incompressible state for the electrons at filling factor $\nu = \frac{n}{np+1}$.

A trial wave function for the resulting state can be constructed by including in the wave function a *vortex-attaching* Jastrow factor $\prod_{i<j}^{N}(z_i - z_j)^p$, with the remaining factor being interpreted as the wave function of the CFs. This gives the trial wave function,

$$\Psi(\mathbf{z}) = \Phi_n(\mathbf{z}) \prod_{i<j}^{N} (z_i - z_j)^p \tag{1.20}$$

where $\Phi_n(\mathbf{z})$ is the $\nu = n$ IQH ground state wave function. This resulting wave function is, however, in multiple LLs. The ideal CF trial wave function for electrons confined to the LLL is simply given by LLL projection of this wave function,

$$\Psi(\mathbf{z}) = \mathcal{P}_{LLL} \Phi_n(\mathbf{z}) \prod_{i<j}^{N} (z_i - z_j)^p \tag{1.21}$$

Within the above mean-field picture, one may also expect the edge excitation of the system to correspond to the edge states of the CFs, which leads to the (unprojected) edge state trial wave functions,

$$\Phi_{\text{edge}}(\mathbf{z}) = \Phi_{n,\text{edge}}(\mathbf{z}) \prod_{i<j}^{N} (z_i - z_j)^p \tag{1.22}$$

where $\Phi_{n,\text{edge}}(\mathbf{z})$ is a $\nu = n$ IQH edge state. The ideal edge states can then be constructed by LLL projection of these states.

Now let us consider the N electron system from the point of view of the Parton theory, where each electron is split into m fictitious Partons, with species i having a charge that is a rational multiple, f_i, of the electrons. One can force the Partons to move in groups of m (i.e. to form an electron) by including an additional dynamical gauge field [92]. Ignoring this gauge field, if the effective filling fractions for each species are all integers $\nu_i = \frac{N}{f_i N_\phi} = n_i$ then we expect each species to separately form an IQH state. We then have an FQH state for the electrons at $\nu^{-1} = \sum_{i=1}^{m} \nu_i^{-1}$.

The corresponding trial wave function is then,

$$\Psi(\mathbf{z}) = \prod_{i=1}^{m} \Phi_{n_i}(\mathbf{z}) \tag{1.23}$$

Again ignoring the dynamical gauge field, one would also expect the edge states to correspond to edge states of the individual Parton species which leads to the trial wave

functions,

$$\Psi_{\text{edge}}(\mathbf{z}) = \prod_{i=1}^{m} \Phi_{n_i,\text{edge}}(\mathbf{z}) \tag{1.24}$$

More generally, edge state trial wave functions can be formed by linear combinations of these products of IQH edge states. As for the CF wave functions, one can form LLL ground and edge state trial wave functions by simply projecting these Parton trial wave functions onto the LLL. The wave functions presented here are *chiral* Parton wave functions. Non-chiral Parton wave functions contain complex conjugate IQH wave functions and will not be considered in this work.

Note that for both the Parton and CF edge state trial wave functions it is not obvious in general if the given set of edge states for a particular state are orthogonal to each other or even if they form a linearly independent set.

1.3 Rational conformal field theory

In this work, the relevant data to form a two-dimensional field theory is a set of fields $\{\phi_j(z,\bar{z})\}$, with $z \in \mathbb{C}$, and their correlation functions $\langle \phi_{j_1}(z_1,\bar{z}_1)\phi_{j_2}(z_2,\bar{z}_2)\ldots\rangle$ with $|z_1| > |z_2| > \ldots$. In CFT this set of fields is infinite with each field in principle being a *local* expression in the underlying degrees of freedom. Each field ϕ_j has an associated holomorphic and anti-holomorphic conformal dimension denoted by h_j and $\bar{h}_j$ respectively.

Within correlation functions it is assumed[3] the *operator product expansion* (OPE) holds,

$$\phi_i(z,\bar{z})\phi_j(w,\bar{w}) = \sum_k \frac{C_{ijk}\phi_k(w,\bar{w})}{(z-w)^{h_i+h_j-h_k}(\bar{z}-\bar{w})^{\bar{h}_i+\bar{h}_j-\bar{h}_k}} \tag{1.25}$$

so long as there exists a circle that only contains z and w and no other points in the correlation function, where C_{ijk} are known as the structure constants of theory. In

[3]This assumption can be taken to be a defining axiom of CFTs.

radial quantisation, we form a vector space of kets by formal linear combinations of the states $|\phi_{j_1}(z_1,\bar{z}_1)\phi_{j_2}(z_2,\bar{z}_2)\ldots\rangle$ with $1>|z_1|>|z_2|>\ldots$ and the space of bras to be spanned by $\langle\phi_{j_1}(z_1,\bar{z}_1)\phi_{j_2}(z_2,\bar{z}_2)\ldots|$ with $|z_1|>|z_2|>\cdots>1$. Inner products are defined by the correlation functions, $\langle\phi_{j_1}(z_1,\bar{z}_1)\phi_{j_2}(z_2,\bar{z}_2)\ldots|\phi_{j'_1}(z'_1,\bar{z'}_1)\phi_{j'_2}(z'_2,\bar{z'}_2)\ldots\rangle = \langle\phi_{j_1}(z_1,\bar{z}_1)\phi_{j_2}(z_2,\bar{z}_2)\ldots\phi_{j'_1}(z'_1,\bar{z'}_1)\phi_{j'_2}(z'_2,\bar{z'}_2)\ldots\rangle$.

By the OPE assumption, it is clear that all ket states must be linear combinations of the kets $|\phi_j(0,0)\rangle \equiv |\phi_j\rangle$, which is also known as state-operator correspondence. To every field ϕ_j we assume there exists a conjugate field $\phi_j^\dagger$ with this mapping being anti-linear and $\phi_j^{\dagger\dagger}=\phi_j$. We then define the Hermitian conjugate between the bras and kets as $\langle\phi_j| \equiv \lim_{z,\bar{z}\to 0}\bar{z}^{-h}z^{-\bar{h}}\langle\phi_j^\dagger(\bar{z}^{-1},z^{-1})|$. If the resulting inner product on the space of kets is positive definite the CFT is said to be *unitary*.

Within a given CFT we can define the *chiral algebra* $\mathcal{A}$ to be the set of purely holomorphic fields $\{\phi(z)\}$ of the CFT (i.e. those which have a holomorphic dependence on position when inserted in any correlation function[4]). For a field $\phi(z)\in\mathcal{A}$ with holomorphic scaling dimension h, where $\bar{h}=0$ for all purely holomorphic fields, we define the *modes* as $\phi_n \equiv \oint \frac{dz}{2\pi i} z^{n+h-1}\phi(z)$ where $n+h\in\mathbb{Z}$ and one can take the contour of integration to be a circle centred at the origin. The OPEs between any two holomorphic fields must only contain holomorphic fields which implies that the commutation or anti-commutation relations between any of the modes of fields of $\mathcal{A}$ must be expressable as sums of modes of fields of $\mathcal{A}$ (see [20] on how these commutation relations are inferred). Note that if the fields have integral or half-integral scaling dimensions then one would need to consider commutation or anti-commutation relations respectively. One can also think of $\mathcal{A}$ as the algebra formed by the modes of these fields which then allows one to define the representations of $\mathcal{A}$ as being representations of this algebra.

Within any CFT, $\mathcal{A}$ will at least contain the identity field $\mathbf{1}(z)$ and the energy-momentum tensor $T(z)$. For the Virasoro minimal models, the chiral algebra can be

[4]Of course, we can get singularities when the field approaches another in a correlation function.

taken to be the (enveloping algebra of) Virasoro algebra formed by the modes of $T(z)$, L_n. For the Wess-Zumino-Witten (WZW) models $\mathcal{A}$ is the algebra generated by the modes of the conserved currents $J^a(z)$ [93].

A CFT is *rational* if its Hilbert space can be decomposed as $\mathcal{H} = \bigoplus_{ij} \mathcal{H}_i \otimes \overline{\mathcal{H}}_j$ where the direct sum is finite and $\mathcal{H}_i$ and $\overline{\mathcal{H}}_j$ are irreducible representations of $\mathcal{A}$ and $\overline{\mathcal{A}}$ respectively with $\overline{\mathcal{A}}$ being the anti-chiral copy of $\mathcal{A}$ (formed by the corresponding anti-holomorphic fields). A rational CFT (RCFT) is further said to be diagonal if the decomposition of the Hilbert space is $\mathcal{H} = \bigoplus_i \mathcal{H}_i \otimes \overline{\mathcal{H}}_i$, where $\overline{\mathcal{H}}_i$ is the anti-chiral copy of $\mathcal{H}_i$. Within each $\mathcal{H}_j \otimes \overline{\mathcal{H}}_j$ there exists a distinguished state whose corresponding field $\phi_j(z)$ we call the *primary* field of $\mathcal{H}_j \otimes \overline{\mathcal{H}}_j$[5]. The correlation function of a set of primary fields can be expressed as,

$$\langle \phi_{j_1}(z_1, \bar{z}_1)\phi_{j_2}(z_2, \bar{z}_2)\dots\rangle = \sum_a |\mathcal{F}_a(z_1, z_2, \dots)|^2 \tag{1.26}$$

where $\mathcal{F}_a(z_1, z_2, \dots)$ are holomorphic functions known as *conformal blocks* and the number of labels a is finite. The *fusion rules* are formal expressions $\phi_i \times \phi_j = \sum_k N_{ij}^k \phi_k$ where we think of N_{ij}^k as being the number of "ways" the primary fields ϕ_i and ϕ_j can fuse to ϕ_k. For a given set of primary fields, the corresponding conformal blocks are in one-to-one correspondence with the number of ways the primary fields can fuse to the identity field. For example, in the Ising model, we have the fields σ and ψ with the fusion rules $\sigma \times \sigma = \mathbf{1} + \psi$, $\psi \times \sigma = \sigma$ and $\psi \times \psi = \mathbf{1}$. Thus, a correlation function of four σ's can have two conformal blocks corresponding to the fusion channels $(\sigma(\sigma(\sigma\sigma))) \to (\sigma(\sigma\psi)) \to (\sigma\sigma) \to \mathbf{1}$ and $(\sigma(\sigma(\sigma\sigma))) \to (\sigma(\sigma\mathbf{1})) \to (\sigma\sigma) \to \mathbf{1}$. If a field J can only have one result when fusing with any other field (i.e. $J \times \phi = \phi'$) then J is said to be a *simple current*.

[5]The precise notion of primary can depend on the chiral algebra. It is typically one of the fields with the lowest scaling dimension of the given representation, although this does not necessarily need to be the case.

Chapter 2

Scaling Property of Real-Space Entanglement Spectra

Consider some many-body system in its ground state $|\Psi\rangle$. Let us then bipartition the physical space of the system into two regions A and B, with the dividing line known as the real-space cut. The ground state can then be expressed as a Schmidt decomposition,

$$|\Psi\rangle = \sum_i e^{-\frac{\xi_i}{2}} |A_i\rangle \otimes |B_i\rangle \tag{2.1}$$

where $\{|A_i\rangle\}$ and $\{|B_i\rangle\}$ are orthonormal bases of the A and B subsystems respectively, and ξ_i are real numbers. The set $\{\xi_i\}$ is called the *real-space entanglement spectrum* (RSES) and the individual ξ_i are referred to as entanglement levels or pseudo-energies. By tracing out the B system, the density matrix of A can be expressed as $\rho_A = \sum_i e^{-\xi_i} |A_i\rangle \langle A_i|$ and so the RSES can equivalently be defined as the eigenvalues of $-\ln \rho_A$. When applied to an FQHE ground state one typically takes the real-space cut to be rotationally invariant, in which case the ξ_i can be labelled by the (L_z^A, N_A) quantum numbers of $|A_i\rangle$ where L_z^A and N_A are the angular momentum and number of particles in A respectively.

In their pioneering work, Li and Haldane [30] suggested and numerically substantiated that such entanglement spectra can contain certain features which are universal for the underlying phase of matter. In particular, they found that the low-lying entan-

glement spectrum of an orbital partition, which approximates the real-space partition, of the Moore-Read trial wave function and the corresponding Coulomb ground state resembled that of the (perturbed) CFT which describes the edge dynamics of the system. Many works since have shown this to be the case for many FQHE and IQHE states [31–34, 94, 95].

In the work of Qi, Katsura and Ludwig (QKL) it is suggested that this can be understood by modelling the interaction between the two real-space regions as only occurring between the edge degrees of freedom of the two subsystems. This then allows one to understand the RSES as the entanglement spectrum of the two interacting edges at the real-space cut. QKL then used certain boundary CFT techniques and the results of Calabrese and Cardy [96, 97] to argue what form the RSES should take in the thermodynamic limit. This method to understand the RSES is termed the QKL cut-and-glue approach.

In Dubail, Read and Rezayi's (DRR) work it is argued that the RSES of wave functions that can be expressed as CFT correlation functions, where the generalised screening hypothesis applies, has a scaling property in that the RSES can be expressed as the spectrum of an operator in the CFT of the form,

$$S_{ES} = \sum_i \frac{\alpha_j}{L^{h_j-1}} \oint \frac{dz}{2\pi i} z^{h_j-1} \phi_j(z) \tag{2.2}$$

where L is the length of the real-space cut, α_i are numerical constants, $\phi_j(z)$ are local operators of the CFT with scaling dimension h_j and S_{ES} is referred to as the entanglement action. This then gave an explanation as to why the RSES resembles a physical edge spectrum as this CFT is the same CFT one expects to describe the edge by the MR conjecture. At large, but finite, L the above expansion can be approximated by truncating it to a finite number of terms which allows one to model the RSES at a finite system size.

It is not obvious from the existing literature whether this should apply to generic

FQHE ground state wave functions. Furthermore, this scaling property has so far only been directly tested for Laughlin ground-state wave functions, where the scaling of the coefficients was not tested.

In this chapter, it shall be argued, using the QKL cut-and-glue approach, that the scaling property of the RSES should be a generic feature of the low pseudo-energy levels of the RSES of ground states of chiral FQHE ground states, where chiral refers to the fact the edge excitations of the system can only move in one direction. We will then directly test this for the case of the $\nu = 2/3$ bosonic Composite Fermion trial wave function on the sphere with real-space cut along the equator. In Chapter 3 we will see that this wave function can be written as a CFT correlation function where the RSES can be understood from DRR's arguments. However, in this chapter, we will make no reference to the CFT construction of this wave function, to emphasise how the RSES can be modelled in a phenomenological manner.

2.1 From cutting and gluing to the scaling property

We will now argue that the DRR scaling property holds for the RSES of chiral quantum Hall wave functions. First, we review the cut-and-glue approach in Sec. 2.1.1, which then allows us to state our starting assumption, and then the edge structure that will be assumed is discussed in Sec. 2.1.2. Finally, in Sec. 2.1.3 we show, given the assumptions of the cut-and-glue approach, that the RSES can be converted to a boundary-critical phenomenon, where we then use renormalisation group arguments to show the existence of the scaling property.

It should be noted that the application of the cut-and-glue method only models the ES below the *entanglement gap*, [30, 33, 98] i.e., for a range of low entanglement pseudo-energies as we shall discuss in a moment.

2.1.1 Cut-and-glue approach

Consider a system in a fractional quantum Hall ground state, $|G\rangle$, and a spatial bipartition into two regions A and B, where we will write the Schmidt decomposition of $|G\rangle$ as, $|G\rangle = \sum_i e^{-\xi_i/2} |i_A\rangle \otimes |i_B\rangle$, where ξ_i are real numbers, and $\{|i_A\rangle\}$ and $\{|i_B\rangle\}$ form orthonormal bases for subsystems A and B respectively. Several works have pointed out that there is a gap in the entanglement spectrum, $\{\xi_i\}$, [30, 33, 98]. Let Ξ be the set of indices, i, such that ξ_i is below the entanglement gap. We will assume that for $i \in \Xi$, $|i_A\rangle$ and $|i_B\rangle$ are edge states of the A and B systems respectively, i.e., these kets do not have excitations deep in the bulk. We will further assume that $|G_{\text{edge}}\rangle = \sum_{i\in\Xi} e^{-\xi_i/2} |i_A\rangle \otimes |i_B\rangle$ is the ground state of some "physical" *gapped* Hamiltonian only involving edges of the A and B subsystems, H_{edge}.

This assumption can also be reformulated using more physically insightful assumptions. Write the Hamiltonian of the system as $H = H_A + H_B + H_{\text{AB}}$, where H_A and H_B are the Hamiltonians for subsystems A and B respectively, and H_{AB} is the interaction between them. If we turn off this interaction then one would expect at low energies the Hilbert space "looks" like $(\mathcal{H}_{A,\text{bulk}} \otimes \mathcal{H}_{A,\text{edge}}) \otimes (\mathcal{H}_{B,\text{bulk}} \otimes \mathcal{H}_{B,\text{edge}})$. Now assume that at low energies of the full Hamiltonian H we are still at low energies in the non-interacting Hamiltonian, $H_A + H_B$. We can then write $H = H_{\text{edge}} + H_{A,\text{bulk}} + H_{B,\text{bulk}} + \Delta H$, where H_{edge} only involves the edge degrees of freedom (including the interactions between the edges), $H_{A,\text{bulk}}$ and $H_{B,\text{bulk}}$ are the Hamiltonians of the bulks of A and B respectively, and ΔH includes the bulk-edge interaction, both between A and B and within either system, and the bulk-bulk interactions between the A and B systems. Even for the long-range Coulomb interaction, one would expect the energy scale for $H_{\text{edge}} + H_{A,\text{bulk}} + H_{B,\text{bulk}}$ to be larger than the energy scale for ΔH. Thus, let us further assume that ΔH can be considered a *perturbation* of $H_{\text{edge}} + H_{A,\text{bulk}} + H_{B,\text{bulk}}$. Further, the ground state of $H_{\text{edge}} + H_{A,\text{bulk}} + H_{B,\text{bulk}}$ is such that both the A and B are in their individual ground states and the coupled edges are in the ground state of H_{edge}. This

would then imply the assumption given in the previous paragraph (at least to zeroth order in the perturbation, ΔH).

As given here, this assumption is stronger than that given by QKL. There is now at least some numerical evidence that one can make such an assertion [99, 100]. The main point is that this approach reduces the problem to finding the entanglement spectrum between the edges of A and B in $|G_{\text{edge}}\rangle$.

2.1.2 Minimal edges of chiral quantum Hall phases

Before going on to understand the entanglement structure of $|G_{\text{edge}}\rangle$, we must first detail the edge theory of these chiral phases. In the following, we will assume that the required edge theory to describe the edges of A and B is that of a minimal edge. The Hamiltonian of our two interacting edges can be written, $H_{\text{edge}} = H_0 + \textit{perturbations}$, where H_0 has full conformal symmetry and does not contain any interactions between the edges. The perturbations include all interactions between the A and B edges and any other terms involving only one edge that also break conformal symmetry. We shall now detail the structure of the edge A under H_0, where the structure of the edge of B is simply the anti-chiral copy.

We will assume that the Wick rotated edge theory, with the Hamiltonian H_0, is described by a *rational* CFT whose chiral algebra $\mathcal{A}$ is generated by repeated OPEs of a finite set of fields $V_i(w)$ and their conjugates $V_i^\dagger(w)$, where $w = x + i\tau$ with x being the spatial coordinate along the edge and τ being the imaginary time. In the absence of any bulk excitations, the space of states forms the vacuum representation of $\mathcal{A}$ and so can be generated by the modes of $V_i(w)$ and $V_i^\dagger(w)$ applied on the vacuum, $|0\rangle$. It is assumed that $V_i(w)$ and $V_i^\dagger(w)$ create excitations on the edge with a charge equivalent and opposite to that of the underlying particle respectively (i.e. $\pm$ the electron charge in most cases).

In the case of chiral abelian FQH states the edge theory the V operators can be

expressed in terms of vertex operators of p independent chiral boson fields $\varphi^{(i)}(w)$ as $V_{\epsilon^j}(w) =: e^{i\sum_{k=1}^{p}\epsilon_k^j\varphi^{(k)}(w)} :$ and $V^\dagger_{\epsilon^j}(w) =: e^{-i\sum_{k=1}^{p}\epsilon_k^j\varphi^{(k)}(w)} :$, where ϵ^j are a basis for an integer lattice Λ with $\epsilon^i \cdot \epsilon^j = K_{ij}$, K is a positive definite matrix with integer entries, and $: * :$ denotes normal ordering. This is the same K-matrix of the Wen-Zee effective Chern-Simons theory that described the bulk of the corresponding state [13]. Furthermore, there is a vector t known as the charge vector, where the charge density on the edge is $\sum_k t_k i\partial\varphi^{(k)}(w)$. As we shall see in Chap. 3 there are also many non-abelian states with the general edge structure outlined in this section.

If $O(w)$ creates some excitation on the A edge then the operator on the B edge which creates the same physical excitation is given $\overline{O}^\dagger(w)$. This follows from the fact that B edge theory is the time-reversed version of A (as the corresponding excitations move in opposite directions on either edge).

2.1.3 Entanglement spectrum as a surface critical problem

In Sec. 2.1.1 we discussed how the problem of computing the RSES can be converted to that of computing the ES between the edges of A and B in $|G_{\text{edge}}\rangle$. We can understand this ES by first understanding the structure of overlaps with the edge ground state of the form, $\langle a|\,\overline{\langle b|}\,|G_{\text{edge}}\rangle$, where $|a\rangle$ and $\overline{|b\rangle}$ are edge states of A and B respectively.

As all states in this two-edge system can be generated by modes of the various local fields acting on the vacuum state, determining the above overlap is equivalent to the computation of correlators of the form, $\langle 0|\,\phi_1(x_1,\tau_1)\phi_2(x_2,\tau_2)\ldots|G_{\text{edge}}\rangle$, where $\phi_i(x_i,\tau_i)$ is a local operator evolving in imaginary time, τ, by H_0, $\tau_1 > \tau_2 > \cdots > 0$, and $|0\rangle$ is the vacuum of H_0. Furthermore, as we can write $|G_{\text{edge}}\rangle = \lim_{\tau\to\infty} e^{-\tau H_{\text{edge}}}|0\rangle \,/\, \langle G_{\text{edge}}|0\rangle$, this is equivalent to computing correlators of fields, at $\tau > 0$, in a Euclidean quantum field theory, which is a CFT evolving according to H_0 for $\tau > 0$ and for $\tau \leq 0$ is a perturbed CFT evolving according to H_{edge}.

As any excitations along the real-space cut must be gapped, H_{edge} must be gapped.

Thus, for $\tau < 0$ we have short-ranged correlations, with a correlation length related to the energy gap. Hence, if we "integrate out" the degrees of freedom for $\tau < 0$ we will be left with a CFT on a semi-infinite cylinder with a *local* boundary perturbation at the boundary, $\tau = 0$. In full, this means the action takes the form $S = S_{CFT} + S_b$, where S_b is local to the boundary and takes the form, $S_b = \sum_i \lambda_i \int_{\tau=0} dx \phi_i(x)$, with $\phi_i(x)$ being local boundary operators and λ_i being numerical coefficients that do not depend on the real-space cut length L (when the real-space cut length is large compared to the correlation length). The short-distance cut-off for this field theory on the semi-infinite cylinder should be taken to be of the order of the magnetic length l_B.

In what follows we shall only be interested in overlaps which correspond to modes of the correlators with wavelength comparable to L. Thus, we can use an RG procedure to compare the overlaps for two different real-space cut lengths. For now let us concentrate on real-space cut lengths larger than some L', $L > L'$. We can then take a particular real-space cut and perform standard RG until the circumference of the semi-infinite cylinder is L'. Under this RG the bulk action S_{CFT} will be invariant, but S_b will change. Thus, we can compare two real-space cuts by comparing the resulting S_b's after this RG procedure. Let $S_b(L)$ denote the resulting boundary action *after* this procedure.

For a large L, $S_b(L)$ will be very close to some fixed point which will enforce some *fixed point boundary condition.* This boundary condition can be understood as a boundary state $|G_*\rangle$, where the correlators with this boundary condition are computed as $\langle 0| \, \phi_1(x_1, \tau_1)\phi_2(x_2, \tau_2) \ldots |G_*\rangle$. One can think of $|G_*\rangle$ as the RG fixed point of $|G_{\text{edge}}\rangle$. We now wish to determine $|G_*\rangle$.

The $V_i(w)$ operators create excitations on the edge which correspond to some bulk excitation that has been moved to the edge. Hence, a natural fixed point boundary condition that one would expect is that when we make a particular excitation on the A edge this should be equivalent to making the corresponding excitation on the B edge,

as the two edges are not spatially separated. This then gives $V_i(w)\,|G_*\rangle = \overline{V}_i^\dagger(w)\,|G_*\rangle$. Written in terms of modes this gives,

$$[V_{i,n} - \overline{V}_{i,-n}^\dagger]\,|G_*\rangle = 0 \tag{2.3}$$

One can show by Schur's lemma that $|G_*\rangle$ is completely determined by Equation 2.3 up to a multiplication by a complex number as the space of states forms an irreducible representation of $\mathcal{A}$, which is a standard result in boundary CFT. Furthermore, $|G_*\rangle$ has the property that, with a particular normalisation, $\langle a|\,\overline{\langle b|}\,|G_*\rangle = \langle a|b\rangle$. In the langauge of boundary CFT, $|G_*\rangle$ is an Ishibashi state [101, 102].

Next, for a large but finite L we must have that $S_b(L)$ will be the fixed point action plus *irrelevant* perturbations. Thus, our correlators take the form $\langle 0|\,\phi_1(x_1,\tau_1)\phi_2(x_2,\tau_2)\ldots e^{-\delta S_b(L)}\,|G_*\rangle$, where $\delta S_b(L)$ must be composed of irrelevant boundary perturbations. Eq. 2.3 indicates that all boundary operators correspond to local operators of the A edge (i.e. fields of $\mathcal{A}$). Thus, $\delta S_b(L)$ must take the form,

$$\delta S_b(L) = \sum_i \frac{\beta_i}{L^{h_i-1}} \int dx' \phi_i(x') \tag{2.4}$$

where $\phi_i(x')$ are local operators of the A edge with corresponding scaling dimension h_i and β_i are numerical constants. The L dependence of each term follows directly from the RG procedure that defines $S_b(L)$. As $\delta S_b(L)$ is an irrelevant perturbation, we must require that only operators with $h_i > 1$ appear[1]. We use a prime on the x coordinate as a reminder that this integral should be along the edge of the semi-infinite cylinder with circumference L', as $S_b(L)$ is the boundary perturbation after the RG procedure.

Finally, we thus have that so long as $\langle a|\,\overline{\langle b|}\,|G_{\text{edge}}\rangle$ corresponds to long wavelengths of a correlator we have,

[1]One may be concerned about marginally irrelevant perturbations. In the cases considered the marginal perturbations are those of scaling dimension one fields where the integral of these around the edge of the cylinder is equivalent to a sum of zero modes of these scaling dimension one fields. The zero modes of scaling dimension one fields all commute with Virasoro mode operators. Hence, these perturbations of scaling dimension one fields must produce yet another fixed point boundary condition. This then implies that these perturbations are all exactly marginal.

$$\langle a|\,\overline{\langle b|}\,|G_{\text{edge}}\rangle = \langle a|\,\overline{\langle b|}e^{-\delta S_b(L)}\,|G_*\rangle = (\langle a|\,e^{-\delta S_b(L)})\overline{\langle b|}\,|G_*\rangle = \langle a|\,e^{-\delta S_b(L)}\,|b\rangle \tag{2.5}$$

where in the second equality we have used the fact $\delta S_b(L)$ is composed entirely of operators of the A edge. Thus, we have found that overlaps with the ground state are encoded in a local boundary perturbation $\delta S_b(L)$. One may be concerned that Eq. 2.5 depends on the normalisation of $|G_*\rangle$, however, any change in the normalisation of $|G_*\rangle$ can be absorbed into $e^{-S_b(L)}$ by adding a constant to the action, $S_b(L)$.

Now we have determined the form of overlaps with the ground state it is a rather simple matter to compute the reduced density matrix of A and thus the ES. First, let $\{|i\rangle\}$ be an orthonormal basis for A and let $\{\overline{|i\rangle}\}$ be the corresponding basis of B. The reduced density matrix is simply given by,

$$\begin{aligned}\rho_A &= \text{Tr}_B[|G_{\text{edge}}\rangle\,\langle G_{\text{edge}}|] = \text{Tr}_B[\sum_{ijkl}(\langle i|\,e^{-\delta S_b(L)}\,|j\rangle)\,|i\rangle\,\overline{|j\rangle}\,\langle k|\,\overline{\langle l|}(\langle l|\,e^{-\delta S_b^\dagger(L)}\,|k\rangle)] \\ &= e^{-\delta S_b(L)}e^{-\delta S_b^\dagger(L)}\end{aligned} \tag{2.6}$$

We then define the entanglement action, S_{ES} by $e^{-S_{ES}} = e^{-\delta S_b(L)}e^{-\delta S_b^\dagger(L)}$. As pointed out by DRR, we can use the Baker-Campbell-Hausdorff formula to express S_{ES} as an expansion in commutators involving $\delta S_b(L)$ and $\delta S_b^\dagger(L)$. The key point is that the commutator of two operators that are integrals of local operators, must itself be the integral of a local operator. We are thus led to the conclusion that the reduced density matrix of A takes the form,

$$\rho_A = e^{-S_{ES}} \qquad S_{ES} = \sum_i \frac{\alpha_i}{L^{h_i-1}}\int dx'\phi_i(x') \tag{2.7}$$

where, once again, $\phi_i(x')$ are local operators of the A edge with corresponding scaling dimension h_i and α_i are numerical constants. The fact that $\delta S_b(L)$ has only operators with $h_i > 1$ implies that S_{ES} must only contain terms with $h_i > 1$. Thus, we can interpret S_{ES} as an *irrelevant boundary perturbation*. The fact that the reduced density

matrix is Hermitian also implies that S_{ES} is Hermitian ($S_{ES}^{\dagger} = S_{ES}$).

We have thus shown that the scaling property of the RSES can be shown from the QKL cut-and-clue approach.

2.2 Modeling the RSES of the Bosonic $\nu = 2/3$ Composite Fermion Wave Function

We will now demonstrate how the general result of Sec. 2.1 can be applied to understand the RSES of the bosonic $\nu = 2/3$ CF wave function of N particles on the sphere with the real-space cut along the equator. Firstly, in Sec. 2.2.1 the edge structure of this $\nu = 2/3$ state will be detailed, along with how certain observables, such as angular momentum, are related to it. Then, a model is developed by arguing what edge operators should and should not appear in S_{ES}. We will then present a numerical test of this model in Sec. 2.3.

2.2.1 Edge structure of the $\nu = 2/3$ state

It can be shown that the effective bulk Chern-Simons theory that one expects for a given CF state is equivalent to the effective bulk theory of the hierarchy state at the same filling fraction [12, 103]. Hence, the minimal edge theory of a given CF state should be the same as that for the corresponding hierarchy state.

The bosonic $\nu = 2/3$ hierarchy state can be thought of as a $\nu = 1/2$ droplet with a $\nu = 1/6$ droplet of quasi-particles. Following Wen [19], the edge theory can then be constructed as a $\nu = 1/2$ edge, described by a chiral boson field $\tilde{\varphi}^{(1)}$, combined with a $\nu = 1/6$ edge described by another chiral boson field $\tilde{\varphi}^{(2)}$. Following a Wick rotation and a mapping to the complex plane $z = e^{\frac{2\pi}{L}(\tau + ix)}$, the boson fields have the mode expansions,

$$\tilde{\varphi}^{(j)} = \tilde{\varphi}_0^{(j)} - i\tilde{a}_0^{(j)} \ln z + i \sum_{n\neq 0} \frac{1}{n} \tilde{a}_n^{(j)} z^{-n} \tag{2.8}$$

where,

$$[\tilde{a}_n^{(i)}, \tilde{a}_m^{(j)}] = n\delta_{n+m,0}\delta_{ij} \quad [\tilde{\varphi}_0^{(j)}, \tilde{a}_0^{(k)}] = i\delta_{jk} \tag{2.9}$$

and all other commutation relations are trivial. Further, the $a_0^{(i)}$ operators measure the $U(1)$ charge of their corresponding boson field.

The charge density operators are $J^{(1)}(z) = i\frac{1}{\sqrt{2}}\partial\tilde{\varphi}^{(1)}$ and $J^{(2)}(z) = i\frac{1}{\sqrt{6}}\partial\tilde{\varphi}^{(2)}$ for the $\nu = 1/2$ and $\nu = 1/6$ edges respectively, with the underlying particle having charge 1. Either edge can support excitations that have charge 1/2. As the total charge of both edges must be an integer, the lattice, Λ, of this theory has a basis $\epsilon^1 = (\sqrt{2}, 0)$ and $\epsilon^2 = (1/\sqrt{2}, \sqrt{3/2})$. The vacuum state, $|0\rangle$, is defined such that $\tilde{a}_n^{(j)}|0\rangle = 0$ for all $n \geq 0$ and $j = 1, 2$. All states in the Hilbert space can then be generated by applying operators to the vacuum state, that are polynomials in $\tilde{a}_{-n}^{(j)}$ $(n > 0)$, $e^{\pm i\sum_j \epsilon_j^1 \tilde{\varphi}_0^{(j)}}$ and $e^{\pm i\sum_j \epsilon_j^2 \tilde{\varphi}_0^{(j)}}$.

To numerically test the model we develop, we must be able to correctly label the angular momentum quantum number in our effective edge theory. In our case, the edge is rotationally symmetric. In Appendix 2.A we show that, the angular momentum relative to the ground state (or relative to the edge vacuum $|0\rangle$), ΔM, is given by,

$$\Delta M = L_0 + \sqrt{2}(Q^{(1)} - 1/2)\tilde{a}_0^{(1)} + \sqrt{6}(Q^{(2)} - 1/2)\tilde{a}_0^{(2)} \tag{2.10}$$

where $Q^{(1)}$ and $Q^{(2)}$ are the amount of charge in the $\nu = 1/2$ and the $\nu = 1/6$ droplets respectively, and L_0 is the zeroth Virasoro mode which is given by $L_0 = \frac{1}{2}((\tilde{a}_0^{(1)})^2 + (\tilde{a}_0^{(2)})^2) + \sum_{n>0}(\tilde{a}_{-n}^{(1)}\tilde{a}_n^{(1)} + \tilde{a}_{-n}^{(2)}\tilde{a}_n^{(2)})$.

Finally, in the next subsection, we will use a more convenient basis of fields given by,

$$\varphi^{(1)} = -\frac{\sqrt{3}}{2}\tilde{\varphi}^{(1)} - \frac{1}{2}\tilde{\varphi}^{(2)} \qquad \varphi^{(2)} = \frac{1}{2}\tilde{\varphi}^{(1)} - \frac{\sqrt{3}}{2}\tilde{\varphi}^{(2)} \tag{2.11}$$

Let $\Delta Q^{(1)}$ and $\Delta Q^{(2)}$ be the electromagnetic charge added to the $\nu = 1/2$ and the $\nu = 1/6$ edges respectively. In this new basis of fields the $U(1)$ charge of $\varphi^{(1)}$ is given by $-\sqrt{\frac{3}{2}}(\Delta Q^{(1)} + \Delta Q^{(2)})$ and the $U(1)$ charge of $\varphi^{(2)}$ is given by $\frac{1}{\sqrt{2}}(\Delta Q^{(1)} - 3\Delta Q^{(2)})$. Thus, we can interpret the $\varphi^{(1)}$ as the charged mode and $\varphi^{(2)}$ as the neutral mode[2].

2.2.2 The entanglement action

We now construct the model entanglement actions. To use our effective description we must specify what state of A our edge vacuum corresponds to, which is equivalent to specifying $Q^{(1)}$ and $Q^{(2)}$. For the results of Sec. 2.1 to apply we must pick the vacuum state such that it corresponds to the state with *minimum* entanglement pseudo-energy in hemisphere A. Such a state will have $N/2$ particles in A. If we let ΔN_A be the change in the number of particles in A from this minimum state, then this choice of vacuum means that the $U(1)$ charge of $\varphi^{(1)}$ is given by $-\sqrt{\frac{3}{2}}\Delta N_A$. In general, this vacuum state does not correspond to the lowest angular momentum eigenstate of the reduced density matrix of A in the $N_A = N/2$ sector. To compare this model to the numerical RSES we need to understand the effective theory near this lowest angular momentum state (i.e. for those states where the RSES can be easily computed). In what follows we shall first discuss what form S_{ES} takes for the minimum pseudo-energy vacuum choice and then we shall detail how this can be transformed to give an effective description around the lowest angular momentum state.

The local operators that can appear in S_{ES} can be labelled by two tuples of positive integers, $\mathbf{k}^{(1)}$ and $\mathbf{k}^{(2)}$ with $\mathbf{k}^{(i)} = (k_1^{(i)}, k_2^{(i)}, \ldots, k_{p_i}^{(i)})$, where the corresponding operator is given by $\phi_{(\mathbf{k}^{(1)},\mathbf{k}^{(2)})}(z) =: \prod_{r=1}^{p_1} i\partial^{k_r^{(1)}}\varphi^{(1)}(z) \prod_{s=1}^{p_2} i\partial^{k_s^{(2)}}\varphi^{(2)}(z) :$. Vertex terms in $\varphi^{(1)}$ are strictly forbidden, as S_{ES} must conserve the electromagnetic charge. The Wen-Zee effective Chern-Simons theory indicates there that both edge mode $U(1)$ charges are conserved at very low energy and long length scales[13]. We will assume that the

[2]i.e. $i\partial\varphi^{(1)}$ will couple directly to the electromagnetic field and $i\partial\varphi^{(2)}$ will not.

conservation of these $U(1)$ charges is not broken in ρ_A at least to the orders in $1/\sqrt{N}$ that we will be testing. By this assumption, there are then no vertex terms in $\varphi^{(2)}(z)$ in S_{ES}. We also fitted model S_{ES} to the numerically calculated RSES that contains the possible vertex operator terms up to scaling dimension 2. The coefficients of the vertex operator terms were found to be several orders of magnitude lower than those of the terms at the corresponding scaling dimension. The scaling dimension of each operator is simply given by $h_{(\mathbf{k}^{(1)},\mathbf{k}^{(2)})} = \sum_{r=1}^{p_1} k_r^{(1)} + \sum_{s=1}^{p_2} k_s^{(2)}$.

Noting that with the real-space cut on the equator $L \propto \sqrt{N}$, we can express S_{ES} in radial quantisation coordinates, $z = e^{\frac{2\pi}{L}(\tau+ix)}$, as, $S_{ES} = \sum_{j,h_j>1} \frac{K_j}{\sqrt{N}^{h_j-1}} \oint \frac{dz}{2\pi i} z^{h_j-1}\phi_j(z)$ where j is a shorthand notation for $(\mathbf{k}^{(1)}, \mathbf{k}^{(2)})$, K_j are numerical constants. Note that the operators that result from integrating these local operators, $\phi_j(z)$, are not linearly independent [104, 105]. For example, through integration by parts we have $\oint dzz : \partial^2\varphi^{(2)}(z) := -\oint dz : \partial\varphi^{(2)}(z) :$.

Let us now discuss how this entanglement action can be understood near the lowest angular momentum state. In Appendix 2.A we show that, in the $\Delta N_A = 0$ sector, the lowest angular momentum state and the state with the lowest entanglement pseudo-energy differ in angular momentum by $O(N)$. From Eq. 2.10 the lowest angular momentum state, in the $N_A = N/2$ sector, $|\hat{0}\rangle$, must correspond to a state which is just some $U(1)$ charge of the neutral mode added to the vacuum, $|\hat{0}\rangle = e^{i\kappa\varphi_0^{(2)}} |0\rangle$ for some κ. As the angular momentum depends on the charge of the neutral mode quadratically, we have that $\kappa = O(\sqrt{N})$. We then define a new neutral mode with a shifted $U(1)$ charge, $i\partial\hat{\varphi}^{(2)}(z) \equiv i\partial\varphi^{(2)}(z) - \frac{\kappa}{z}$. The lowest angular momentum state, $|\hat{0}\rangle$, will be the vacuum of these shifted fields. We can rewrite S_{ES} in terms of this new neutral mode, which will "reshuffle" the various terms. For example, $z : (i\partial\varphi^{(2)})^2 := z : (i\partial\hat{\varphi}^{(2)})^2 : -2\kappa i\partial\hat{\varphi}^{(2)} + \frac{\kappa^2}{z}$, which will now give terms of scaling dimension one. Let $\hat{\phi}_j(z)$ be the $\phi_j(z)$ with $\varphi^{(2)} \to \hat{\varphi}^{(2)}$. We can then express,

$$S_{ES} = \sum_{h_j \geq 1} \frac{\hat{K}_j}{\sqrt{N}^{h_j - 1}} \oint \frac{dz}{2\pi i} z^{h_j - 1} \hat{\phi}_j(z) \tag{2.12}$$

where $\hat{K}_j$ can generally now be expanded as $\hat{K}_j = a + \frac{b}{\sqrt{N}} + \frac{c}{N} + \ldots$, as $\kappa = O(N)$.

To create an approximate model we truncate at some finite h_j. The possible operators can be reduced by the fact the system is symmetric under the exchange of the two hemispheres, A and B. It is not obvious how this symmetry is manifest in our effective description. In Appendix 2.B we argue, although not entirely rigorously, that this transformation in the effective description is given by, $i\partial\varphi^{(1)} \to -i\partial\varphi^{(1)}$ and $i\partial\hat{\varphi}^{(2)} \to i\partial\hat{\varphi}^{(2)}$. A numerical test[3] for this symmetry can be found in Ref. [1]. We can then only have terms with $\mathbf{k}^{(1)}$ having an even number of components.

We shall now present two approximations of S_{ES} at with truncations at scaling dimensions 2 and 3. The models with all linearly independent terms, respecting the hemisphere swapping symmetry, up to scaling dimensions 2 and 3 are given by,

$$\hat{S}_{ES}^{\{2\}} = \oint \frac{dz}{2\pi i} \hat{\alpha} i\partial\hat{\varphi}^{(2)}(z) + z\left[\frac{\hat{\beta}}{2} : (i\partial\varphi^{(1)}(z))^2 : + \frac{\hat{\gamma}}{2} : (i\partial\hat{\varphi}^{(2)}(z))^2 :\right] \tag{2.13}$$

and

$$\hat{S}_{ES}^{\{3\}} = \hat{S}_{ES}^{\{2\}} + \oint \frac{dz}{2\pi i} z^2 \left[\hat{\delta} : (i\partial\hat{\varphi}^{(2)}(z))^3 : + \hat{\epsilon} : (i\partial\hat{\varphi}^{(2)}(z))(i\partial\varphi^{(1)}(z))^2 :\right] \tag{2.14}$$

respectively where $\hat{\alpha}$, $\hat{\beta}$, $\hat{\gamma}$, $\hat{\delta}$ and $\hat{\epsilon}$ are model parameters that require fitting. Eqs. 2.13 and 2.14 define the two models we shall test against the numerically calculated RSES.

[3]In this test the real-space cut is moved off the equator slightly and the additional terms not satisfying this symmetry are included with the coefficients shown to go to zero as the real-space cut moves to the equator.

2.3 Numerical Tests

We now present two numerical tests for our effective model of the RSES of the bosonic $\nu = 2/3$ Composite Fermion wave function on the sphere with the real-space cut on the equator. The first test demonstrates how well the effective description can be fit to the numerically computed RSES, over multiple N_A sectors. We then test how the fitted model parameters vary with the system size.

2.3.1 Fitting the model

In all cases presented here, the RSES has been calculated numerically using the methods of Rodriguez et al. [106] where the projection to the LLL has been approximated using the Jain-Kamila procedure [108] and inner products have been calculated using Monte-Carlo integration (see Ref. [107] for details). The parameters in the model entanglement actions, $S_{ES}^{\{2\}}$ and $S_{ES}^{\{3\}}$, are then fit using a least-squares procedure, which is detailed in Appendix 2.C along with the procedure used for error estimation. One subtlety that should be mentioned, is that the least-squares fitting procedure used here cannot determine the sign of the parameters $\hat{\alpha}$, $\hat{\delta}$ and $\hat{\epsilon}$, as simultaneously changing the sign of these parameters will produce the same spectrum. The sign of such parameters would have to be determined by some other means.

The resulting numerically calculated and fitted RSES for the case of $N = 58$ bosons can be seen in Fig. 2.1, where the spectra are shown over the $N_A = 29, 28, 27, 26$ sectors.

One can see that the fitted low-order entanglement action, $S_{ES}^{\{2\}}$, is in good agreement with the numerically calculated spectrum over the $N_A = 29, 28, 27$ sectors. There is an improvement by adding the higher order terms of $S_{ES}^{\{3\}}$, where we can see some of the higher order level splitting being reproduced. One can also see that at higher angular momentum both effective models, $S_{ES}^{\{2\}}$ and $S_{ES}^{\{3\}}$, begin to break down. This is due to the presence of the higher order terms in the entanglement action whose coefficients are small, but have matrix elements which grow much faster, as momentum

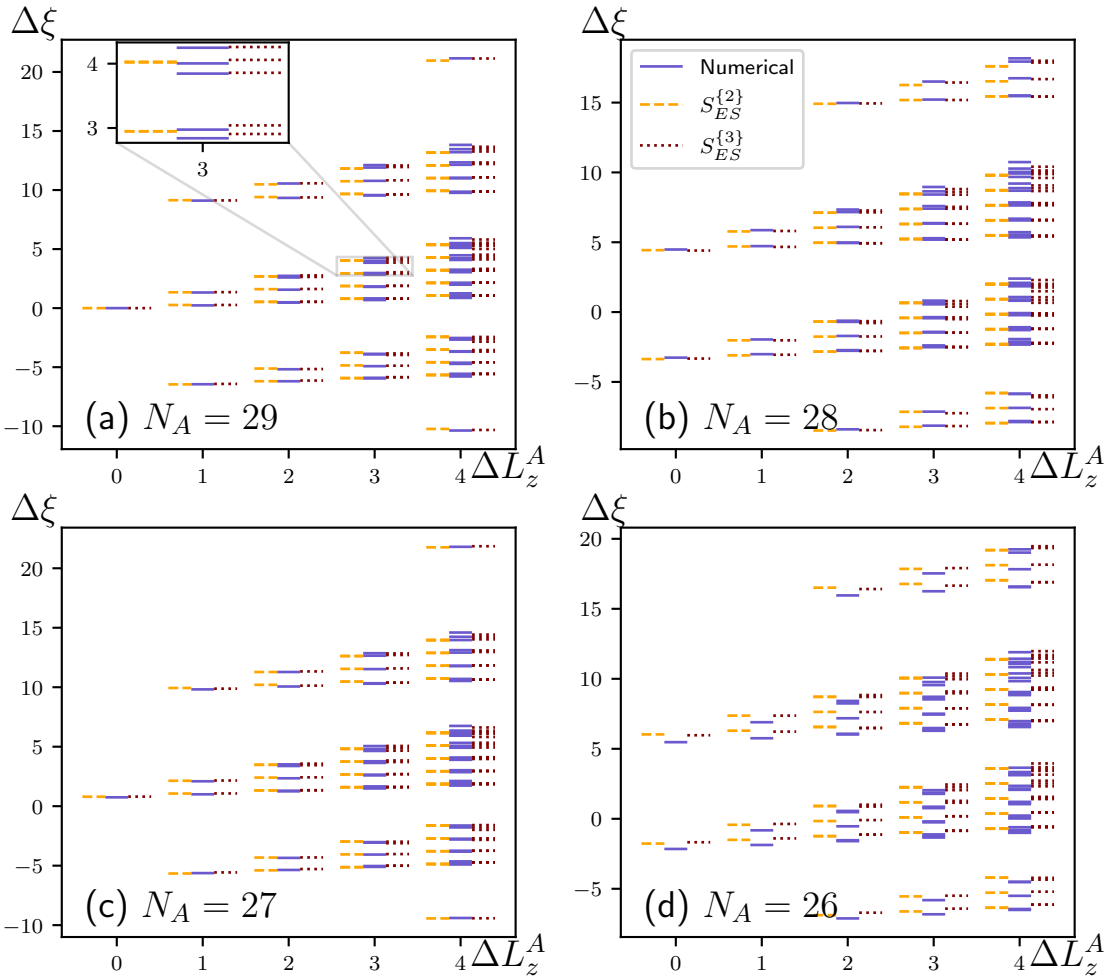

Figure 2.1: Comparison between the numerically calculated RSES (blue-solid), using the methods of Refs. [106, 107], and the models, $S_{ES}^{\{2\}}$ (Eq. 2.13) (yellow-dashed) and $S_{ES}^{\{3\}}$ (Eq. 2.14) (red-dotted), fitted using the procedure of Appendix 2.C, in the case of $N = 58$ bosons on a sphere, in the $\nu = 2/3$ bosonic CF wave function with real-space cut on the equator over the (a) $N_A = 29$, (b) $N_A = 28$, (c) $N_A = 27$ and (d) $N_A = 26$ sectors. ΔL_z^A is the angular momentum relative to the lowest possible for the given N_A sector and $\Delta\xi$ is the entanglement pseudo-energy relative the level at $N_A = 29$ and $\Delta L_z^A = 0$. Error bars have not been included and are too small to be visible.

is increased, compared to the lower order terms included in both models. This also explains the observed deviation at $N_A = 26$, as at scaling dimension 4 one would expect the $:(\partial\varphi^{(1)})^4:$ term to be present which would give a $(a_0^{(1)})^4 \propto (\Delta N)^4$. This term is not present in either model and would lead to their suddenly large inaccuracy at larger ΔN_A.

2.3.2 Parameter scaling

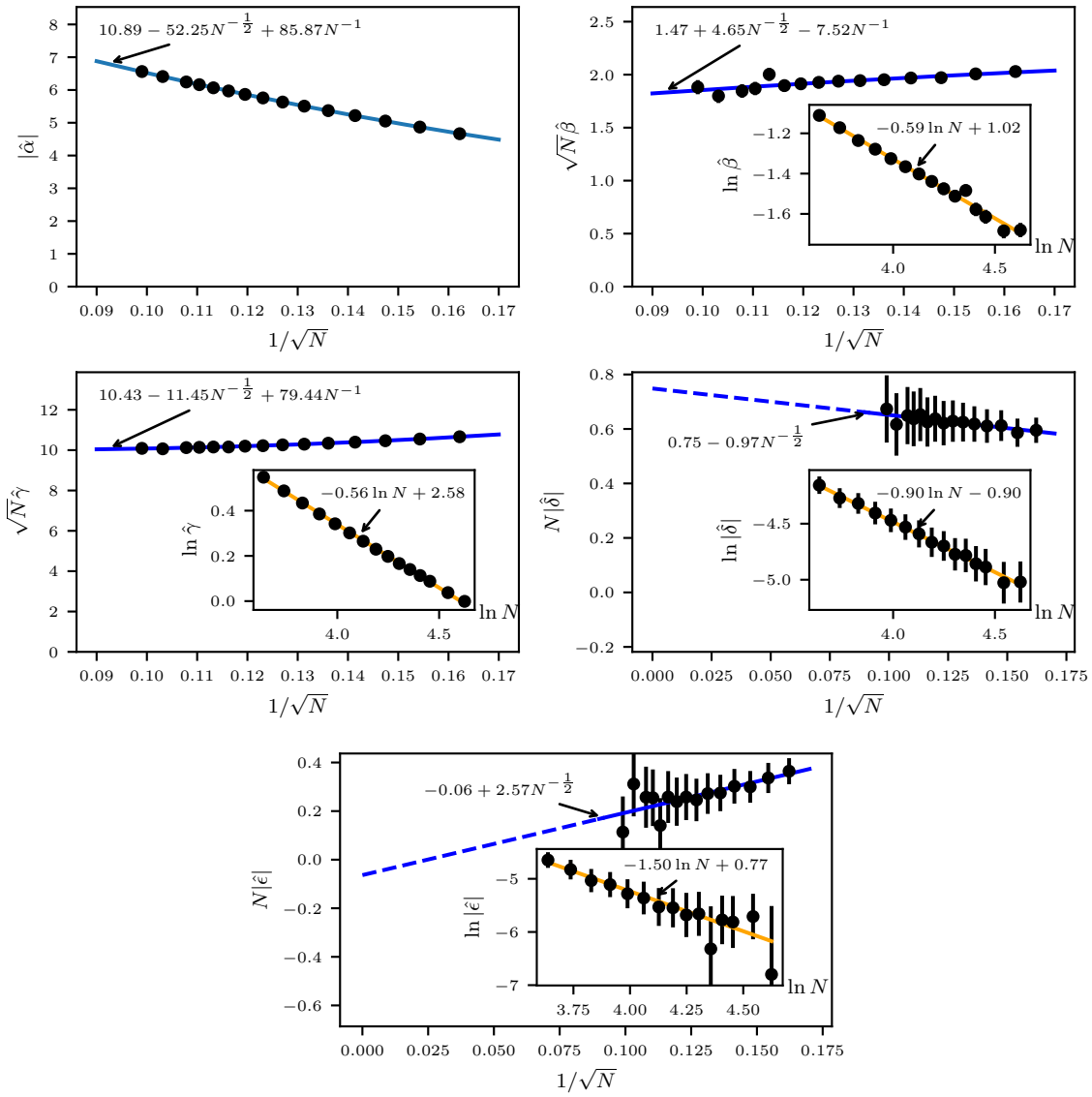

Figure 2.2: The N dependence of the fitted $\hat{\alpha}$, $\hat{\beta}$, $\hat{\gamma}$, $\hat{\delta}$ and $\hat{\epsilon}$ parameters in the $S_{ES}^{\{3\}}$ model. There is a sign ambiguity when fitting the parameters $\hat{\alpha}$, $\hat{\delta}$ and $\hat{\epsilon}$, and hence we have only presented their absolute values. The N dependence of all three parameters can be fit to the given functional form (blue line) (see discussion of Sec. 2.2). Inset log plots are given for all parameters except $\hat{\alpha}$. Error bars have been included, but in many cases are too small to be visible. Our procedures for error estimation are given in Appendix 2.C.

To test how the parameters of each model vary with the system size, N, we have repeated the procedure of Sec. 2.3.1 to estimate these parameters for a variety of system

sizes between $N = 38$ and $N = 102$. One should keep in mind again that the sign of parameters $\hat{\alpha}$, $\hat{\delta}$ and $\hat{\epsilon}$ cannot be determined by the fitting procedure used; we have thus taken the absolute value of any parameter values presented in this section. As discussed in Sec. 2.2 each parameter should vary with N as, $a/\sqrt{N}^{h-1} + b/\sqrt{N}^{h} + c/\sqrt{N}^{h+1} + \ldots$, where h is the scaling dimension of the term in the entanglement action which this particular parameter is a coefficient of. We have then fitted the N dependence of each parameter to this functional form (whilst keeping h fixed to the expected value). For each parameter which decays to zero for large N, we have also performed a linear regression for the $\ln N$ dependence of the logarithm of the parameter. This allows us to check that the fit to the expected N dependence has not been too biased, by estimating the exponent of the leading order contribution.

The result of this test for the parameters of $S_{ES}^{\{3\}}$ can be seen in Fig. 2.2. One can see that all parameters can be fit very well to their expected N dependence. Furthermore, the linear regressions of $\ln\hat{\beta}$ and $\ln\hat{\gamma}$ vs. $\ln N$ both indicate $\hat{\beta} \sim N^{-0.59}$ and $\hat{\gamma} \sim N^{-0.56}$, which is close to the expected leading order scaling of $N^{-1/2}$. One should note that the presence of the higher order terms in $1/\sqrt{N}$ will cause the estimation of this leading order exponent to be slightly off and one can also visually see the presence of such terms from the curvature in the $\ln\hat{\gamma}$ plot. The dependence of $\hat{\delta}$ on N has the estimation of the leading order exponent gives $\hat{\delta} \sim N^{-0.90}$, which is close to the expected leading dependence, N^{-1}. However, the estimation of the leading order exponent for $\hat{\epsilon}$ indicates that the fitted $\hat{\epsilon}$ will scale as $\sim N^{-3/2}$ at large system size, which is also evident in the small $N\hat{\epsilon}$-axis intercept of the fitted N dependence. The scaling of $\hat{\epsilon}$ is still consistent with the predictions of Sec. 2.2. We have that, through integration by parts, $-\oint dz z^2 : (i\partial\hat{\varphi}^{(2)})(i\partial\varphi^{(1)})^2 := \oint \frac{z^3}{3}[: (i\partial^2\hat{\varphi}^{(2)})(i\partial\varphi^{(1)})^2 : + : (i\partial\hat{\varphi}^{(2)})\partial(i\partial\varphi^{(1)})^2 :$. Hence, the $\hat{\epsilon}$ term can be generated by scaling dimension 4 terms. In general, $\hat{\epsilon}$ can then be expanded as $\hat{\epsilon} = a/N + b/N^{3/2} + \ldots$. If it is the case that $a = 0$ then $\hat{\epsilon}$ would scale as $\hat{\epsilon} \sim N^{-3/2}$, which may suggest an additional symmetry.

2.4 Summary and outlook

In this chapter, it has been argued, using the QKL cut-and-glue approach, that the scaling property of RSES should be a generic feature of chiral FQHE ground states. This provides deeper insight into the RSES by emphasising the locality of the effective entanglement action, that reproduces the RSES, and allows one to understand the hierarchy of entanglement level splittings as a consequence of the scaling of the various terms in the entanglement action. A numerical test for this scaling property was then carried out in the case of the RSES of the $\nu = 2/3$ bosonic CF wave function on the sphere with real-space cut along the equator, by fitting a model entanglement action, truncated at finite order, to the RSES. These fitted model RSES were found to accurately reproduce the numerically calculated RSES, where the scaling of the various model parameters was found to be consistent with the RSES scaling property. Furthermore, these model entanglement actions were made with no reference to the CFT construction of the $\nu = 2/3$ wave functions, which is discussed in Chap. 3, to emphasise how this scaling property could be used to model the RSES in a phenomenological manner.

Generally speaking, the RSES of non-chiral FQHE ground states are less well understood compared with the chiral ground states. The main difficulty is that the number of states at a given momentum in the edge CFT of a non-chiral state is infinite and so the usual entanglement level state counting that one can perform for chiral states is no longer possible. It would then be interesting to understand if the scaling property still holds for states with non-chiral edges. If this is so, the scaling property could be used as an alternative to entanglement level counting, where one could identify the topological order of a given ground state by investigating which edge theory can most accurately model the low pseudo-energy entanglement levels with a local entanglement action. Some efforts in this direction have been made recently, in the case of non-chiral topological phases with strong time-reversal symmetry breaking, where effective edge

"velocities" in the RSES are significantly different for edge modes of opposite chirality [109].

2.A Angular Momentum Calculations

2.A.1 Angular momentum in the effective edge theory

We will now show how the angular momentum of the effective edge theory of $\nu = 2/3$ can be computed.

As was stated in Sec. 2.2, the $\nu = 2/3$ can be thought of as a $\nu = 1/2$ droplet with a $\nu = 1/6$ droplet on top, which is composed of quasi-particles [76, 84]. For the purpose of clarity, we shall work in the disk geometry for the moment. Following the Halperin-Haldane construction one can write a wave function for this case as,

$$\psi(\mathbf{z}) = \int \prod_{k=1}^{N_q} d^2w \prod_{i<j}^{N_q} (w_i - w_j)^2 e^{-\sum_i \frac{|w_i|^2}{4l_{B*}^2}} \prod_{i=1}^{N_q}\prod_{j=1}^{N} (\bar{w}_i - \partial_{z_j}) \prod_{i<j}^{N} (z_i - z_j)^2 e^{-\sum_i \frac{|z_i|^2}{4l_B^2}} \tag{2.15}$$

where N is the number of particles, N_q is the number of quasi-particles, l_B is the magnetic length for the underlying particles and l_{B*} is the effective magnetic length for the quasi-particles.

By transforming $z \to e^{i\theta} z$, the angular momentum of this wave function can be computed as,

$$M = Q^{(1)}(Q^{(1)} - 1) + 3Q^{(2)}(Q^{(2)} - 1) \tag{2.16}$$

where, $Q^{(1)} = N - \frac{N_q}{2}$, and $Q^{(2)} = \frac{N_1}{2}$, are the charges of the $\nu = 1/2$ and $\nu = 1/6$ droplet respectively. For any state that is adiabatically connected to this state, this formula should still apply.

If we add charges $\Delta Q^{(1)}$ and $\Delta Q^{(2)}$ to the $\nu = 1/2$ and $\nu = 1/6$ edges respectively,

then the angular momentum will change by $\Delta M_{\text{charge}} = (\Delta Q^{(1)})^2 + 3(\Delta Q^{(2)})^2 + 2(Q^{(1)} - 1/2)\Delta Q^{(1)} + 6(Q^{(2)} - 1/2)\Delta Q^{(2)}$. Written in terms of the zeroth modes of the effective edge theory we have $\Delta M_{\text{charge}} = \frac{1}{2}(\tilde{a}_0^{(1)})^2 + \frac{1}{2}(\tilde{a}_0^{(2)})^2 + \sqrt{2}(Q^{(1)} - 1/2)\tilde{a}_0^{(1)} + \sqrt{6}(Q^{(2)} - 1/2)\tilde{a}_0^{(2)}$. Furthermore, the angular momentum from the edge phonons is $\Delta M_{\text{phonons}} = \sum_{n>0}(\tilde{a}_{-n}^{(1)}\tilde{a}_n^{(1)} + \tilde{a}_{-n}^{(2)}\tilde{a}_n^{(2)})$. Thus, the total angular momentum is,

$$\Delta M = L_0 + \sqrt{2}(Q^{(1)} - 1/2)\tilde{a}_0^{(1)} + \sqrt{6}(Q^{(2)} - 1/2)\tilde{a}_0^{(2)} \tag{2.17}$$

which gives us Eq. 2.10.

2.A.2 Angular momentum difference is $O(N)$ between lowest M eigenstate and lowest pseudo-energy state

We now show the eigenstate of the reduced density matrix with the lowest angular momentum in the $\Delta N_A = 0$ sector differs in angular momentum from the state with the lowest entanglement pseudo-energy by $O(N)$, as stated in Sec. 2.2.2. First, we show the difference in angular momentum between the lowest angular momentum state and the average angular momentum is $O(N)$. Then, we will demonstrate that the difference in angular momentum from the lowest pseudo-energy state and the average angular momentum is also $O(N)$, which then implies the given statement. When we speak of angular momentum here we mean $M_{\text{sphere}} + NN_\phi/2$, where M_{sphere} is the actual angular momentum on the sphere [4]. We will use coordinate $z = u/v$ throughout.

Firstly, let us assume we are in the $N_A = N/2$ sector and that $N/2$ is odd [5]. From Eq. 2.16 the lowest M configuration is when $Q^{(1)} = (3N_A - 1)/4$ and $Q^{(2)} = (N_A + 1)/4$, with the total angular momentum being $3(N_A - 1)^2/4$ (with no edge phonons). One can also compute the average angular momentum in A. Following Girvin et al. [110], the single particle reduced density matrix of our rotationally symmetric LLL wave

[4] This form of angular momentum means one can more straightforwardly transform from the plane geometry to the sphere geometry in such a way that Eq. 2.16 remains valid.

[5] The following arguments can easily be altered slightly to deal with the even case.

functions is, $\rho(x_1, x_2) = \rho_0 \bar{v}_1^{N_\phi} v_2^{N_\phi} (1 + \bar{z}_1 z_2)^{N_\phi}$ where x is a shorthand for a position on the sphere and ρ_0 is the particle density. Which gives the angular momentum density $M(x) = z\partial_{z_2}\rho(x,x) = N_\phi \rho_0 \frac{|z|^2}{1+|z|^2}$. Now let R be the radius of the sphere and $\mathcal{S} = \nu^{-1}N - N_\phi$ be the shift. We can then find the average angular momentum in A, $\langle M_A \rangle$,

$$\begin{aligned} \langle M_A \rangle &= \int_A R^2 d\Omega M(x) = 2\pi R^2 N_\phi \rho_0 \int_{\frac{\pi}{2}}^{\pi} d\theta \sin(\theta) \frac{\cot^2(\theta/2)}{1+\cot^2(\theta/2)} = \frac{N_\phi N}{8} \\ &= \frac{\nu^{-1}N^2 - \mathcal{S}N}{8} = \frac{3}{4}N_A^2 + O(N) \end{aligned} \tag{2.18}$$

Thus, the difference between the average angular momentum in A and the minimum angular momentum eigenstate of the reduced density matrix in the $N_A = N/2$ sector is $O(N)$.

The angular momentum relative to the lowest pseudo energy state with charges $Q^{(1)}$ and $Q^{(2)}$ in the $\nu = 1/2$ and $\nu = 1/6$ droplets respectively is given by Eq. 2.10. If we let $\zeta = \frac{1}{\sqrt{2}}(Q^{(1)} - 3Q^{(2)} + 1)$, then one can see that the minimum angular momentum in the $N_A = N/2$ sector relative to the minimum pseudo energy state is $\Delta M_{\min} = -\frac{\zeta^2}{2}$. We will now compute this relative angular momentum using the effective edge description.

In the large N limit, we can approximate S_{ES} with $S_{ES}^{\{2\}}$ and thus our partition function can be written as $Z = \mathrm{Tr} e^{-S_{ES}^{\{2\}}} = \frac{e^{-\frac{\beta+\gamma}{24}}}{\eta\left(\frac{i\beta}{2\pi}\right)\eta\left(\frac{i\gamma}{2\pi}\right)} \sum_{q\in\Lambda} e^{-\frac{\beta}{2}q_1^2 - \frac{\gamma}{2}q_2^2 - \alpha q_2}$, where $\eta(\tau)$ is the Dedekind eta-function. Using Poisson resummation (Ref. [20]) and that $\eta(-1/\tau) = \sqrt{-i\tau}\eta(\tau)$, we get,

$$\begin{aligned} Z =& e^{-\frac{\beta+\gamma}{24} + \frac{\pi^2}{6}(1/\beta + 1/\gamma)} \left(\prod_{n=1}^{\infty} \frac{1}{1 - e^{-\frac{4\pi^2}{\beta}n}} \right) \left(\prod_{m=1}^{\infty} \frac{1}{1 - e^{-\frac{4\pi^2}{\gamma}m}} \right) \\ &\times \mathrm{Vol}(\Lambda)^{-1} \sum_{p\in\Lambda^*} e^{-\frac{2\pi^2}{\beta}p_1^2 - \frac{2\pi^2}{\gamma}(p_2 + \frac{\alpha}{2\pi i})^2} \end{aligned} \tag{2.19}$$

where $\mathrm{Vol}(\Lambda)$ is the unit cell volume of Λ. Noting that $\alpha, \beta, \gamma \propto 1/\sqrt{N}$ we must have that at large N,

$$\ln Z = \frac{\pi^2}{6}\left(\frac{1}{\beta}+\frac{1}{\gamma}\right)+\frac{\alpha^2}{2\gamma}-\frac{\beta+\gamma}{24}+\ln \mathrm{Vol}(\Lambda)+\text{subleading corrections} \tag{2.20}$$

From Eq. 2.10 the average relative angular momentum is a linear combination of $\langle L_0\rangle$, $\langle a_0^{(1)}\rangle$ and $\langle a_0^{(2)}\rangle$. Note that $\langle a_0^{(1)}\rangle = 0$ by symmetry. Define a $Z(\omega)$ by transforming $\beta \to \beta-\omega$ and $\gamma \to \gamma-\omega$. Then we have $\langle L_0\rangle = \frac{\partial \ln Z(0)}{\partial \omega} = \frac{\pi^2}{6}\left(\frac{1}{\beta^2}+\frac{1}{\gamma^2}\right)+$ subleading corrections. Next, $\langle a_0^{(2)}\rangle = -\frac{\partial \ln Z}{\partial \alpha} = -\frac{\alpha}{\gamma}$ (for large N). This then gives,

$$\langle \Delta M\rangle = \frac{\pi^2}{6}\left(\frac{1}{\beta^2}+\frac{1}{\gamma^2}\right)-\zeta\frac{\alpha}{\gamma}+\text{subleading corrections} \tag{2.21}$$

Since $Q^{(1)}+Q^{(2)}=N$ and $Q^{(j)}\geq 0$ we must have that ζ is at most $O(N)$ (i.e. ζ cannot grow any faster than N). It then simply follows that $\langle \Delta M\rangle = O(N)$ in the large N limit, QED.

2.B Hemisphere Swapping Symmetry

In Sec. 2.2 we claimed that the hemisphere swapping symmetry implied that S_{ES} should be invariant under $i\partial\varphi^{(1)} \to -i\partial\varphi^{(1)}$, $i\partial\varphi^{(2)} \to i\partial\varphi^{(2)}$. Whilst we do not have rigorous proof for this statement, we wish to give a strong motivation for it. We shall first detail how this symmetry is manifest in the $\nu=2$ RSES. Then, with the knowledge of the $\nu=2$ RSES, we deduce how this symmetry should be manifest in the $\nu=2/3$ state using the composite fermion description.

Let $\psi_{1,m}$ and $\psi_{2,m}$ be the LLL and 2nLL orbitals on the sphere with $2Q$ flux quanta passing through, where the form of $\psi_{1,m}$ is given in 1 and $\psi_{2,m}(u,v) = \mathcal{N}_{2,m}v^{Q-m}u^{Q+m}[(Q+1+m)v^*v-(Q+1-m)u^*u]$ with $m=-Q-1,-Q,\ldots,Q,Q+1$ and $\mathcal{N}_{2,m}$ is a normalisation factor. The wave function of the full $\nu=2$ state can be written in second quantised notation as $|\nu=2\rangle = \prod_{m=-Q}^{Q} c_{1,m}^\dagger \prod_{n=-Q-1}^{Q+1} c_{2,n}^\dagger |0\rangle$.

To compute the RSES one must rewrite this state in terms of orbitals that are orthogonal on the A and B hemispheres separately [111, 112]. We then define the

correlation matrix to be $C_{ij}^{A,m} = \int_A d\Omega \psi_{i,m}^*(u,v)\psi_{j,m}(u,v)$. Let $\psi_{+,m}$ and $\psi_{-,m}$ be the orbitals that correspond to the highest eigenvalue, $\lambda_+^{A,m}$ and the lowest eigenvalue $\lambda_-^{A,m}$ of the correlation matrix respectively. As these orbitals diagonalise the correlation matrix they must be orthogonal on the A and B hemispheres separately. One can then verify that the $\nu = 2$ state can be written in terms of these orbitals simply as $|\nu = 2\rangle = \prod_m c_{+,m}^\dagger \prod_n c_{-,m}^\dagger |0\rangle$.

By writing $c_{\pm,m} = \sqrt{\lambda_\pm^{A,m}} c_{\pm,m}^A + \sqrt{1-\lambda_\pm^{A,m}} c_{\pm,m}^B$, where $c_{\pm,m}^A$ and $c_{\pm,m}^B$ is the $c_{\pm,m}$ orbital restricted to the A and B hemispheres respectively, one can then Schmidt decompose the state $|\nu = 2\rangle$. The resulting entanglement Hamiltonian for A is $S_{ES}^A = \sum_{\pm,m} \ln\left[\frac{1-\lambda_\pm^{A,m}}{\lambda_\pm^{A,m}}\right] c_{\pm,m}^{A\dagger} c_{\pm,m}^A$.

Under the transformation $u \to v$, $v \to u$, the Landau level orbitals transform as $\psi_{1,m} \to \psi_{1,-m}$ and $\psi_{2,m} \to -\psi_{2,-m}$. By first considering the transformation properties of the correlation matrix, one can also show under this transformation $\psi_{\pm,m} \to -\psi_{\mp,-m}$. Furthermore, the transformation properties of the correlation matrix gives, $\lambda_\pm^{A,m} = \lambda_\pm^{B,-m}$. Note that an eigen-orbital of the A correlation matrix with the lowest eigenvalue, at a particular angular momentum, must be an eigen-orbital of the B correlation matrix with the highest eigenvalue, at the same angular momentum (i.e. the orbital $\psi_{\pm,m}$ will have eigenvalue $\lambda_\mp^{B,m}$ for the corresponding B correlation matrix). Finally, we note that under this transformation an orbital entirely on the A hemisphere will be mapped to an orbital entirely on the B hemisphere, so we have $c_{\pm,m}^{A\dagger} c_{\pm,m}^A \to c_{\mp,-m}^{B\dagger} c_{\mp,-m}^B$. Putting this all together, one finds that this transformation gives $S_{ES}^A \to S_{ES}^B$. This should be the case as under this transformation our entire wave function is invariant.

Due to the fact that the number of electrons in each orbital are separately conserved we also have that under $c_{\pm,m}^{B\dagger} c_{\pm,m}^B \to 1 - c_{\pm,m}^{A\dagger} c_{\pm,m}^A$ we have $S_{ES}^B \to S_{ES}^A$ up to an additive constant. Putting these two transformations together maps S_{ES}^A onto itself. Let $\partial_x \phi_\pm$ represent the electron density in the $\pm$ orbitals at the edge. These combined

Parameter	Value	Error
$\hat{\alpha}$	5.514	6.2×10^{-4}
$\sqrt{N}\hat{\beta}$	2.024	3.1×10^{-3}
$\sqrt{N}\hat{\gamma}$	10.22	1.7×10^{-3}

Parameter	Value	Error
$\hat{\alpha}$	5.472	6.6×10^{-4}
$\sqrt{N}\hat{\beta}$	2.039	3.4×10^{-3}
$\sqrt{N}\hat{\gamma}$	10.30	1.7×10^{-3}
$N\hat{\delta}$	0.6461	2.8×10^{-3}
$N\hat{\epsilon}$	-0.3113	4.4×10^{-3}

Table 2.1: Fitted parameters for the $S_{ES}^{\{2\}}$ (left) model (Eq. 2.13) and $S_{ES}^{\{3\}}$ (right) model (Eq. 2.14) of the RSES of $N = 58$ bosons on the sphere in the $\nu = 2/3$ CF wave function with the real-space cut along the equator.

transformations can be written in terms of these modes as $\partial\phi_{\pm} \to -\partial\phi_{\mp}$. Thus, written in terms of these modes we can say S_{ES}^{A} is invariant under $\partial\phi_{\pm} \to -\partial\phi_{\mp}$.

When describing the RSES of the $\nu = 2/3$ we expect from CF theory that there must exist two modes at the real-space cut $\partial\phi_{\pm}$ which can be interpreted as the density of CFs in the effective $c_{\pm,m}^{\dagger}$ orbitals. We then expect as written in terms of these modes S_{ES} is invarient under $\partial\phi_{\pm} \to -\partial\phi_{\mp}$.

The transformation between these CF modes and the charge and neutral modes are given by[1, 12, 50, 52],

$$\begin{pmatrix} \varphi^{(1)} \\ \varphi^{(2)} \end{pmatrix} = \begin{pmatrix} -\sqrt{\frac{3}{2}} & -\sqrt{\frac{3}{2}} \\ -\frac{1}{\sqrt{2}} & \frac{1}{\sqrt{2}} \end{pmatrix} \begin{pmatrix} \phi_{+} \\ \phi_{-} \end{pmatrix} \tag{2.22}$$

Hence, we can now interpret the neutral mode as representing the difference in densities of Composite Fermions in the $\pm$ orbitals at the edge. Thus, we see that if S_{ES}^{A} is invariant under $\partial_x\phi_{\pm} \to -\partial_x\phi_{\mp}$, then in terms of the charged and neutral modes it must be invariant under $i\partial\varphi^{(1)} \to -i\partial\varphi^{(1)}$, $i\partial\varphi^{(2)} \to i\partial\varphi^{(2)}$.

2.C Fitting Procedure and Fitted Parameters

Given some numerically calculated spectrum, $\xi_{RSES}^{(i)}$ we fit any given model spectrum, $\xi_{\text{Model}}^{(i)}$, by minimising,

$$R = \sum_i \frac{(\Delta\xi^{(i)}_{RSES} - \Delta\xi^{(i)}_{\text{Model}})^2}{2\sigma_i^2} e^{-\frac{(N_A^{(i)} - N/2)^2}{8}} \tag{2.23}$$

where $\Delta\xi$ is the entanglement pseudo-energy relative to the lowest level of the lowest angular momentum sector for the given N_A sector, and σ_i are the entanglement level errors. The factor $e^{-\frac{(N_A^{(i)} - N/2)^2}{8}}$ is used to control how much the N_A sectors away from $N/2$ are included in the fitting procedure. The choice of 8 in the denominator in the exponent sets the variance of this Gaussian weight to be 2, so that only the $|\Delta N_A| \leq 2$ contribute significantly to R. Errors in the model parameters can be estimated by treating this as a log-likelihood function.

For the specific case shown in Fig. 2.1 full estimates of the errors of the numerical levels, σ_i, have been made. The fitted values can be seen in Tables 2.1. The parameters in Fig. 2.2 have been fitted using numerical data where σ_i has been crudely estimated to be $\sigma \sim 0.1$ for *all* cases.

Chapter 3

CFT Approach to Parton Wave Functions

It is expected that the effective field theory, at extremely low energies and long wavelengths, of many FQHE states is given by some form of Chern-Simons gauge theory [12, 13, 52, 113–116]. These Chern-Simons gauge theories can only be well-defined on manifolds with boundaries by the introduction of extra degrees of freedom at the boundary which are described by a two-dimensional CFT [43, 91]. Thus, one would then expect the edge degrees of freedom of a given FQH state to be also described by the corresponding CFT. Furthermore, in second quantisation, the ground state wave function of a given system can be written as $\langle 0| \, c(z_1)c(z_2)\ldots|G\rangle$ where $|G\rangle$ is the ground state and $c(z)$ is the electron annihilation operator, which can be interpreted as a correlation function of a 3d euclidean field theory which has the action of the FQH system for imaginary time $\tau < 0$ and is the free field action for $\tau > 0$. At "long-wavelengths" this field theory is the Chern-Simons field theory for $\tau < 0$ and so we expect the "long-wavelength" properties of the ground state wave function to be described by the edge CFT, in some sense. A natural choice, then, for a ground-state trial wave function that is likely to be in a phase of matter described by a given Chern-Simons theory would then be the wave function generated by the corresponding CFT.

Indeed, this is one of the motivating ideas in Moore and Read's pioneering work

where the idea to generate new trial wave functions with CFT was first proposed, which allowed for the construction of ground, quasi-particle and edge [46] state trial wave functions, and, importantly, allows one to simply "read-off" the topological order of a given wave function provided the MR conjecture holds. This conjuncture was later superseded by the *generalised screening hypothesis*, where, if this holds, the adiabatic braiding of quasi-particles is given by the monodromy of the given conformal block wave function, as argued by Read [47], and there exists an isometric isomorphism[1] between the CFT states to the space of edge-state wave functions in the thermodynamic limit, as argued by Dubail, Read and Rezayi (DRR) [35]. This isometric isomorphism, roughly speaking, means the edge degrees of freedom, as given by the trial wave functions, could indeed be described by the same CFT used to generate the trial wave functions. Furthermore, this map from CFT states to edge states allows one to directly model the edge state dynamics at finite system size with the CFT [105] so long as there exists a so-called "special parent Hamiltonian" for the given space of edge states.

As well as giving theoretical predictions of a trial wave function's topological properties, these CFT constructions allow for the analytic computation of arbitrarily precise matrix product state (MPS) representations of the corresponding wave functions [117–119]. These MPS representations can be used for efficient computation of various observables and importantly allows for the possibility of numerically testing the implications of generalised screening [120].

In this chapter, we will demonstrate how these CFT constructions can be extended to the projected and unprojected chiral Parton wave functions in the planar geometry. More specifically, it is demonstrated that all ground and edge state chiral Parton trial wave functions can be generated by unitary CFTs where to each wave function we can associate a chiral algebra $\mathcal{A}$ such that $\mathrm{CFT}_{\mathcal{A}}$ is the "smallest" CFT that can generate the ground and edge state trial wave functions of the corresponding Parton state. It is then

[1] An isometric isomorphism is a linear map between two Hilbert spaces that preserves the inner product.

shown that the symmetric Parton states, that is an integer quantum Hall states raised to an integer power, can be generated using the $\hat{\mathfrak{u}}(1) \oplus \widehat{\mathfrak{su}}(n)_m$ WZW models, which one would expect based on Wen's mean-field arguments [92]. A generalised screening hypothesis for these states is formulated, and we then discuss how one can use RG arguments to motivate an extension of DRR's results to describe the edge states and the RSES of the ground state. We then numerically test these extensions of DRR's results for the edge state trial wave function inner products in the cases of the $\nu = 2/5$ CF wave functions and the ϕ_2^2 Parton wave function.

In Sec. 3.1 we review how these CFT constructions have been applied previously. Then in Sec. 3.2 we show how IQH ground and edge state wave functions can be generated using CFT. These IQH constructions then allow us in Sec. 3.3 to show how all chiral Parton ground and edge state trial wave functions can be generated by CFT, and give examples of the CF wave functions and symmetric Parton states. Next, in Sec. 3.4 we formulate the generalised screening hypothesis for these wave functions and discuss the implications for edge state inner products and the RSES. Finally, in Sec. 3.5 we present the numerical tests.

Throughout this chapter, we will only work on the planar geometry where we will not include the Gaussian factors of the wave functions and we will denote the ket of a wave function as $|\Psi\rangle\rangle$. These Gaussian factors are moved into the integration measure such that inner products take the form,

$$\langle\langle \Psi_2 | \Psi_1 \rangle\rangle = \frac{1}{N!} \int \prod_{i=1}^{N} D^2 z_i \overline{\Psi_2(\mathbf{z})} \Psi_1(\mathbf{z}) \tag{3.1}$$

where $D^2 z = d^2 z \exp(-|z|^2/2)$. Note that we will work in units where $l_B = 1$.

3.1 CFT approach to FQHE trial wave functions: a review

As given in previous works, [14, 34, 47, 104, 105, 121], many FQH trial wave functions can be expressed as a CFT correlation function of an operator $\Omega(z)$. In each case, the CFT in question is that defined by the chiral algebra $\mathcal{A}$ generated by OPEs of $\Omega(z)$ and its conjugate $\Omega^\dagger(z)$. We write this CFT as $\mathrm{CFT}_\mathcal{A}$. Each $\mathrm{CFT}_\mathcal{A}$ can be *represented* by fields in $\mathrm{CFT}_{U(1)} \otimes \mathrm{CFT}_\chi$, where $\mathrm{CFT}_{U(1)}$ is a chiral boson CFT and CFT_χ is a CFT referred to as the statistics sector. With this representation $\Omega(z)$ can be expressed as,

$$\Omega(z) =: e^{i\varphi(z)/\sqrt{\nu}} : \chi(z) \tag{3.2}$$

where $\varphi(z)$ is the chiral boson field, $: * :$ denotes normal ordering, $\chi(z)$ is a primary field of CFT_χ, and ν is the filling fraction of the wave function that will be generated. It should be noted that $\mathrm{CFT}_\mathcal{A}$ is not formally equivalent to $\mathrm{CFT}_{U(1)} \otimes \mathrm{CFT}_\chi$. However, $\mathrm{CFT}_\mathcal{A}$ can be conformally embedded in $\mathrm{CFT}_{U(1)} \otimes \mathrm{CFT}_\chi$.

We will now summarise how, given such a CFT, the ground and edge state ansätz can be generated. The generalised screening hypothesis is then detailed along with how the topological properties of the trial wave function can be extracted from the properties of the CFT if this holds. Constructions involving explicit anti-symmetrisation or symmetrisation of correlation functions will not be discussed here.

3.1.1 CFT construction of ground and edge state ansätze

Starting from the $\Omega(z)$ definition in Eq. 3.2, we can write the ground state wave function of N particles as,

$$\Psi_{\langle 0|}(\mathbf{z}) = \langle 0| C(N) \prod_{i=1}^{N} \Omega(z_i) |0\rangle \tag{3.3}$$

where $C(N)$ is a unitary operator known as the *background charge* which has a $U(1)$

charge $-\frac{N}{\sqrt{\nu}}$ and is used to ensure the correlation function is non-zero. In $\mathrm{CFT}_{\mathcal{A}}$ it can be defined by $C^\dagger(N)\Omega(z)C(N) = z^{-\frac{N}{\nu}}\Omega(z)$ and $\langle 0|\, C(N) = \lim_{z\to\infty} z^{-\frac{N^2}{\nu}} \langle 0|\, e^{-i\frac{N}{\sqrt{\nu}}\varphi(z)}$, where $C^\dagger(N)\,|0\rangle$ can also be expressed as modes of $\Omega(z)$ and $\Omega^\dagger(z)$ applied on $|0\rangle$[2]. Note that this correlation function can be computed entirely in the Hilbert space of the vacuum representation of $\mathcal{A}$, $\mathcal{H}_0$.

Following Refs. [35, 46], we can generate trial edge states from an *edge state mapping* that maps a CFT state $\langle v| \in \mathcal{H}_0^*$ to a many-body wave function $|\Psi_{\langle v|}\rangle\rangle$, which is defined in second-quantisation by,

$$|\Psi_{\langle v|}\rangle\rangle \equiv \langle v|\, C(N) e^{\int d^2z e^{-\frac{|z|^2}{4}} \Omega(z)\otimes c^\dagger(z)}\, |0\rangle \otimes |0\rangle\rangle \tag{3.4}$$

By $U(1)$ charge conservation, when $|v\rangle$ has a definite $U(1)$ charge, q, only one term in the expansion of this exponential contributes, with the resulting many-body state having exactly $N + \sqrt{\nu}q$ particles and a wave function given by,

$$\Psi_{\langle v|}(\mathbf{z}) = \langle v|\, C(N) \prod_{i=1}^{N+q\sqrt{\nu}} \Omega(z_i)\, |0\rangle \tag{3.5}$$

As an extra aside, one can also generate trial wave functions for quasi-particle states, roughly speaking, by inserting primary fields, $\phi(w)$, of $\mathcal{A}$ at the positions of the quasi-particles. More formally, this is done by inserting the chiral vertex operators (see Ref. [40–42] for a definition of chiral vertex operators) of $\mathcal{A}$ into the generating correlation function.

3.1.2 The generalised screening hypothesis

In Laughlin's plasma analogy, one maps the inner products of wave functions to expectation values of observables of a one-component plasma. A field-theoretic generalization of this involves mapping wave function inner products to correlation functions of a field

[2]For the Laughlin wave functions this construction works for any N. For Moore-Read states this is defined by N even and for the $\mathbb{Z}_k$ Read-Rezayi states this is defined if N is divisible by k.

theory that is a "perturbation" of $\mathrm{CFT}_{\mathcal{A}}$. In order to express inner products in terms of just the CFT we first need to be able to generate the complex conjugate of these wave functions. To this end, we denote the anti-chiral copy of $\Omega(z)$ as $\overline{\Omega}(\bar{z})$. Complex conjugate wave functions can then be expressed with correlation functions within $\overline{\mathcal{H}}_0$, which is the anti-chiral copy of the vacuum representation of $\mathcal{A}$.

The squared norm of the ground state trial wave function can then be expressed as,

$$\begin{aligned} Z_N \equiv & \langle\langle \Psi_{\langle 0|}|\Psi_{\langle 0|}\rangle\rangle = \frac{1}{N!}\int D^2\mathbf{z}|\Psi_{\langle 0|}(\mathbf{z})|^2 \\ = & \frac{1}{N!}\int D^2\mathbf{z}\,\langle \overline{C}(N)\prod_{i=1}^{N}\overline{\Omega}(\bar{z}_i)C(N)\prod_{i=1}^{N}\Omega(z_i)\rangle = \langle \overline{C}(N)C(N)e^{(-1)^{2h}\int D^2z\overline{\Omega}(\bar{z})\Omega(z)}\rangle \end{aligned} \tag{3.6}$$

where h is the scaling dimension of Ω and the $(-1)^{2h}$ factor is included to account for the minus signs picked up in rearranging the operators (this only matters when $\Omega(z)$ has half-integral spin). By $U(1)$ charge conservation, the background charges ensure that only one term contributes from the exponential. We have thus expressed the ground state norm as the partition function of a "perturbed" CFT[3]. As $\langle v|$ can be expressed as modes of local fields acting on $\langle 0|$, edge-state inner products can be mapped to correlation functions of this field theory. We will denote correlation functions of this field theory by $\langle \phi_1(w_1,\bar{w}_2)\phi_1(w_2,\bar{w}_2)\ldots\rangle_* \equiv \langle \overline{C}(N)C(N)\mathcal{R}\phi_1(w_1,\bar{w}_2)\phi_1(w_2,\bar{w}_2)\ldots e^{(-1)^{2h}\int D^2z\overline{\Omega}(\bar{z})\Omega(z)}\rangle/Z_N$, where $\mathcal{R}$ indicates radial ordering. Note that correlation functions involving ϕ with singular OPEs with Ω require some form of regularisation. This will be of no conceptual concern here.

For a large N, the configurations of the $\overline{\Omega}(\bar{z})\Omega(z)$ insertions that are the dominant configurations to the partition function will have a particular density $\rho(z,\bar{z})$ on long length scales, with this $\rho(z,\bar{z})$ being the actual density of particles in the ground state $|\Psi_{\langle 0|}\rangle\rangle$. As pointed out in Ref. [35], $\rho(z,\bar{z})$ can be computed from a saddle-point

[3]We use "perturbed" very loosely here as there is no notion of the term added to the action being small.

approximation, with the density being entirely determined by the $U(1)$ sector. The resulting density profile is that of a droplet of radius $R = l_B\sqrt{\frac{2N}{\nu}}$ with a uniform density of $\frac{\nu}{2\pi l_B^2}$ inside the droplet.

The *generalised screening hypothesis* is that under renormalization group transformations (RG), the field theory flows to a massive infra-red fixed point inside the droplet and flows back to $\mathrm{CFT}_{\mathcal{A}}$ outside the droplet. Flow towards a massive infra-red fixed point, inside the droplet, implies that connected correlation functions decay exponentially (i.e. short-range correlations).

Of course, the obvious question at this point is for which wave functions does generalised screening actually occur. Ultimately, this must be tested numerically, either by directly testing for some form of screening [122–124] or indirectly by testing its implications [35, 45, 105, 120]. In the case of Laughlin's wave functions, generalised screening is equivalent to the screening phase of the plasma analogy which occurs for $\nu \gtrsim \frac{1}{71}$. For other wave functions that can be constructed by a CFT, this question is less well explored. It is argued by Read [47] that if generalised screening does not occur then the ground state trial wave function cannot represent a gapped phase of matter. In brief, if generalised screening does not occur then there are local operators of the perturbed field theory which are long-range correlated in the quantum Hall droplet. These then map to long-range correlations in the actual ground state trial wave function, which is inconsistent with the ground state wave function being gapped.

Let us now discuss in what sense *screening* is occurring. Consider now some disk D inside the droplet, which is far away from the droplet edge. Within $\mathrm{CFT}_{\mathcal{A}}$ we have the OPE, $i\partial\varphi(z)\Omega(w) \sim \sqrt{\nu}^{-1}\Omega(w)/(z-w)$. We must then have,

$$\begin{aligned}\frac{\sqrt{\nu}}{2} \times \left\langle \oint_{\partial D} \frac{dz}{2\pi i} i\partial\varphi(z) + \oint_{\partial D} \frac{d\bar{z}}{2\pi i} i\overline{\partial}\overline{\varphi}(\bar{z}) \right\rangle_* &= (\text{Average number of particles in } D) \\ &= \frac{\nu A_D}{2\pi l_B^2}\end{aligned} \tag{3.7}$$

where A_D and ∂D is the area and boundary of D respectively. Let $\langle \phi(w)\bar{\phi}(\bar{w})\ldots\rangle_*$ be a correlation involving the fields $\phi(w)\bar{\phi}(\bar{w})$ and some other fields, where $w \in D$ and all the other field insertions are far away from D. Just as for the partition function, the dominant contributions to this correlation function will be from $\overline{\Omega}(\bar{z})\Omega(z)$ insertions with a particular density profile, where the number of these insertions in D given by this density profile will be denoted by N_D. Let the $U(1)$ charge of $\phi(w)$ be written as $Q_{U(1)}$. We then have,

$$\begin{aligned}&\frac{\sqrt{\nu}}{2}\left\langle \left(\oint_{\partial D} \frac{dz}{2\pi i} i\partial\varphi(z) + \oint_{\partial D} \frac{d\bar{z}}{2\pi i} i\overline{\partial}\overline{\varphi}(\bar{z}) \right) \phi(w)\bar{\phi}(\bar{w})\ldots \right\rangle_* \\ &= (\sqrt{\nu}Q_{U(1)} + N_D)\left\langle \phi(w)\bar{\phi}(\bar{w})\ldots\right\rangle_*\end{aligned} \tag{3.8}$$

Provided w is far away from ∂D short-range correlation within the droplet implies,

$$\begin{aligned}&\frac{\sqrt{\nu}}{2}\left\langle \left(\oint_{\partial D} \frac{dz}{2\pi i} i\partial\varphi(z) + \oint_{\partial D} \frac{d\bar{z}}{2\pi i} i\overline{\partial}\overline{\varphi}(\bar{z}) \right) \phi(w)\bar{\phi}(\bar{w})\ldots \right\rangle_* \\ &= \frac{\sqrt{\nu}}{2}\left\langle \oint_{\partial D} \frac{dz}{2\pi i} i\partial\varphi(z) + \oint_{\partial D} \frac{d\bar{z}}{2\pi i} i\overline{\partial}\overline{\varphi}(\bar{z}) \right\rangle_* \left\langle \phi(w)\bar{\phi}(\bar{w})\ldots\right\rangle_* \\ &= \frac{\nu A_D}{2\pi l_B^2}\left\langle \phi(w)\bar{\phi}(\bar{w})\ldots\right\rangle_*\end{aligned} \tag{3.9}$$

Equating Eq. 3.8 with Eq. 3.9 we find,

$$N_D = \frac{\nu A_D}{2\pi l_B^2} - \sqrt{\nu}Q_{U(1)} \tag{3.10}$$

In words, there are on average $\sqrt{\nu}Q_{U(1)}$ fewer $\overline{\Omega}(\bar{z})\Omega(z)$ in the vicinity of w when $\phi(w)\bar{\phi}(\bar{w})$ has been inserted into the correlation function. Thus, the $\overline{\Omega}(\bar{z})\Omega(z)$ insertions behave analogously to a screened plasma, where field insertions such as $\phi(w)\overline{\phi}(\bar{w})$ can be thought of as fixed charges.

In the case where the correlation function $\langle \phi(w)\bar{\phi}(\bar{w})\ldots\rangle_*$ corresponds to the norm squared of a quasi-particle wave function, the density of the configurations of $\overline{\Omega}(\bar{z})\Omega(z)$ insertions will be equal to the particle density in the quasi-particle wave function.

Therefore, the physical charge of the quasi-particle generated by $\phi(w)$ is simply given by $-\sqrt{\nu}Q_{U(1)}$.

3.1.3 Implications of generalised screening

In Ref. [35], by slightly modifying the edge state mapping of Eq. 3.4 by $\Omega(z) \rightarrow \sqrt{\lambda_N}\Omega(z)$, where λ_N is an adjustable parameter, it was shown that the generalised screening hypothesis implies that the edge-state inner products could be expressed as,

$$\langle\langle \Psi_{\langle w|} | \Psi_{\langle v|} \rangle\rangle / Z_N = \langle v| \, R^{2L_0} e^S \, |w\rangle \tag{3.11}$$

where L_0 is the zeroth Virasoro mode, and S is an operator referred to as the inner product action that takes the form,

$$S = \sum_j \frac{\alpha_j}{\sqrt{N}^{h_j-1}} \oint_{|z|=1} \frac{dz}{2\pi i} z^{h_j-1} \phi_j(z) \tag{3.12}$$

where α_j are constants and the $\phi_j(z)$ fields belonging to $\mathcal{A}$ with corresponding scaling dimension h_j such that $h_j > 1$. The λ_N parameter is used to cancel the $h_j = 1$ term (corresponding to the a_0 mode of $\varphi(z)$). As $N \rightarrow \infty$, $S \rightarrow 0$. In other words, the edge state map becomes an isometric isomorphism in the thermodynamic limit. Furthermore, as each term scales as $\sqrt{N}^{-(h_j-1)}$, for large but finite N the inner products can be accurately modelled using only a small number of low scaling dimension terms [104]. We will show how this can be generalised in Sec. 3.4. From this result, DRR could then show the RSES has the scaling property discussed in Chap. 2.

It was argued by Read [47] that generalised screening implied that the transformation of a quasihole wave function after adiabatic braiding of the quasiholes was given by the monodromy of the wave function along the braid, up to the usual area dependant magnetic Berry phase factor. This argument only relies on the assumption of generalised screening and the fact that the quasihole trial wave function is *holomorphic* in the quasihole coordinates. Thus, if generalised screening holds the anyonic charges

or superselection sectors [125] of the quasiholes that can be generated by this CFT construction are in the one-to-one correspondence with the irreducible representations of $\mathcal{A}$.

3.1.4 Example: Laughlin's wave functions

To generate Laughlin's wave function for filling factor $\nu = \frac{1}{p}$ one can use the CFT of a single chiral boson field $\phi(z)$ with the mode expansion,

$$\phi(z) = -ia_0^{(\phi)} \ln z + i \sum_{n \neq 0} a_n^{(\phi)} \frac{z^{-n}}{n} \tag{3.13}$$

along with the unitary Klein factor operator F_ϕ, where these operators have the commutation relations,

$$[a_n^{(\phi)}, a_m^{(\phi)}] = n\delta_{n+m,0} \qquad [a_n^{(\phi)}, F_\phi] = \sqrt{p}\delta_{n,0} F_\phi \tag{3.14}$$

We have that $(a_n^{(\phi)})^\dagger = a_{-n}^{(\phi)}$. The vacuum state $|0\rangle$ is the unique state defined by $a_n^{(\phi)}|0\rangle = 0$ for $n \geq 0$ and $\langle 0|0\rangle = 1$. The Hilbert space of this theory, $\mathcal{H}_0$, is generated by applying polynomials in $a_n^{(\phi)}$, F_ϕ and $F_\phi^\dagger$ on $|0\rangle$. Finally, the energy-momentum tensor of this CFT is given by $T(z) = -\frac{:(\partial\phi(z))^2:}{2}$ where $: * :$ denotes normal ordering.

Let $V_\phi(z)$ and $V_\phi^\dagger(z)$ be the vertex operators defined by,

$$V_\phi(z) \equiv F_\phi : e^{i\sqrt{p}\phi(z)} : \qquad V_\phi^\dagger(z) \equiv F_\phi^\dagger : e^{-i\sqrt{p}\phi(z)} : \tag{3.15}$$

It can be checked that both these operators have conformal dimension $h = \frac{p}{2}$. Strictly speaking, products of vertex operators such as $V_\phi(z)V_\phi(w)$ are only well-defined for $|z| > |w|$. One can, however, define their products when $|z| < |w|$ by analytic continuation. For $|z| > |w|$ one can show[4] $V_\phi(z)V_\phi(w) = (z-w)^p F_\phi^2 : e^{i\sqrt{p}(\phi(z)+\phi(w))} :$.

[4]By using $e^A e^B = e^B e^A e^{[A,B]}$, if $[A,B]$ commutes with A and B, then we have $e^{-\sqrt{p}a_n^{(\phi)} z^{-n}/n} e^{\sqrt{p}a_{-n}^{(\phi)} w^n/n} = e^{\sqrt{p}a_{-n}^{(\phi)} w^n/n} e^{-\sqrt{p}a_n^{(\phi)} z^{-n}/n} e^{p(w/z)^n/n}$. Further using $e^{\sqrt{p}a_0^{(\phi)} \ln z} F = z^p F e^{\sqrt{p}a_0^{(\phi)} \ln z}$, which gives $V_\phi(z)V_\phi(w) = e^{p\ln z + p\sum_{n>0}(w/z)^n/n} F_\phi^2 : e^{i\sqrt{p}(\phi(z)+\phi(w))} := e^{p\ln z + p\ln(1-w/z)} F_\phi^2 : e^{i\sqrt{p}(\phi(z)+\phi(w))} := (z-w)^p F_\phi^2 : e^{i\sqrt{p}(\phi(z)+\phi(w))} :$

By analytically continuing the expression of the right-hand side we have $V_\phi(z)V_\phi(w) = (-1)^p V_\phi(w)V_\phi(z)$. Using the same method we also have $V_\phi(z)V_\phi^\dagger(w) = (-1)^p V_\phi^\dagger(w)V_\phi(z)$ as well as the OPE,

$$V_\phi(z)V_\phi^\dagger(w) = \frac{1}{(z-w)^p} + \frac{\sqrt{p}i\partial\phi(w)}{(z-w)^{p-1}} + \dots \tag{3.16}$$

Let $\mathcal{A}_p$ be the chiral algebra generated by repeated OPEs of the $V_\phi(z)$ and $V_\phi^\dagger(z)$ fields. Note that in the case that p is odd $\mathcal{A}_p$ is a chiral superalgebra with the $V_\phi(z)$ field being fermionic. From the OPE of Eq. 3.16 it follows that the $a_n^{(\phi)}$ can be expressed in terms of the $V_{\phi,k}$ and $V_{\phi,k}^\dagger$ modes. Furthermore, $V_{\phi,-p/2}\left|0\right\rangle = F_\phi\left|0\right\rangle$, $V_{\phi,-p/2}^\dagger\left|0\right\rangle = F_\phi^\dagger\left|0\right\rangle$ and $F_\phi^\dagger V_{\phi,k}F_\phi = V_{\phi,k+p}$, which implies the states $F_\phi^n\left|0\right\rangle$ can be generated by applying the $V_{\phi,k}$ and $V_{\phi,k}^\dagger$ modes on $\left|0\right\rangle$. Hence, all states of $\mathcal{H}_0$ can be generated by repeated application of the modes $V_{\phi,k}$ and $V_{\phi,k}^\dagger$ on $\left|0\right\rangle$. Thus, $\mathcal{H}_0$ forms the vacuum representation of $\mathcal{A}_p$.

Using $V_\phi(z)F_\phi^n : e^{i\sqrt{p}\sum_{j=1}^n \phi(w_j)} := \prod_{j=1}^n (z-w_j)^p : e^{i\sqrt{p}(\phi(z)+\sum_{j=1}^n \phi(w_j))} :$, one can show that,

$$\Psi_{\langle 0|}(\mathbf{z}) \equiv \langle 0|\, F_\phi^{-N} \prod_{i=1}^N V_\phi(z_i)\left|0\right\rangle = \prod_{i<j}^N (z_i - z_j)^p \tag{3.17}$$

We have thus generated the $\nu = \frac{1}{p}$ Laughlin wave function using $\Omega(z) = V_\phi(z)$ and $C(N) = F_\phi^{-N}$.

Now let us consider the edge state map. Using $[a_n^{(\phi)}, V_\phi(z)] = \sqrt{p}z^n V_\phi(z)$ and $a_n\left|0\right\rangle = 0$ for $n \geq 0$, we then have for $n > 0$,

$$\Psi_{\langle v|a_n^{(\phi)}}(\mathbf{z}) = \langle v|\, a_n^{(\phi)} F_\phi^{-N} \prod_{i=1}^N V_\phi(z_i)\left|0\right\rangle = \sqrt{p}P_n(\mathbf{z})\Psi_{\langle v|}(\mathbf{z}) \tag{3.18}$$

where $P_n(\mathbf{z}) = \sum_{i=1}^N z_i^n$. This then implies that the image of the edge state map is in fact equivalent to the null space of the $\nu = \frac{1}{p}$ parent Hamiltonian, H_m [104].

3.2 IQH wave functions as CFT correlation functions

We now turn to the seemingly esoteric task of using CFT to express the ground-state and edge excitation wave functions for IQH states. This will be the fundamental building block for constructing Parton-type wave functions.

3.2.1 $\nu = 1$

This is the $p = 1$ case of the Laughlin wave functions discussed in Sec. 1.2.1. To distinguish this case, however, we will denote the chiral boson field as $\varphi(z)$, the Klein factor by F, the modes by a_n and the vertex operators by $V(z)$ and $V^\dagger(z)$. $V(z)$ and $V^\dagger(z)$ both have conformal dimension $\frac{1}{2}$, and Eq. 3.16 implies the modes V_k and $V_k^\dagger$ with $k \in \mathbb{Z}+\frac{1}{2}$ have the *anti-commutation* relations $\{V_k, V_l^\dagger\} = \delta_{k+l,0}$. Furthermore, the OPEs $V(z)V(w)$ and $V^\dagger(z)V^\dagger(w)$ are non-singular which implies $\{V_k, V_l\} = \{V_k^\dagger, V_l^\dagger\} = 0$. Thus, the vertex operators are in fact free complex fermion fields, which is just one way of expressing the usual bosonisation relations [126].

The ground state wave function is given by,

$$\Psi_{\langle 0|}(\mathbf{z}) = \langle 0| F^{-N} \prod_{i=1}^{N} V(z_i) |0\rangle = \det[z_1^{N-1}, z_2^{N-2}, \ldots, z_N^0] \tag{3.19}$$

We note that the image of the edge state map must be the null space of the parent Hamiltonian H_1. However, for fermions, the null space of H_1 is trivially just the space of states with all the particles in the LLL.

Given this, we must have that for any Slater determinant state there exists a CFT state $\langle v|$ that will generate it. Let $\langle v|$ be a state that generates the Slater determinant $\Psi_{\langle v|}(\mathbf{z}) = \det[z_1^{m_1}, z_2^{m_2}, \ldots, z_N^{m_N}]$. Now we consider the state generated by $\langle v| V_k$. First, we note that this state will generate a wave function with $N-1$ particles (as the correlation function must be $U(1)$ charge neutral). We then have that,

$$\begin{aligned}\Psi_{\langle v|V_k}(\mathbf{z}) &= \langle v|\, V_k F^{-N} \prod_{i=2}^{N} V(z_i)\,|0\rangle = \langle v|\, F^{-N} V_{k-N} \prod_{i=1}^{N-1} V(z_i)\,|0\rangle \\ &= \oint \frac{dz_1}{2\pi i} z_1^{-(N-k-1/2)-1} \Psi_{\langle v|}(\mathbf{z})\end{aligned} \tag{3.20}$$

where we should recall that $\Psi_{\langle v|}(\mathbf{z})$ is an N particle wave function. If $(N-k-1/2) \in \{m_1, m_2, \ldots, m_N\}$ with $m_j = N-k-1/2$, then we have (by expanding the Slater determinant along the first column),

$$\Psi_{\langle v|V_k}(\mathbf{z}) = (-1)^{j-1} \det[z_2^{m_1}, \ldots, z_j^{m_{j-1}}, z_{j+1}^{m_{j+1}}, \ldots, z_N^{m_N}] \tag{3.21}$$

Otherwise, if $(N-k-1/2) \notin \{m_1, m_2, \ldots, m_N\}$ then we have $\Psi_{\langle v|V_k}(\mathbf{z}) = 0$.

Now consider the state $\Psi_{\langle v|V_k^\dagger}(\mathbf{z})$ with $N+k>0$. By $U(1)$ charge conservation this is an $N+1$ particle wave function. From the anti-commutation relation $\{V_k^\dagger, V(z)\} = z^{k-1/2}$ and $V_k^\dagger\,|0\rangle = 0$ for $k>0$ we have that,

$$\begin{aligned}&\Psi_{\langle v|V_k^\dagger}(\mathbf{z}) = \langle v|\, V_k^\dagger F^{-N} \prod_{i=1}^{N+1} V(z_i)\,|0\rangle = \langle v|\, F^{-N} V_{k+N}^\dagger \prod_{i=1}^{N+1} V(z_i)\,|0\rangle \\ &= \sum_{j=1}^{N+1} (-1)^{j-1} z_j^{N+k-1/2} \langle v|\, F^{-N} \prod_{i\neq j}^{N} V(z_i)\,|0\rangle = \det[z_1^{N+k-1/2}, z_2^{m_1}, \ldots, z_{N+1}^{m_N}]\end{aligned} \tag{3.22}$$

As $\Psi_{\langle 0|}(\mathbf{z})$ is a Slater determinant, we can then see, inductively, that all Slater determinant states are generated by CFT states of the form $\langle 0|\prod_i V_{k_i}^\dagger \prod_j V_{l_j}$ with $k_i, l_j > 0$.

This mapping is best summarised in the second quantised notation. Firstly, we note that $|\Psi_{\langle 0|}\rangle\rangle/\sqrt{Z_N} = c_{N-1}^\dagger c_{N-2}^\dagger \ldots c_1^\dagger c_0^\dagger\,|0\rangle\rangle$. Then, for $N-k-1/2>0$ we have,

$$|\Psi_{\langle v|V_k}\rangle\rangle = \sqrt{\mathcal{N}(N-k-1/2)}^{-1} c_{N-k-1/2}\,|\Psi_{\langle v|}\rangle\rangle \tag{3.23}$$

and for $N+k-1/2>0$ we have,

$$|\Psi_{\langle v|V_k^\dagger}\rangle\rangle = \sqrt{\mathcal{N}(N+k-1/2)} c_{N+k-1/2}^\dagger\,|\Psi_{\langle v|}\rangle\rangle \tag{3.24}$$

where $\mathcal{N}(m) = \int D^2 z |z^m|^2 = 2\pi 2^m m!$. One can then interpret this edge state mapping as a finite system size non-unitary bosonization. We call this non-unitary as the edge state map does not preserve the inner product.

This simple mapping from $V_k^\dagger$ and V_k to $c_m^\dagger$ and c_m allows us to express edge state inner-products in the CFT as $\langle\langle \Psi_{\langle w|} | \Psi_{\langle v|} \rangle\rangle / Z_N = \langle v| \, e^{\mathcal{S}} \, |w\rangle$, where,

$$\begin{aligned} \mathcal{S} &= \sum_{k>0} \ln[\mathcal{N}(N+k-1/2)] V_{-k} V_k^\dagger - \sum_{0<k\leq N-1/2} \ln[\mathcal{N}(N-k-1/2)] V_{-k}^\dagger V_k \\ &= \sum_{k=-N+1/2}^{\infty} \ln[\mathcal{N}(N+k-1/2)] : V_{-k} V_k^\dagger : \end{aligned} \tag{3.25}$$

For large N and $|(k-1/2)/N| \ll 1$ we can use the Stirling series to expand $\ln[\mathcal{N}(N+k-1/2)] \approx N\ln N - N + (1/2)\ln N + (3/2)\ln(2\pi) + 1/(12N) + (k-1/2)\ln 2N + [(k-1/2)^2 + (k-1/2)]/(2N)$. Then we note the following[5], $\sum_k (k-1/2) : V_{-k} V_k^\dagger := \oint \frac{dz}{2\pi i} z : (\partial V(z)) V^\dagger(z) := \oint \frac{dz}{2\pi i} z [i\partial^2\varphi(z) + : (i\partial\varphi(z))^2 :]/2 = -a_0/2 + L_0$, and $\sum_k (k-1/2)^2 : V_{-k} V_k^\dagger := \oint \frac{dz}{2\pi i} z^2 [: (\partial^2 V(z)) V^\dagger(z) : + z^{-1} : (\partial V(z)) V^\dagger(z) :] = \oint \frac{dz}{2\pi i} z^2 [: (i\varphi(z))^3 : + (3/2)\partial : (i\partial\varphi(z))^2 : + i\partial^3\varphi(z)]/3 + L_0 - a_0/2 = \oint \frac{dz}{2\pi i} z^2 : (i\varphi(z))^3 : /3 - L_0 + (1/6)a_0$. We can then write the inner products in the following form

$$\langle\langle \Psi_{\langle w|} | \Psi_{\langle v|} \rangle\rangle / Z_N = \langle v| \, R^{2L_0} e^S \, |w\rangle \tag{3.26}$$

where $R = \sqrt{2N}$ (i.e. the radius of the droplet) and,

$$S = (N\ln N - N + \ln[2\pi\sqrt{\pi}] - 1/(12N)) a_0 + \frac{1}{6N} \oint \frac{dz}{2\pi i} z^2 : (i\partial\varphi(z))^3 : \tag{3.27}$$

We can remove the a_0 term by replacing $V(z) \to \sqrt{\lambda_N} V(z)$ in the generating correlation function, with $\ln \lambda_N = -(N\ln N - N + \ln[2\pi\sqrt{\pi}] - 1/(12N))$.

Finally, it is instructive to see how the angular momentum operator can be mapped

[5] To derive these one can use $V(z) = \sum_k z^{-k-\frac{1}{2}} V_k$, $V^\dagger(z) = \sum_k z^{-k-\frac{1}{2}} V_k^\dagger$ and $V(z)V^\dagger(w) - 1/(z-w) = \sum_{n=1}^\infty (n!)^{-1} (z-w)^{n-1} : e^{-i\varphi(w)} \partial^n e^{i\varphi(w)} :$. Note that $V(z)V^\dagger(w) - 1/(z-w)$ is the fermionic normal ordering of $V(z)V^\dagger(w)$.

to the CFT. Given that $L_0 |0\rangle = 0$ and $[L_0, V(z)] = V(z)/2 + z\partial V(z)$, then,

$$\begin{aligned}
\sum_{i=1}^{N} z_i \partial_i \Psi_{\langle v|}(\mathbf{z}) &= \langle v| F^{-N} (L_0 - a_0/2) \prod_{i=1}^{N} V(z_i) |0\rangle \\
&= \langle v| (L_0 + (2N-1)a_0/2 + N(N-1)/2) F^{-N} \prod_{i=1}^{N} V(z_i) |0\rangle \\
&= \Psi_{\langle v|(L_0+(2N-1)a_0/2+N(N-1)/2)}(\mathbf{z})
\end{aligned} \tag{3.28}$$

Hence, we can see that the angular momentum operator maps to the CFT as $\sum_i z_i \partial_i \rightarrow L_0 + (2N-1)a_0/2 + N(N-1)/2$.

3.2.2 $\nu = 2$

For $\nu = 2$ the ground state wave function is no longer purely holomorphic (up to Gaussian factors); hence, we cannot write it purely as a chiral CFT correlation function. However, for $\nu = 2$ the highest power of any $\bar{z}$ that appears is one. We can then easily separate the anti-holomorphic dependence from the holomorphic dependence, with the latter given by some chiral CFT correlation functions.

The CFT that we will use is that of two independent copies of the chiral boson theory used to generate the $\nu = 1$ wave functions. We denote the fields by $\varphi^{(i)}(z)$ for $i = 1, 2$, the modes by $a_n^{(i)}$ and the Klein factors by F_i. All the modes of $\varphi^{(1)}(z)$ commute with those of $\varphi^{(2)}(z)$ and F_2, and vice-versa. The two Klein factors, however, anti-commute $\{F_1, F_2\} = 0$. The corresponding vertex operators are denoted by $V_j(z) \equiv F_j : e^{i\varphi^{(j)}(z)} :$ and $V_j^\dagger(z) \equiv F_j^\dagger : e^{-i\varphi^{(j)}(z)} :$, where the modes $V_{j,k}$ and $V_{j,k}^\dagger$ have the anti-commutation relations, $\{V_{i,k}, V_{j,l}\} = 0$ and $\{V_{i,k}, V_{j,l}^\dagger\} = \delta_{ij}\delta_{l+k,0}$. These vertex operators are then two independent species of complex fermions, and the full Hilbert space of the theory can be generated by applying their modes to $|0\rangle$.

To generate the ground state wave function, the $\Omega(z)$ operator will now have to have some anti-holomorphic dependence, $\Omega(z, \bar{z})$. We will consider the operator,

$$\Omega(z,\bar{z}) = V_1(z) + \bar{z}V_2(z) \tag{3.29}$$

In the following, we will only consider the case when N is odd (so that the lowest angular momentum $\nu = 2$ state is unique). Now consider the wave function,

$$\Psi_{\langle 0|}(\mathbf{z}) = \langle 0|\, F_2^{-(N+1)/2} F_1^{-(N-1)/2} \prod_{i=1}^{N} \Omega(z_i,\bar{z}_i)\, |0\rangle \tag{3.30}$$

By expanding out the $\Omega(z_i,\bar{z}_i)$, this correlation function can be expressed as a sum of correlation functions of products of $V_1(z)$ and $V_2(z)$. As the $U(1)$ charge of each boson field is separately conserved, the only terms that will contribute are those with $(N-1)/2$ V_1's and $(N+1)/2$ V_2's. Let P be a permutation of $\{1,2,\ldots,N\}$ such that $P(i) < P(j)$ if $0 < i < j \leq q$ or $q < i < j \leq N$ with q being a fixed integer $(0 < q \leq N)$. Let the set of such permutations be denoted by $\mathcal{P}_{N,q}$. Further letting $C(N) = F_2^{-N_2} F_1^{-N_1}$ and $N_1 = (N-1)/2$, $N_2 = (N+1)/2$, we can express our wave function as,

$$\begin{aligned}
\Psi_{\langle 0|}(\mathbf{z}) &= \sum_{P\in\mathcal{P}_{N,N_1}} \mathrm{sgn}(P)\, \langle 0|\, C(N) \prod_{i=1}^{N_1} V_1(z_{P(i)}) \prod_{j=N_1+1}^{N} \bar{z}_{P(j)} V_2(z_{P(j)})\, |0\rangle \\
&= \sum_{P\in\mathcal{P}_{N,N_1}} \mathrm{sgn}(P)\, \det[z_{P(1)}^{N_1-1}, z_{P(2)}^{N_1-2}, \ldots, z_{P(N_1)}^{0}] \\
&\quad \times \det[\bar{z}_{P(N_1+1)} z_{P(N_1+1)}^{N_2-1}, \bar{z}_{P(N_1+2)} z_{P(N_1+2)}^{N_2-2}, \ldots, \bar{z}_{P(N)} z_{P(N)}^{0}]
\end{aligned} \tag{3.31}$$

where $\mathrm{sgn}(P)$ appears because the $V_j(z)$ anti-commute. This can be simplified to one Slater determinant, with the resulting wave function given by,

$$\Psi_{\langle 0|}(\mathbf{z}) = \det[z_1^{N_1-1}, \ldots, z_{N_1}^{0}, \bar{z}_{N_1+1} z_{N_1+1}^{N_2-1}, \ldots, \bar{z}_N z_N^0] \tag{3.32}$$

This is the non-interacting $\nu = 2$ ground state wave function of N particles (with N odd).

The associated chiral algebra of this state is that generated by repeated OPEs of $V_j(z)$ and $V_j^\dagger(z)$. Note that now the chiral algebra is generated by four fields rather

than just $\Omega(z)$ and $\Omega^\dagger(z)$.

We will now consider the edge state mapping. Assume $\langle v|$ to be a state that generates the Slater determinant,

$$\Psi_{\langle v|}(\mathbf{z}) = \det[z_1^{m_1^{(1)}}, z_2^{m_2^{(1)}}, \ldots, z_{N_1}^{m_{N_1}^{(1)}}, \bar{z}_{N_1+1} z_{N_1+1}^{m_1^{(2)}}, \bar{z}_{N_1+2} z_{N_1+2}^{m_2^{(2)}}, \ldots, \bar{z}_N z_N^{m_{N_2}^{(2)}}] \tag{3.33}$$

By $U(1)$ charge conservation the state $\langle v| V_{2,k}$, with $N_2 - k - 1/2 = m_j^{(2)}$, must generate a $N-1$ particle wave function with,

$$\begin{aligned}
&\Psi_{\langle v|V_{2,k}}(\mathbf{z}) = \langle v| V_{2,k} C(N) \prod_{i=1}^{N-1} \Omega(z_i, \bar{z}_i) |0\rangle \\
&= \sum_{P \in \mathcal{P}_{N-1,N_1}} \mathrm{sgn}(P) \langle v| V_{2,k} C(N) \prod_{i=1}^{N_1} V_1(z_{P(i)}) \prod_{j=N_1-1}^{N-1} \bar{z}_{P(j)} V_2(z_{P(j)}) |0\rangle \\
&= (-1)^{j-1} \sum_{P \in \mathcal{P}_{N+1,N_1}} \det[z_{P(1)}^{m_1^{(1)}}, \ldots, z_{P(N_1)}^{m_{N_1}^{(1)}}] \\
&\quad \times \det[\bar{z}_{P(N_1+1)} z_{P(N_1+1)}^{m_1^{(2)}}, \ldots, \bar{z}_{P(N_1+j-1)} z_{P(N_1+j-1)}^{m_{j-1}^{(2)}}, \bar{z}_{P(N_1+j)} z_{P(N_1+j)}^{m_{j+1}^{(2)}}, \ldots, \bar{z}_{P(N-1)} z_{P(N-1)}^{m_{N_2}^{(2)}}]
\end{aligned} \tag{3.34}$$

This then simplifies to,

$$\begin{aligned}
\Psi_{\langle v|V_{2,k}}(\mathbf{z}) = &(-1)^{j-1} \det[z_1^{m_1^{(1)}}, \ldots, z_{N_1}^{m_{N_1}^{(1)}}, \\
&\bar{z}_{N_1+1} z_{N_1+1}^{m_1^{(2)}}, \ldots, \bar{z}_{N_1+j-1} z_{N_1+j-1}^{m_{j-1}^{(2)}}, \bar{z}_{N_1+j} z_{N_1+j}^{m_{j+1}^{(2)}}, \ldots, \bar{z}_{N-1} z_{N-1}^{m_{N_2}^{(2)}}]
\end{aligned} \tag{3.35}$$

Clearly, if $N_2 - k - 1/2 \notin \{m_1^{(2)}, m_2^{(2)}, \ldots, m_{N_2}^{(2)}\}$ then $\Psi_{\langle v|V_{2,k}}(\mathbf{z}) = 0$.

By the same argument, we also have,

$$\Psi_{\langle v|V_{2,k}^\dagger}(\mathbf{z}) = \det[z_1^{m_1^{(1)}}, \ldots, z_{N_1}^{m_{N_1}^{(1)}}, \bar{z}_{N_1+1} z_{N_1+1}^{N_2+k-1/2}, \bar{z}_{N_1+2} z_{N_1+2}^{m_1^{(2)}}, \ldots, \bar{z}_{N+1} z_{N+1}^{m_{N_2}^{(2)}}] \tag{3.36}$$

One can also easily find analogous expressions for $\Psi_{\langle v|V_{1,k}}(\mathbf{z})$ and $\Psi_{\langle v|V_{1,k}^\dagger}(\mathbf{z})$.

We summarise this edge state mapping in second quantised notation as,

$$|\Psi_{\langle v|V_{i,k}}\rangle\rangle = (-1)^{N-N_i}\tilde{d}_{i,N_1-k-1/2}\,|\Psi_{\langle v|}\rangle\rangle \qquad |\Psi_{\langle v|V_{i,k}^\dagger}\rangle\rangle = (-1)^{N-N_i}\tilde{c}^\dagger_{i,N_1+k-1/2}\,|\Psi_{\langle v|}\rangle\rangle \tag{3.37}$$

where $\tilde{c}^\dagger_{1,m}$ and $\tilde{c}^\dagger_{2,m}$ are the creation operators for *unnormalised* orbitals z^m and $\bar{z}z^{m+1}$ respectively[6], and $\tilde{d}^\dagger_{i,m}$ are creation operators for single particle orbitals such that $\{\tilde{d}_{i,m}, \tilde{c}^\dagger_{j,m'}\} = \delta_{ij}\delta_{mm'}$[7]. These operator mappings are strictly only valid for $N_i - k - 1/2 \geq 0$ for $V_{i,k}$ and $N_i + k - 1/2 \geq 0$ for $V^\dagger_{i,k}$.

To express edge state inner products in the CFT, we first define $R = \sqrt{2N_1}$, $M(m)_{ij} = \{\tilde{c}_{i,m}, \tilde{c}^\dagger_{j,m}\}$ (i.e. $M(m)_{ij}$ is the inner-product matrix of the orbitals z^m and $\bar{z}z^{m+1}$). Then the inner products take the usual form $\langle\langle\Psi_{\langle w|}|\Psi_{\langle v|}\rangle\rangle/Z_N = \langle v|\, e^{\mathcal{S}}\,|w\rangle$, with $\mathcal{S} = \sum_k \sum_{ij}(-1)^{i+j}[\ln M(N_1 + k - 1/2)]_{ij} : V_{i,-k}V^\dagger_{j,k} :$, where the sum of k having the obvious restriction.

By explicit diagonalization and keeping terms up to and including $1/R$, for large N we find,

$$\begin{aligned}\ln M(N_1 + k - 1/2) \approx & 6 \ln R \begin{pmatrix} -\frac{1}{2} & \frac{1}{R^2} \\ \frac{1}{R^2} & \frac{1}{2} \end{pmatrix} \\ & + [N_1 \ln N_1 - N_1 + \ln N_1 + \ln(4\pi\sqrt{\pi}) + (k - 1/2)\ln 2N_1]\mathbf{1}_{2\times 2}\end{aligned} \tag{3.38}$$

where $\mathbf{1}_{2\times 2}$ is the two by two identity matrix. To express this matrix in a form that generalises to other states, we first define the currents, $J^3(z) = [i\partial\varphi^{(2)}(z) - i\partial\varphi^{(2)}(z)]/2$, $J^+(z) = V_2(z)V_1^\dagger(z)$ and $J^-(z) = V_1(z)V_2^\dagger(z)$. These fields have the OPEs, $J^3(z)J^3(w) \sim \frac{1/2}{(z-w)^2}$, $J^3(z)J^\pm(w) \sim \pm\frac{J^\pm(w)}{z-w}$ and $J^+(z)J^-(w) \sim \frac{1}{(z-w)^2} + \frac{2J^3(w)}{z-w}$, which are the OPEs for $\widehat{\mathfrak{su}}(2)_1$ WZW model currents. Finally, we also define $\Phi(z) = [\varphi^{(1)} + \varphi^{(2)}]/\sqrt{2}$ with it's corresponding modes $\tilde{a}_n$. We can now express the inner products as $\langle\langle\Psi_{\langle w|}|\Psi_{\langle v|}\rangle\rangle/Z_N = \langle v|\, R^{2L_0}e^S\,|w\rangle$, where,

[6] i.e. $\langle\langle 0|\, c(z)\tilde{c}^\dagger_{1,m}\,|0\rangle\rangle = z^m e^{-\frac{|z|^2}{4}}$ and $\langle\langle 0|\, c(z)\tilde{c}^\dagger_{2,m}\,|0\rangle\rangle = \bar{z}z^{m+1}e^{-\frac{|z|^2}{4}}$.

[7] Note that N and N_i in these expressions are the N and N_i of the ground state trial wave function and so are constants.

$$S = \sqrt{2}[N_1 \ln N_1 - N_1 + (1/2)\ln N_1 + \ln(2\pi\sqrt{2\pi})]\tilde{a}_0 + 3\ln(2N_1)\left[J_0^3 - \frac{J_0^1}{N_1}\right] \quad (3.39)$$

where, $J^1(z) = (J^+(z) + J^-(z))/2$. Thus, we can see that for $\nu = 2$ we have other divergent terms in S that are zero modes of these extra conserved currents.

Finally, the angular momentum operator $\sum_i z_i\partial_i - \bar{z}_i\overline{\partial}_i$ can be mapped over using the same method for the $\nu = 1$ case to give,

$$\begin{aligned}[\sum_{i=1}^{N} z_i\partial_i - \bar{z}_i\overline{\partial}_i]\Psi_{\langle v|}(\mathbf{z}) &= \langle v|\, F_2^{-N_2}F_1^{-N_1}(L_0 - (1/2)a^{(1)} - (3/2)a_0^{(2)})\prod_{i=1}^{N}\Omega(z,\bar{z})\,|0\rangle \\ &= \langle v|\,[L_0 + (2N_1-1)\tilde{a}_0/\sqrt{2} + N_1(N_1-1) - 1]F_2^{-N_2}F_1^{-N_1}\prod_{i=1}^{N}\Omega(z,\bar{z})\,|0\rangle\end{aligned} \quad (3.40)$$

Hence, the angular momentum operator maps over to the CFT as, $\sum_i z_i\partial_i - \bar{z}_i\overline{\partial}_i \rightarrow [L_0 + \frac{(2N_1-1)\tilde{a}_0}{\sqrt{2}} + N_1(N_1-1) - 1]$.

3.2.3 $\nu = n$

We can now generalise from the $\nu = 2$ case to $\nu = n$. This will require n independent free chiral boson fields $\varphi^{(i)}(z)$ along with their Klein factors F_i and vertex operators $V_j(z) = F_j :e^{i\varphi^{(j)}(z)}:$. The generating Ω operator is given by,

$$\Omega(z,\bar{z}) = \sum_{j=1}^{n}\bar{z}^{j-1}V_j(z) \quad (3.41)$$

Let N_1 be a positive integer. Then for $N = N_1 + n(n-1)/2$ we define $N_i \equiv N_1 + i - 1$ and the background charge operator as $C_n(N) = F_n^{-N_n}F_{n-1}^{-N_{n-1}}\ldots F_1^{-N_1}$. We then have,

$$\Psi_{\langle 0|}(\mathbf{z}) = \langle 0|\, C_n(N) \prod_{i=1}^{N} \Omega(z_i, \bar{z}_i)\, |0\rangle = \det[z_1^{N_1-1}, \ldots, z_{N_1}^0, \bar{z}_{N_1+1} z_{N_1+1}^{N_2-1}, \ldots, \bar{z}_{N_1+N_2} z_{N_1+N_2}^0, \ldots, \bar{z}_{\sum_{i=1}^{n-1} N_i}^{n-1} z_{\sum_{i=1}^{n-1} N_i}^{N_n-1}, \ldots, \bar{z}_N^{n-1} z_N^0] \tag{3.42}$$

which is the non-interacting $\nu = n$ ground state wave function, where the second equality can be shown by a simple extension of the method used for $\nu = 2$.

One can show, again using a simple generalisation of the $\nu = 2$ case, that the edge state mapping has the property,

$$|\Psi_{\langle v|V_{i,k}\rangle}\rangle\rangle = (-1)^{N-N_i} \tilde{d}_{i,N_1-k-1/2}\, |\Psi_{\langle v|}\rangle\rangle \qquad |\Psi_{\langle v|V_{i,k}^\dagger\rangle}\rangle\rangle = (-1)^{N-N_i} \tilde{c}^\dagger_{i,N_1+k-1/2}\, |\Psi_{\langle v|}\rangle\rangle \tag{3.43}$$

where $\tilde{c}^\dagger_{j,m}$ is the creation operator for the *unnormalised* orbital $\bar{z}^{j-1} z^{m+j-1}$ and $\tilde{d}^\dagger_{j,m}$ is the creation operator for a single particle orbital such that $\{\tilde{d}_{i,m}, \tilde{c}^\dagger_{j,m'}\} = \delta_{ij}\delta_{mm'}$. These operator mappings are strictly only valid, once again, for $N_i - k - 1/2 \geq 0$ for $V_{i,k}$ and $N_i + k - 1/2 \geq 0$ for $V^\dagger_{i,k}$. Hence, the edge state mapping will generate the entire space of states of particles restricted to the n lowest Landau levels, with states of the form $\langle 0|$ (product of $V_{i,k}$'s and $V^\dagger_{i,k}$'s) generating the Slater determinant wave functions. We will not calculate the large N form of the edge state inner products here, although this can in principle be done.

The angular momentum operator maps over as, $\sum_i z_i\partial_i - \bar{z}_i\overline{\partial}_i \to L_0 + \frac{2N_1-1}{2}\big(\sum_{i=1}^n a_0^{(i)}\big) + \frac{nN_1(N_1-1)}{2} - \frac{n(n-1)}{2}$.

Finally, we shall now note some further properties of this construction that will be useful later. We can define a Hermitian operator $J_0 \equiv \sum_{i=1}^N (i-1) a_0^{(i)}$ that has the property $[J_0, V_i(z)] = (i-1)V_i(z)$. Furthermore we have $C_n(N) V_j(z) C_n^\dagger(N) \propto z^{N_1+j-1} V_j(z)$. $C(N)^\dagger_n\, |0\rangle$ is a state of the CFT with N fermions. Among all states with N fermions, it is the unique state that minimises $L_0 - J_0$. To see this note that $L_0 - J_0 = \sum_i \frac{(a_0^{(i)}-i+1)^2}{2} + \sum_{i,n>0} a_{-n}^{(i)} a_n^{(i)} +$ constant. The second term is positive

definite so any state that minimises this must be a Heisenberg primary $a_r^{(i)}|v\rangle = 0$ for $r > 0$. Using the Lagrange multiplier method, the first term can easily be shown to be minimised under the constraint $(\sum_i a_0^{(i)})|v\rangle = N|v\rangle$ by a state with $a_0^{(i)}|v\rangle = (N_1 + i - 1)|v\rangle$. In this CFT there can only be one state that is a Heisenberg primary and has a specific amount of $U(1)$ charge for each fermion species. It can be checked that $C^\dagger(N)_n|0\rangle$ is a Heisenberg primary with $a_0^{(i)}C_n^\dagger(N)|0\rangle = (N_1 + i - 1)C_n^\dagger(N)|0\rangle$. Therefore, $C_n^\dagger(N)|0\rangle \propto |v\rangle$, QED.

3.3 CFT construction of ground and edge state Parton trial wave functions

In this section, we will first discuss how generic Parton trial ground and edge state wave functions can be generated using CFT, where a chiral algebra $\mathcal{A}$ can be associated with each ground state trial wave function with $\text{CFT}_\mathcal{A}$, roughly speaking, being the "smallest" CFT that can generate the ground state trial wave function. We will then give the Composite Fermion and symmetric Parton wave functions as examples of this construction in Sec. 3.3.1 and Sec. 3.3.2 respectively.

From the above discussion of the IQH wave functions, we can see that a possible way to generalise the usual CFT construction of wave functions is to use a generating operator $\Omega(z, \bar{z})$ which is composed of r operators ϕ_l for $l = 0, 1, 2 \ldots, r-1$, all with the same conformal dimension, belonging to some CFT which we denote CFT_L (for the moment), where,

$$\Omega(z, \bar{z}) = \sum_{l=0}^{r-1} \bar{z}^l \phi_l(z) \tag{3.44}$$

After the choice of an appropriate background charge operator $C(N)$, the ground state trial wave function can then be expressed as,

$$\Psi_{\langle 0|}(\mathbf{z}) = \langle 0| C(N) \prod_{i=1}^{N} \Omega(z_i, \bar{z}_i) |0\rangle \tag{3.45}$$

Let $\mathcal{A}$ be the chiral algebra generated by repeated OPE of $\phi_l(z)$ and $\phi_l^\dagger(z)$. Let $\mathcal{H}_L$ be the Hilbert space of CFT_L and let $\mathcal{H}_0$ be the space of states in $\mathcal{H}_L$ which are generated by applying the modes of $\phi_l(z)$ and $\phi_l^\dagger(z)$ on $|0\rangle$ (i.e. the vacuum rep. of $\mathcal{A}$). We will assume this construction has the following properties,

(i) CFT_L is *unitary*.

(ii) $\phi_l(z)$ are Virasoro primary fields.

(iii) There exists a conserved $U(1)$ charge with the Hermitian operator a_0 where $\phi_l(z)$ has some charge q and $C(N)$ has charge $-qN$.

(iv) There exists a Hermitian operator J_0 such that $[J_0, \phi_l(z)] = l\phi_l(z)$.

(v) $a_0 |0\rangle = J_0 |0\rangle = L_0 |0\rangle = 0$

(vi) $C(N)\phi_l(z)C^\dagger(N) \propto z^{k(N)+l}\phi_l(z)$ where $k(N)$ is some integer-valued function.

(vii) $C^\dagger(N) |0\rangle \in \mathcal{H}_0$ is a simultaneous eigenstate of a_0, J_0 and L_0, and among all states with the same $U(1)$ charge in $\mathcal{H}_0$ it is the *unique* state that minimises $L_0 - J_0$.

Note that (ii)-(vii) imply that $\mathcal{H}_0$ is an invariant subspace of a_0, J_0, L_0 and $C(N)$. Properties (i)-(iii) trivially hold for the IQH wave functions and (iv)-(vii) were shown to hold in the last paragraph of Sec. 3.2.3, provided the number of particles in the "ground state" N takes the form $N = N_1 r + r(r-1)/2$ with $\nu = r$. We will first demonstrate that these properties hold for Parton states where there always exists N such that the lowest angular momentum wave function with N particles is unique. At the end of this section, we will discuss the more subtle case where there is no unique lowest angular momentum Parton state, which occurs when there exists no number of

particles N such that for each IQH component the expression $N = N_1 r + r(r-1)/2$ holds where r is the filling fraction of the given component and N_1 is a positive integer that can depend on the IQH component.

The general edge state map is then defined as,

$$|\Psi_{\langle v|}\rangle\rangle \equiv \langle v| C(N) e^{\int d^2 z e^{-\frac{|z|^2}{4}} \Omega(z,\bar{z}) \otimes c^\dagger(z)} |0\rangle \otimes |0\rangle\rangle \tag{3.46}$$

We will associate to this wave function the chiral algebra $\mathcal{A}$. A CFT can be defined from $\mathcal{A}$, which we denote $\mathrm{CFT}_{\mathcal{A}}$, provided $\mathcal{A}$ has an energy-momentum tensor. From the general Proposition 5.29 of Ref. [127] it follows that an energy-momentum tensor always exists for $\mathcal{A}$[8]. In general, $\mathcal{H}_0 \neq \mathcal{H}_L$. However, as $\mathcal{H}_0$ is an invariant subspace of $C(N)$, the correlation function of Eq. 3.45 can be computed entirely within $\mathcal{H}_0$[9]. CFT_L has then merely been used as a convenient way to compute a correlation function of $\mathrm{CFT}_{\mathcal{A}}$.

Furthermore, from the definition of the edge state map of Eq. 3.46 it can be seen that all the states of the orthogonal complement of $\mathcal{H}_0$ must map to zero. Thus, the image of the edge state map is not changed when the domain of the map is restricted to $\mathcal{H}_0$.

When formulating a generalised screening hypothesis (as will be discussed later) it is important to consider the wave function as being generated from $\mathrm{CFT}_{\mathcal{A}}$. Roughly speaking, if CFT_L was used instead then there would be "degrees of freedom" within this CFT that would not couple to the perturbation, which would then imply that the perturbed field theory could not flow to a massive IR fixed point.

Note that when we generate a wave function this way the $\bar{z}$ dependence implies this is not a wave function entirely in the LLL. To generate the LLL projected wave

[8]This follows from the fact $\mathcal{A}$ is generated by OPEs of a finite number of Virasoro primary fields. Let P be the projector onto $\mathcal{H}_0$. The energy-momentum tensor of $\mathcal{A}$ is the field, $\tilde{T}(z)$, that corresponds to the state $PT(0)|0\rangle$ where $T(z)$ is the energy-momentum tensor of CFT_L. For all $\phi(z) \in \mathcal{A}$ the singular terms in the OPE $T(z)\phi(w)$ are the same as those in the OPE $\tilde{T}(z)\phi(w)$.

[9]If $\mathcal{H}_0$ was not an invariant subspace of $C(N)$ then one can simply project the background charge operator onto $\mathcal{H}_0$.

function we simply perform the replacement $\bar{z} \to 2\partial$ so that the generating operator becomes $\Omega(z) = \sum_l (2\partial)^l \phi_l(z)$. Thus, the LLL projected wave function can still be generated by $\mathrm{CFT}_{\mathcal{A}}$ and the resulting edge state map is now a map from the vacuum representation of $\mathcal{A}$ to some space of wave functions in the LLL.

We will now show inductively that this construction exists for all chiral Parton wave functions, where the lowest angular momentum state is unique. Suppose we know how to generate some trial wave functions Ψ_1 and Ψ_2 using the operators $\Omega_1(z, \bar{z})$ and $\Omega_2(z, \bar{z})$ from CFT_1 and CFT_2 respectively, with the desired properties. Let $\phi_l^{(i)}(z)$, $a_0^{(i)}, L_0^{(i)}$, $J_0^{(i)}$ and $\mathcal{H}_0^{(i)}$ be the $\phi_l(z)$, a_0, L_0, J_0 and $\mathcal{H}_0$ for CFT_i respectively. We can then generate the trial wave function $\Psi_1\Psi_2$ using the CFT $\mathrm{CFT}_L = \mathrm{CFT}_2 \otimes \mathrm{CFT}_1$ as follows. Let $C(N) = C_1(N)C_2(N)$, where $C_i(N)$ is the background charge operator used to generate Ψ_i, and $\Omega(z, \bar{z}) = \Omega_1(z, \bar{z})\Omega_2(z, \bar{z})$. We then have,

$$\begin{aligned} \Psi_{\langle 0|}(\mathbf{z}) &= \langle 0| \, C(N) \prod_{i=1}^{N} \Omega(z_i, \bar{z}_i) \, |0\rangle \\ &\propto \langle 0| \left[C_2(N) \prod_{i=1}^{N} \Omega_2(z_i, \bar{z}_i) \right] |0\rangle \, \langle 0| \left[C_1(N) \prod_{j=1}^{N} \Omega_1(z_j, \bar{z}_j) \right] |0\rangle \\ &= \Psi_1(\mathbf{z})\Psi_2(\mathbf{z}) \end{aligned} \tag{3.47}$$

where $\propto$ appears as, depending on the conformal spin of the Ω_i's, we may obtain an additional minus one factor from rearranging the Ω_i's. Thus, simply by the fact the resulting correlation function will factorise, we can generate $\Psi_1\Psi_2$ from a CFT correlation function.

One can expand $\Omega(z, \bar{z}) = \sum_l \bar{z}^l \phi_l(z)$ where each $\phi_l(z) = \sum_{l_1 l_2} \delta_{l_1+l_2,l} \phi_{l_1}^{(1)}(z)\phi_{l_2}^{(2)}(z)$. As $\phi_l^{(i)}(z)$ are Virasoro primary fields it then follows that $\phi_l(z)$ are also Virasoro primary fields, which gives (ii). Clearly CFT_L is unitary as CFT_i are unitary which gives (i). Next, we define $a_0 = a_0^{(1)} + a_0^{(2)}$, $L_0 = L_0^{(1)} + L_0^{(2)}$ and $J_0 = J_0^{(1)} + J_0^{(2)}$, which can easily be shown to have the desired properties for (iii)-(v). As $C_1(N)C_2(N)\phi_{l_1}^{(1)}(z)\phi_{l_2}^{(2)}(z)C_2^\dagger(N)$ $C_1^\dagger(N) \propto z^{k_1(N)+k_2(N)+l_1+l_2}\phi_{l_1}^{(1)}(z)\phi_{l_2}^{(2)}(z)$, it follows that

$C(N)\phi_l(z)C^\dagger(N) \propto z^{k_1(N)+k_2(N)+l}\phi_l(z)$ which gives (vi).

Let P be the projector onto $\mathcal{H}_0$. As $\phi_l(z)$ has a well defined $U(1)$ charge for both $a_0^{(1)}$ and $a_0^{(2)}$ then $\mathcal{H}_0$ is an invariant subspace of $a_0^{(i)}$ and as $a_0^{(i)}$ are Hermitian $[a_0^{(i)}, P] = 0$. In fact, within $\mathcal{H}_0$, $a_0^{(1)} \propto a_0^{(2)}$. Furthermore, $C^\dagger(N)\left|0\right\rangle \in \mathcal{H}_0^{(1)} \otimes \mathcal{H}_0^{(2)}$ must have the property that among all states with the same $a_0^{(i)}$ charges in $\mathcal{H}_0^{(1)} \otimes \mathcal{H}_0^{(2)}$ it must be the unique state which minimises $L_0 - J_0$. Now write $C^\dagger(N)\left|0\right\rangle = \left|x\right\rangle + \left|y\right\rangle$ where $\left|x\right\rangle \in \mathcal{H}_0$ and $\left|y\right\rangle \in \mathcal{H}_0^\perp$ (i.e. $\mathcal{H}_0^\perp$ is the orthogonal complement of $\mathcal{H}_0$). As $\prod_{i=1}^N \Omega(z_i, \bar{z}_i)\left|0\right\rangle \in \mathcal{H}_0$ and $\left\langle 0\right| C(N) \prod_{i=1}^N \Omega(z_i, \bar{z}_i)\left|0\right\rangle \neq 0$ then $PC^\dagger(N)\left|0\right\rangle \neq 0 \Rightarrow \left|x\right\rangle \neq 0$. From $[a_i^{(i)}, P] = [L_0, P] = [J_0, P] = 0$ it follows that $\left|x\right\rangle$ must be a simultaneous eigenstate of $a_0^{(i)}$, L_0 and J_0 with the same eigenvalues as $C^\dagger(N)\left|0\right\rangle$. Hence, from the uniqueness property of $C^\dagger(N)\left|0\right\rangle$ we have $C^\dagger(N)\left|0\right\rangle = \left|x\right\rangle$. This then implies that property (vii) holds, QED.

Consider the state $\left|v\right\rangle \in \mathcal{H}_0^{(1)} \otimes \mathcal{H}_0^{(2)}$ with, $\left|v\right\rangle = \left|v_1\right\rangle \otimes \left|v_2\right\rangle$ and $\left|v_i\right\rangle \in \mathcal{H}_0^{(i)}$. By the factorisation of the resulting correlation function we must have that, $\Psi_{\langle v_1|\otimes\langle v_2|}(\mathbf{z}) \propto \Psi^{(1)}_{\langle v_1|}(\mathbf{z})\Psi^{(2)}_{\langle v_2|}(\mathbf{z})$, where $\Psi^{(i)}_{\langle v_i|}(\mathbf{z})$ is the wave function resulting from the edge state map of CFT_i (i.e. the edge state map associated with Ψ_i). Thus, the image of the edge state map must be spanned by wave functions which are products of wave functions from the images of the edge state maps of CFT_1 and CFT_2.

Finally, assume that under the edge state map for Ψ_i the angular momentum operator maps to the CFT is $L_0^{(i)} + v_i(N)a_0^{(i)}+$ constant with $v_i(N)$ being some real-valued function, which holds for the $\nu = r$ IQH case so long as $N = N_1 r + r(r-1)/2$ for some positive integer N_1. We then have that for the edge state map of $\Psi_1\Psi_2$ the angular momentum operator maps to the CFT as $L_0^{(1)} + v_1(N)a_0^{(1)} + L_0^{(2)} + v_2(N)a_0^{(2)}+$ constant. Recall that in $\mathcal{H}_0$, $a_0^{(1)} \propto a_0^{(2)}$, which implies that within $\mathcal{H}_0$ the angular momentum operator maps over as $L_0 + v(N)a_0+$ constant for some function $v(N)$. Thus, the edge state counting for a fixed number of particles and angular momentum has an upper bound given by the state counting in $\mathcal{H}_0$ for the corresponding L_0 and a_0 eigenvalues.

We will now briefly discuss the case where the lowest angular momentum Parton

state is not unique. An example of this is the Parton state formed as a product of a $\nu = 4$ and a $\nu = 2$ wave function, $\phi_4\phi_2$. At $\nu = 4$, we only have a unique lowest angular momentum state when $N = 4N_1 + 6$ for some positive integer N_1. For $\nu = 2$ there is only a unique lowest angular momentum ground state for $N = 2N_1 + 1$. Clearly, there cannot exist an N such that there is a unique lowest angular momentum state for the $\nu = 4$ and $\nu = 2$ components. In these cases, it is not obvious if such a well-defined background charge operator exists. One can get around this by simply not using a background charge. From the discussion of Sec. 3.2 it can be seen that one can generate all IQH ground and edge state wave functions using CFT correlation functions of the form $\langle v| \prod_{i=1}^{N} \Omega(z_i, \bar{z}_i) |0\rangle$. Furthermore, for any state expressible as $\langle v| \prod_{i=1}^{N} \Omega(z_i, \bar{z}_i) |0\rangle$ we can still expand $\Omega(z, \bar{z}) = \sum_l \bar{z}^l \phi_l(z)$ and then associate a chiral algebra $\mathcal{A}$ generated by these $\phi_l(z)$ and $\phi^\dagger(z)$ where this correlation function can be expressed as a correlation function of the vacuum representation of $\mathcal{A}$. One can then perform all the same inductive steps used earlier in this section, not involving the background charge, to show that all chiral Parton ground and edge state wave functions can be expressed in this way. Thus, for these more subtle cases, the only part of this construction one may not have is the well-defined background charge operator. This is of no conceptual concern as the background charge operator is mostly a tool to simplify edge state counting.

3.3.1 Composite Fermion wave functions

The unprojected CF ground state trial wave function at $\nu = \frac{r}{rp+1}$, with $r, p \in \mathbb{Z}^+$, is simply a product of a $\nu = r$ IQH ground state and a $\nu = \frac{1}{p}$ Laughlin ground state trial wave function. To generate this wave function we then can use the CFT used to generate the $\nu = n$ ground state discussed in Sec. 1.2.1, which we will denote $\text{CFT}_{\nu=r}$, combined with the CFT used to generate the $\nu = \frac{1}{p}$ Laughlin wave function discussed in Sec. 1.2.1 which we denote $\text{CFT}_{\mathcal{A}_p}$. In this section we will denote the chiral boson

fields, the Klein factors and the vertex operators of $\text{CFT}_{\nu=r}$ as $\tilde{\varphi}^{(j)}(z)$, $\tilde{F}_j$ and $\tilde{V}_j(z)$ respectively.

We now define the CF vertex operators by $V_j(z) \equiv \tilde{V}_j(z)V_\phi(z)$ along with their corresponding Klein factors $F_i \equiv \tilde{F}_i F_\phi$, where the generating $\Omega(z,\bar{z})$ is given by,

$$\Omega(z,\bar{z}) = \sum_{j=1}^{r} \bar{z}^{j-1} V_j(z) \tag{3.48}$$

Defining the background charge to be $C(N) = C_r(N)F_\phi^{-N}$ where $C_r(N)$ is the $\nu = r$ background charge, the ground state wave function is then given by,

$$\Psi_{\langle 0|}(\mathbf{z}) = \langle 0|\, C(N) \prod_{i=1}^{N} \Omega(z_i,\bar{z}_i)\, |0\rangle \propto \Phi_r(\mathbf{z}) \prod_{i<j} (z_i - z_j)^p \tag{3.49}$$

where $\Phi_r(\mathbf{z})$ is the $\nu = r$ ground state wave function of Eq. 3.42 and the $\propto$ sign appears as for p odd we can get additional minus signs when passing the F_ϕ and $V_\phi(z)$ through the $\tilde{V}_j(z)$. We have thus generated the $\nu = \frac{r}{rp+1}$ CF trial ground state wave function without explicit anti-symmetrisation.

From the discussion at the beginning of this section, we know that the image of the edge state map must be spanned by wave functions of the form $\Phi_{r,\text{edge}}\Psi_{p,\text{edge}}$ where $\Phi_{r,\text{edge}}$ and $\Psi_{p,\text{edge}}$ are edge state wave functions for the $\nu = r$ and $\nu = \frac{1}{p}$ states respectively. $\Psi_{p,\text{edge}}$ always takes the form $P(\mathbf{z})\prod_{i<j}^{N}(z_i - z_j)^p$ with $P(\mathbf{z})$ being a symmetric polynomial. Thus, the image of the edge state map is spanned by $[P(\mathbf{z})\Phi_{r,\text{edge}}(\mathbf{z})]\prod_{i<j}^{N}(z_i - z_j)^p$. However, $P(\mathbf{z})\Phi_{r,\text{edge}}$ is still a $\nu = r$ edge state wave function. Hence, the image of the edge state is in fact given by wave functions of the form $\Phi_{r,\text{edge}}(\mathbf{z})\prod_{i<j}^{N}(z_i - z_j)^p$, which is the space of CF edge state trial wave functions.

Let $\mathcal{A}_{r,p}$ be the chiral algebra generated by repeated OPEs of $V_j(z)$ and $V_j^\dagger(z)$, where $V_j^\dagger(z) = F_j^\dagger : e^{i\varphi^{(j)}(z)} :$. We will now discuss the structure of $\mathcal{A}_{r,p}$. First note that $V_i(z)V_j(w) \sim V_i^\dagger(z)V_j^\dagger(w) \sim 0$. We also have the OPEs,

$$V_i(z)V_j^\dagger(w) \sim \frac{\delta_{ij}}{(z-w)^{K_{ij}}} + \frac{i\partial\varphi^{(i)}(w)}{(z-w)^{K_{ij}-1}} + \dots \tag{3.50}$$

where $\varphi^{(i)}(z) = \tilde{\varphi}^{(i)}(z) + \sqrt{p}\phi(z)$ and K is the K-matrix corresponding to this CF state given by $K_{ij} = p + \delta_{ij}$. We denote the modes of $\varphi^{(i)}(z)$ as $a_n^{(i)}$.

From state-operator correspondence, we can deduce what other fields must belong to $\mathcal{A}$ by understanding what states belong to $\mathcal{H}_0 \subset \mathcal{H}_L$, where we take $\mathcal{H}_L$ to be the Hilbert space of $\mathrm{CFT}_{\nu=n} \otimes \mathrm{CFT}_{\mathcal{A}_p}$. First, define the field $\mathcal{J}(z) = \frac{1}{\sqrt{np+1}}\big[i\partial\phi(z) - \sqrt{p}\sum_{j=1}^{n} i\partial\tilde{\varphi}^{(j)}(z)\big]$ and the space of "gauge invariant" states $\mathcal{H}_G$ by $\mathcal{J}_n |v\rangle = 0, n \geq 0, \Leftrightarrow |v\rangle \in \mathcal{H}_G$. Note that $[\mathcal{J}_n, a_m^{(j)}] = 0$. One can pick a basis of $\mathcal{H}_L$ of the form $[\prod_{n_k} \mathcal{J}_{-n_k}][\prod_{j=1}^{r}\prod_{n_l^{(j)}} a^{(j)}_{-n_l^{(j)}} F_j^{s_j}]F_\phi^s |0\rangle$ with $n_k, n_l^{(j)} \in \mathbb{Z}^+$ and $s, s_j \in \mathbb{Z}$. Clearly, any ket of $\mathcal{H}_G$ can only be a linear combination of the basis elements of the form $[\prod_{j=1}^{r}\prod_{n_l^{(j)}} a^{(j)}_{-n_l^{(j)}} F_j^{s_j}]F_\phi^s |0\rangle$ (i.e. those that do not involve $\mathcal{J}_n$). Furthermore, condition $\mathcal{J}_0 |v\rangle = 0$ implies that $|v\rangle$ can only be a linear combination of the basis elements with $s = 0$. Thus, the kets $[\prod_{j=1}^{r}\prod_{n_l^{(j)}} a^{(j)}_{-n_l^{(j)}} F_j^{s_j}] |0\rangle$ form a basis for $\mathcal{H}_G$.

As $\mathcal{J}(z)V_j(w) \sim \mathcal{J}(z)V_j^\dagger(z) \sim 0 \Rightarrow [\mathcal{J}_n, V_j(z)] = [\mathcal{J}_n, V_j^\dagger(z)] = 0$, we have $\mathcal{H}_0 \subseteq \mathcal{H}_G$. Now note that $F_i^\dagger V_j(z) F_i = z^{p+\delta_{ij}} V_j(z)$ and $V_{j,-\frac{p+1}{2}} |0\rangle = F_j |0\rangle$ and $V^\dagger_{j,-\frac{p+1}{2}} |0\rangle = F_j^\dagger |0\rangle$. It then follows that the states $\prod_j F_j^{s_j} |0\rangle$ can be generated by applying the modes of $V_j(z)$ and $V_j^\dagger(z)$ on the vacuum, which then gives $\prod_j F_j^{s_j} |0\rangle \in \mathcal{H}_0$. In addition, the OPEs of Eq. 3.50 imply that the $a_n^{(j)}$ modes can be expressed in terms of the $V_{j,k}$ and $V^\dagger_{j,k}$ modes. Hence, $[\prod_{j=1}^{r}\prod_{n_l^{(j)}} a^{(j)}_{-n_l^{(j)}} F_j^{s_j}] |0\rangle \in \mathcal{H}_0$. It then follows that $\mathcal{H}_0 = \mathcal{H}_G$.

Thus, we can see that the edge excitations that $\mathcal{H}_0$ will map to correspond to r bosonic branches of excitations, when the various $U(1)$ charges are fixed, as one would expect based on the standard CF theory.

Within $\mathcal{A}_{r,p}$ we also have the following currents with scaling dimension one,

$$\begin{aligned} J^a(z) \equiv & \sum_{ij} T^a_{ij} : V_i(z) V_j^\dagger(z) : \\ \Phi(z) \equiv & \frac{1}{\sqrt{n(np+1)}} \sum_{j=1}^{r} \varphi^{(j)}(z) \end{aligned} \tag{3.51}$$

where T^a are the generators of $SU(r)$ and the $U(1)$ operator that is the zero mode of

$i\partial\Phi(z)$, a_0, is related to the number of particles added to the edge by $\Delta N = \sqrt{\nu}a_0$ under the edge state map. These fields form the $\hat{\mathfrak{u}}(1) \oplus \widehat{\mathfrak{su}}(r)_1$ current algebra and form a basis of the space of fields of conformal dimension one which are $U(1)$ neutral with respect to $\partial\Phi(z)$. It can be straightforwardly shown that the space of states with a fixed total $U(1)$ charge in $\mathcal{H}_0$ can be generated by applying the modes of $i\partial\Phi(z)$ and $J^a(z)$ on a state of the form $\prod_j F^{s_j} |0\rangle$. Consequently, each space of fixed total $U(1)$ charge forms an irreducible representation of $\hat{\mathfrak{u}}(1) \oplus \widehat{\mathfrak{su}}(r)_1$. This can be thought of as non-abelian bosonisation [128] for CFs.

The angular momentum operator expressed in the CFT must be the sum of the $\nu = r$ and the $\nu = \frac{1}{p}$ angular momentum operators. Keeping in mind the $\mathcal{J}_0 = 0$ in $\mathcal{H}_0$, this gives the mapping of the angular momentum operator to be $L_0 + \left[\frac{(2N_1-1)}{2} + \frac{2N-1}{2\sqrt{p}}\right]\sqrt{\nu}a_0 +$ constant, where $N_1 = N/r - (r-1)/2$ (i.e. the N_1 defined for $\nu = r$ wave functions). Hence, the edge excitation state counting at fixed particle number and angular momentum must be bounded from above by the state counting at fixed total $U(1)$ charge, of $\Phi(z)$, and L_0.

In principle, one can then go on to use $\mathrm{CFT}_{\mathcal{A}_{r,p}}$ to generate quasiparticle trial wave functions. This has been discussed in detail in many other works (see Ref. [52] and references therein).

3.3.2 Symmetric Parton wave functions

To generate the symmetric parton wave function $[\Phi_r(\mathbf{z})]^r$ (i.e. the $\nu = r$ ground state raised to the m^{th} power with $m \in \mathbb{Z}^+$), we can use m copies of the CFT used to generate the $\nu = r$ ground state, $\mathrm{CFT}_L \equiv \bigotimes^m \mathrm{CFT}_{\nu=r}$. This gives a CFT with rm chiral bosons denoted $\tilde{\varphi}^{(ij)}(z)$ for $i = 1, 2, \ldots, m$ and $j = 1, 2, \ldots, r$, where we think of i as the "species" index and j as the "Landau level" index. The corresponding Klein factor and vertex operator for $\tilde{\varphi}^{(ij)}(z)$ will be written as $\tilde{F}_{ij}$ and $\tilde{V}_{ij}(z)$ respectively.

To generate Φ_r^m we simply need an Ω which is a product of the Ω's that generate

the $\nu = r$ ground state for each species,

$$\Omega(z, \bar{z}) = \prod_{i=1}^{m} \left[\sum_{j=1}^{r} \bar{z}^{j-1} \tilde{V}_{ij}(z) \right] \tag{3.52}$$

Let $C_r^{(i)}(N)$ be the background charge operator that can be used to generate the $\nu = r$ ground state using the i^{th} species. We define $C(N) = \prod_{i=1}^{m} C_r^{(i)}(N)$. This then gives,

$$\Psi_{\langle 0|}(\mathbf{z}) = \langle 0| \, C(N) \prod_{i=1}^{N} \Omega(z_i, \bar{z}_i) \, |0\rangle \propto [\Psi_r(\mathbf{z})]^m \tag{3.53}$$

which is the desired ground state wave function. From the discussion at the start of this section, it is clear that the image of the edge state map will be the space of wave functions spanned by products of m $\nu = r$ edge state wave functions.

We will now show that the above correlation function is a conformal block of the $\hat{\mathfrak{u}}(1) \oplus \widehat{\mathfrak{su}}(r)_m$ WZW model. First, we define the following currents,

$$\begin{aligned} \mathcal{J}^a(z) \equiv & \sum_{ijk} t^a_{ij} : \tilde{V}_{ik}(z) \tilde{V}^\dagger_{jk}(z) : \\ J^a(z) \equiv & \sum_{ijk} T^a_{ij} : \tilde{V}_{ki}(z) \tilde{V}^\dagger_{kj}(z) : \\ \Phi(z) \equiv & \frac{1}{\sqrt{rm}} \sum_{ij} \tilde{\varphi}^{(ij)}(z) \end{aligned} \tag{3.54}$$

where t^a and T^a are the generators for $SU(m)$ and $SU(r)$ respectively. Using the fermionic version of Wick's theorem one can show that these currents have the OPEs, $i\partial\Phi(z)\mathcal{J}^a(w) \sim i\partial\Phi(z)J^a(w) \sim \mathcal{J}^a(z)J^b(w) \sim 0$ and,

$$\begin{aligned} \mathcal{J}^a(z)\mathcal{J}^b(w) \sim & \frac{r\mathrm{Tr}[t^a t^b]}{(z-w)^2} + \frac{i\sum_c \tilde{f}^{abc}\mathcal{J}^c(w)}{(z-w)} \\ J^a(z)J^b(w) \sim & \frac{m\mathrm{Tr}[T^a T^b]}{(z-w)^2} + \frac{i\sum_c f^{abc}J^c(w)}{(z-w)} \\ i\partial\Phi(z)i\partial\Phi(w) \sim & \frac{1}{(z-w)^2} \end{aligned} \tag{3.55}$$

where f^{abc} and $\tilde{f}^{abc}$ are the structure constants defined by $[T^a, T^b] = i\sum_c f^{abc}T^c$ and

$[t^a, t^b] = i\sum_c \tilde{f}^{abc}t^c$ respectively. Note that for $\mathfrak{su}(n)$ the normalised Killing form, $K(T^a, T^b) = \frac{1}{2n}\mathrm{Tr}[\mathrm{ad}(T^a)\mathrm{ad}(T^b)]$ with $\mathrm{ad}(T^a)$ being the adjoint representation, can also be expressed as $K(T^a, T^b) = \mathrm{Tr}[T^aT^b]$ where the trace is taken the the fundemental representation. Thus, these currents must form the $\hat{\mathfrak{u}}(1) \oplus \widehat{\mathfrak{su}}(r)_m \oplus \widehat{\mathfrak{su}}(m)_r$ current algebra with $i\partial\Phi(z)$ being the $\hat{\mathfrak{u}}(1)$ current, $J^a(z)$ being the $\widehat{\mathfrak{su}}(r)_m$ currents and $\mathcal{J}^a(z)$ being the $\widehat{\mathfrak{su}}(m)_r$ currents. Furthermore, it was shown by Affleck [129] that the total energy-momentum tensor of CFT_L can be expressed as $T(z) = T^{\hat{\mathfrak{u}}(1)}(z) + T^{\widehat{\mathfrak{su}}(r)_m}(z) + T^{\widehat{\mathfrak{su}}(m)_r}(z)$ where $T^{\hat{\mathfrak{u}}(1)}(z)$, $T^{\widehat{\mathfrak{su}}(r)_m}(z)$ and $T^{\widehat{\mathfrak{su}}(m)_r}(z)$ are the Sugowara energy-momentum tensors of the currents $i\partial\Phi(z)$, $J^a(z)$ and $\mathcal{J}^a(z)$ respectively. This is then a conformal embedding of the $\hat{\mathfrak{u}}(1) \oplus \widehat{\mathfrak{su}}(r)_m \oplus \widehat{\mathfrak{su}}(m)_r$ current algebra.

The total Hilbert space of the theory $\mathcal{H}_L$ can then be decomposed into irreducible representations of this current algebra, $\mathcal{H}_L = \bigoplus \mathcal{M}_{q,\lambda,\tilde{\lambda}}$ where $\mathcal{M}_{q,\lambda,\tilde{\lambda}}$ is an irreducible module of $\hat{\mathfrak{u}}(1) \oplus \widehat{\mathfrak{su}}(r)_m \oplus \widehat{\mathfrak{su}}(m)_r$ with $U(1)$ charge q, highest weight λ with respect to $J^a(z)$ and highest weight $\tilde{\lambda}$ with respect to $\mathcal{J}^a(z)$. The branching rules for this decomposition are discussed in detail in Ref. [130]. Let $\phi_{q\lambda\tilde{\lambda}}(z)$ denote a WZW primary of $\mathcal{M}_{q\lambda\tilde{\lambda}}$. As discussed in Refs. [130–132], the correlation function $\langle 0|\prod_i \phi_{q_i,\lambda_i,\tilde{\lambda}_i}|0\rangle$ has the decomposition,

$$\langle 0|\prod_i \phi_{q_i,\lambda_i,\lambda_i'}(z_i)|0\rangle = \mathcal{F}^{\hat{\mathfrak{u}}(1)}(\mathbf{z})\left[\sum_{ab} C_{ab}\mathcal{F}_a^{\widehat{\mathfrak{su}}(r)_m}(\mathbf{z})\mathcal{F}_b^{\widehat{\mathfrak{su}}(m)_r}(\mathbf{z})\right] \tag{3.56}$$

where C_{ab} are constants, $\mathcal{F}^{\hat{\mathfrak{u}}(1)}(\mathbf{z})$ is a conformal block of the $U(1)$ vertex operators $\langle 0|\prod_j :e^{iq_j\Phi(z_j)}:|0\rangle$, $\mathcal{F}_a^{\widehat{\mathfrak{su}}(r)_m}(\mathbf{z})$ is a conformal block of the $\widehat{\mathfrak{su}}(r)_m$ WZW model related to the correlation function $\langle 0|\prod_i \phi_{\lambda_i}(z_i,\bar{z}_i)|0\rangle$, and $\mathcal{F}_b^{\widehat{\mathfrak{su}}(m)_r}(\mathbf{z})$ is a conformal block of the $\widehat{\mathfrak{su}}(m)_r$ WZW model related to the correlation function $\langle 0|\prod_i \phi_{\tilde{\lambda}_i}(z_i,\bar{z}_i)|0\rangle$.

Now expand $\Omega(z,\bar{z}) = \sum_{l=0}^{r(m-1)} \bar{z}^l V_l(z)$ where

$$V_l(z) = \sum_{i_1,i_2,\ldots i_m} \delta_{\sum_j i_j, l+m}\tilde{V}_{1i_1}(z)\tilde{V}_{2i_2}(z)\ldots\tilde{V}_{mi_m}(z) \tag{3.57}$$

We have $\mathcal{J}^a(z)V_l(w) \sim \mathcal{J}^a(z)V_l^\dagger(z) \sim 0$ so $V_l(z)$ and $V_l^\dagger(z)$ transform as the identity

field with respect to the $\mathcal{J}^a(z)$ currents. The $V_l(z)$ operators belong to a more general space of fields of the form $\sum_{i_1,i_2,\ldots,i_m} S^{i_1 i_2 \ldots i_m} \prod_{j=1}^{m} \tilde{V}_{j i_j}(z)$, where S is a symmetric rank m tensor. Under the action of $J^a(z)$ these fields form the rank m totally symmetric tensor representation WZW primary fields which are represented by a Young diagram of one row of m boxes, which we denote $\lambda(1)$. We will use $\lambda(n)$ to denote the $\widehat{\mathfrak{su}}(r)_m$ representation corresponding to the Young diagram of n rows of m boxes. The $V_l^\dagger(z)$ are also WZW primaries with respect to $J^a(z)$ belonging to the conjugate representation of $\lambda(1)$ which is $\lambda(1)^\dagger = \lambda(r-1)$. $V_l(z)$ and $V_l^\dagger(z)$ are also primary fields with respect to $i\partial\Phi(z)$ with $U(1)$ charges $q(1)$ and $q(-1)$ respectively, where $q(n) \equiv n\sqrt{\frac{m}{r}}$. In short, $V_l(z)$ and $V_l^\dagger(z)$ are primary fields of $\mathcal{M}_{q(1)\lambda(1)0}$ and $\mathcal{M}_{q(-1)\lambda(r-1)0}$ respectively. Note that the $\phi_{\lambda(n)}$ $\widehat{\mathfrak{su}}(r)_m$ primary fields are simple currents with fusion rules $\phi_{\lambda(n_1)} \times \phi_{\lambda(n_2)} = \phi_{\lambda([n_1+n_2] \mod r)}$ [133].

Now let us consider the correlation function $\langle \prod_j V_{l_j}^\dagger(w_j) \prod_i V_{l_i}(z_i) \rangle$. By Eq. 3.56 we know this must decompose into conformal blocks of the $\hat{\mathfrak{u}}(1)$, $\widehat{\mathfrak{su}}(r)_m$ and $\widehat{\mathfrak{su}}(m)_r$ WZW models. As the $\phi_{\lambda(1)}$ and $\phi_{\lambda(r-1)}$ $\widehat{\mathfrak{su}}(r)_m$ WZW primaries are simple currents there can only be one $\widehat{\mathfrak{su}}(r)_m$ conformal block in the decomposition. Furthermore, there is only one conformal block for a set of identity fields of $\widehat{\mathfrak{su}}(m)_r$ which is trivially a constant. We then have $\langle \prod_j V_{l_j}^\dagger(w_j) \prod_i V_{l_i}(z_i) \rangle = C \mathcal{F}^{\hat{\mathfrak{u}}(1)}(\mathbf{w};\mathbf{z}) \mathcal{F}^{\widehat{\mathfrak{su}}(r)_m}(\mathbf{w};\mathbf{z})$ where $\mathcal{F}^{\hat{\mathfrak{u}}(1)}(\mathbf{w};\mathbf{z})$ is the $\hat{\mathfrak{u}}(1)$ conformal block of the correlation function $\langle \prod_j : e^{iq(-1)\Phi(w_j)} : \prod_k : e^{iq(1)\Phi(z_k)} : \rangle$, $\mathcal{F}^{\widehat{\mathfrak{su}}(r)_m}(\mathbf{w};\mathbf{z})$ is the $\widehat{\mathfrak{su}}(r)_m$ conformal block of the correlation function $\langle \prod_j \phi_{\lambda(r-1)}(w_j, \bar{w}_j)$ $\prod_k \phi_{\lambda(1)}(z_k, \bar{z}_k) \rangle$ and C is a constant. By the cluster decomposition property in quantum field theory we have that $C = \prod_i C_i$ where the constant C_i only depends on the i^{th} field insertion. These C_i can then be absorbed in the normalisation of the $\phi_{\lambda(1)}$ and $\phi_{\lambda(r-1)}$ fields, which then gives,

$$\langle \prod_j V_{l_j}^\dagger(w_j) \prod_i V_{l_i}(z_i) \rangle = \mathcal{F}^{\hat{\mathfrak{u}}(1)}(\mathbf{w};\mathbf{z}) \mathcal{F}^{\widehat{\mathfrak{su}}(r)_m}(\mathbf{w};\mathbf{z}) \tag{3.58}$$

We can then express the ground state wave function in terms of these conformal blocks.

One would then expect that primary fields of the $\widehat{\mathfrak{su}}(r)_m$ WZW model could be used to generate quasiparticle wave functions with their braiding given by the monodromy of the corresponding conformal blocks. However, we will not consider quasiparticles here.

Now let $\mathcal{A}(r)_m$ be the chiral algebra generated by repeated OPEs of $V_l(z)$ and $V_l^\dagger(z)$, which is the chiral algebra we associate with this state. As usual, $\mathcal{H}_0$ is the space of states generated by applying the modes of this chiral algebra on $|0\rangle$, which forms the vacuum representation of $\mathcal{A}(r)_m$. We will now discuss the structure of $\mathcal{A}(r)_m$ by understanding $\mathcal{H}_0$.

We first define the "gauge" invariant states $\mathcal{H}_G$ by $\mathcal{J}_n^a |v\rangle = 0, n \geq 0, \Leftrightarrow |v\rangle \in \mathcal{H}_G$. Any $|v\rangle \in \mathcal{H}_G$ must be such that it is a sum of states belonging to the $\mathcal{M}_{q,\lambda,0}$ modules, where $\tilde{\lambda} = 0$ corresponds to vacuum representation of $\mathcal{J}^a(z)$. Furthermore, we can express $\mathcal{M}_{q,\lambda,0} \cong \mathcal{M}_q \otimes \mathcal{M}_\lambda \otimes \mathcal{M}_0$ where $\mathcal{M}_q$, $\mathcal{M}_\lambda$ and $\mathcal{M}_0$ are irreducible modules of $\hat{\mathfrak{u}}(1)$, $\widehat{\mathfrak{su}}(r)_m$ and $\widehat{\mathfrak{su}}(m)_r$ respectively. Clearly any gauge invariant state of $\mathcal{M}_{q,\lambda,0}$ must be a linear combination of states of the form $|v\rangle \otimes |w\rangle \otimes |0\rangle$ where $|v\rangle \in \mathcal{M}_q$, $|w\rangle \in \mathcal{M}_\lambda$ and $|0\rangle$ is the vacuum state of $\mathcal{M}_0$. Thus, the space of gauge invariant states in $\mathcal{M}_{q,\lambda,0}$ which we denote $\mathcal{M}_{q,\lambda} \subset \mathcal{M}_{q,\lambda,0}$ must be such that $\mathcal{M}_{q,\lambda} \cong \mathcal{M}_q \otimes \mathcal{M}_\lambda$. Using the branching rules of Ref. [130] we have the decomposition $\mathcal{H}_G = \bigoplus_{n\in\mathbb{Z}} \mathcal{M}_{q(n),\lambda(n \mod r)}$.

We will now show that $\mathcal{H}_0 = \mathcal{H}_G$. First as $[\mathcal{J}_n^a, V_l(z)] = [\mathcal{J}_n^a, V_l^\dagger(z)] = 0$ $\mathcal{H}_0$ must be a subspace of $\mathcal{H}_G$, $\mathcal{H}_0 \subset \mathcal{H}_G$. By $U(1)$ charge conservation and from the $\widehat{\mathfrak{su}}(r)_m$ fusion rules we must have that if $|v\rangle \in \mathcal{M}_{q(n)\lambda(n \mod r)}$ then $V_l(z)|v\rangle \in \mathcal{M}_{q(n+1)\lambda(n+1 \mod r)}$ and $V_l^\dagger(z)|v\rangle \in \mathcal{M}_{q(n-1)\lambda(n-1 \mod r)}$. In Appendix 3.A we show that $i\partial\Phi(z) \in \mathcal{A}(r)_m$ and $J^a(z) \in \mathcal{A}(r)_m$. These properties then imply that $\mathcal{M}_{q(n)\lambda(n \mod r)} \subset \mathcal{H}_0$ (as we can generate each state of $\mathcal{M}_{q(n)\lambda(n \mod r)}$ from the application of modes of fields fo $\mathcal{A}(r)_m$). Thus, $\mathcal{H}_0 = \mathcal{H}_G$ and we then have the decomposition,

$$\mathcal{H}_0 = \bigoplus_{n\in\mathbb{Z}} \mathcal{M}_{q(n),\lambda(n \mod r)} \tag{3.59}$$

Under the edge state map, the angular momentum operator can be expressed in

the CFT simply as a sum of the CFT mapped angular momentum operators for each individual species under the IQH edge state map which gives $\sum_i z_i\partial_i - \bar{z}_i\overline{\partial}_i \to L_0 + \frac{(2N_1-1)\sqrt{mr}}{2}a_0+$ constant, where $N_1 = N/r - (r-1)/2$. Thus, under the edge state map, the edge state counting for n particles added to the system at a specific angular momentum is bounded from above by the state counting at the corresponding L_0 eigenvalue in $\mathcal{M}_{q(n),\lambda(n)}$.

3.4 Generalised screening, edge state inner products and the RSES

We will now discuss how the generalised screening hypothesis can be generalised to the wave functions generated by the CFT construction of Sec. 3.3. We then go on in Sec. 3.4.1 to discuss how DRR's edge state inner product result can be generalised to these wave functions. Finally, in Sec. 3.4.2, we then discuss how the scaling property of the RSES of these wave functions is implied by generalised screening, which is again a simple generalisation of DRR's argument. Throughout this section, we will only consider unprojected wave functions (i.e. those with $\bar{z}$ dependence) for simplicity. All arguments and discussions here also apply to the projected wave functions with the replacement $\bar{z} \to 2\partial$. Throughout this section, we will only discuss Parton states with a unique lowest angular momentum wave function, which thus satisfy all the properties (i)-(vii) of Sec. 3.3 and have well-defined background charge operators. One can, in principle, reapply these discussions to the other cases, although one may encounter extra subtleties.

Consider now a ground state trial wave function generated by the general construction of Sec. 3.3. The full $\text{CFT}_{\mathcal{A}}$, will contain the anti-chiral copy of the chiral algebra $\overline{\mathcal{A}}$ as well as $\mathcal{A}$, where these two algebras are independent. We will denote the anti-chiral version of $\phi_l(z)$ by $\bar{\phi}_l(\bar{z}) \in \overline{\mathcal{A}}$. Let the anti-chiral version of the generating operator

$\Omega(z,\bar{z})$ be written as $\overline{\Omega}(z,\bar{z}) = \sum_l z^l \bar{\phi}_l(\bar{z})$. Further, let $\overline{C}(N)$ be the anti-chiral copy of the background charge operator $C(N)$. The complex conjugate of the ground state wave function can then be expressed as $\overline{\Psi_{\langle 0|}(\mathbf{z})} = \overline{\langle 0|\overline{C}(N)} \prod_{i=1}^{N} \overline{\Omega}(z_i,\bar{z}_i)\overline{|0\rangle}$. One can then repeat the calculation shown in Sec. 3.1.2 to show that the norm of the ground state wave function is given by,

$$Z_N \equiv \langle\langle \Psi_{\langle 0|}|\Psi_{\langle 0|}\rangle\rangle = \langle \overline{C}(N)C(N)e^{(-1)^{2h}\int D^2 z \overline{\Omega}(z,\bar{z})\Omega(z,\bar{z})}\rangle \tag{3.60}$$

where h is the scaling dimension of the fields $\phi_l(z)$ that appear in the definition of $\Omega(z,\bar{z})$. We then interpret Z_N as the partition function of a field theory which is a "perturbation" of $\mathrm{CFT}_{\mathcal{A}}$, where we will use the same notation as Sec. 3.1.2 to denote the correlation functions of this field theory. Once again the use of the word "perturbed" should be used with caution as there is no sense in which this addition to the CFT action is small. We will not be concerned with how this field theory is properly regularised when operators with singular OPEs with $\phi_l(z)$ or $\bar{\phi}_l(\bar{z})$ are inserted into a correlation function[10].

As for the cases discussed in Sec.3.1.2, one can use a saddle-point approximation, where we are looking for saddle points of $\ln|\Psi_{\langle 0|}(\mathbf{z})|^2$, to determine the course-grained density profile of the configuration of the $\overline{\Omega}(z,\bar{z})\Omega(z,\bar{z})$ insertions that dominate the partition function. As the Parton wave functions are constructed as products of integer quantum Hall wave functions, an obvious solution, in these cases, is a density profile of a disk with a uniform density of $\frac{\nu}{2\pi l_B^2}$, where $\nu^{-1} = \sum_i n_i^{-1}$ and n_i is the filling fraction of the i^{th} integer quantum Hall factor of the trial wave function. Thus, up to exponentially small corrections, the $\overline{\Omega}(z,\bar{z})\Omega(z,\bar{z})$ insertions are confined to the droplet of radius $R = \sqrt{\frac{2N}{\nu}}$.

We can then state the generalised screening hypothesis as before. That is, under

[10]The way that is suggested in Ref. [47] is to limit the integration of the $\overline{\Omega}(z,\bar{z})\Omega(z,\bar{z})$ perturbation such that z does not pass within some distance ϵ of any operator that is inserted into the correlation function. The resulting correlation function depends on ϵ in such a way that it diverges as $\epsilon \to 0$. By suitable renormalization these divergences can be cancelled in a systematic manner.

renormalisation group flow it is assumed that the perturbed field theory flows to a massive infrared fixed point inside the droplet and flows back to $\mathrm{CFT}_{\mathcal{A}}$ outside the droplet.

We now wish to discuss a slightly different formulation that will be useful when discussing edge-state inner products. In the formulation above we have placed the background charge operators at the left of the correlation function and so they are equivalent to some field being placed at infinity. Recall property (vi), discussed in Sec. 3.3, that $C(N)\phi_l(z)C^\dagger(N) \propto z^{k(N)+l}\phi_l(z)$, with $k(N) \in \mathbb{Z}$. One can use this property to move the background charge to the right of the correlation function and, thus, we can express Z_N as,

$$Z_N = \langle e^{(-1)^{2h}\int D^2 z \overline{\tilde{\Omega}}(z,\bar{z})\tilde{\Omega}(z,\bar{z})} \overline{C}(N)C(N)\rangle \tag{3.61}$$

where $\overline{\tilde{\Omega}}(z,\bar{z})\tilde{\Omega}(z,\bar{z}) = \overline{C}(N)C(N)\overline{\Omega}(z,\bar{z})\Omega(z,\bar{z})C^\dagger(N)\overline{C}^\dagger(N)$. Having the background charge operator at the right of the correlation function is equivalent to some local field placed at $z = 0$. Simply moving the background charge like this will not affect the configurations of the $\overline{\tilde{\Omega}}(z,\bar{z})\tilde{\Omega}(z,\bar{z})$ which are the dominant contributions to the partition function. Hence, the $\overline{\tilde{\Omega}}(z,\bar{z})\tilde{\Omega}(z,\bar{z})$ should still be confined to the droplet of radius R. As the transformation of any field $\phi(z,\bar{z})$ from the background charge $\overline{C}(N)C(N)\phi(z,\bar{z})C^\dagger(N)\overline{C}^\dagger(N)$ is expressible as a sum of local fields at the same position as $\phi(z,\bar{z})$ (with coefficients that may depend on this position), we must have that if the perturbed field theory with the background charge at infinity is short range correlated in the droplet then the field theory with the background charge at the origin is also short-range correlated. Hence, if generalised screening holds when the background charge is on the left of the correlation function then it also holds after it has been moved to the right.

Let $\tilde{S}_{FQH}$ denote the action of this field theory with the background charge operator placed on the right of the correlator. One expects that this can be expressed as $\tilde{S}_{FQH} =$

$S_{\mathrm{CFT}_{\mathcal{A}}} + \delta S$ where $S_{\mathrm{CFT}_{\mathcal{A}}}$ is the action of $\mathrm{CFT}_{\mathcal{A}}$ and δS is the "perturbation". As the $\overline{\tilde{\Omega}}(z,\bar{z})\tilde{\Omega}(z,\bar{z})$ are confined to the droplet, one expects that δS is localised to the droplet (on long length scales).

3.4.1 Edge-state inner products

We will now generalise the result of DRR [35] to the wave functions considered here, where we will use many of the boundary CFT methods used in Chap. 2. In what follows we will only be interested in inner products that correspond to the "scaling region". Roughly speaking, these are inner products between edge states where the fluctuation of the radius of the droplet δR for either state is such that $\frac{\delta R}{R} \ll 1$. For a more precise definition of this, we refer the reader to Sec. III.C of [35].

Firstly, we note that we can use the anti-chiral $\overline{\Omega}(z,\bar{z})$ to generate the complex conjugate of the wave function $\Psi_{\langle v|}(\mathbf{z})$ as $\overline{\Psi_{\langle v|}(\mathbf{z})} = \overline{\langle v|}\overline{C}(N)\prod_{i=1}^{N}\overline{\Omega}(z_i,\bar{z}_i)\overline{|0\rangle}$, where $\overline{\langle v|}$ is the anti-chiral copy of $\langle v|$. The edge-state inner products can then be expressed as,

$$\langle\langle \Psi_{\langle w|}|\Psi_{\langle v|}\rangle\rangle = \langle v|\,\overline{\langle w|}e^{(-1)^{2h}\int D^2 z\overline{\tilde{\Omega}}(z,\bar{z})\tilde{\Omega}(z,\bar{z})}\overline{C}(N)C(N)\,|0\rangle\,\overline{|0\rangle} \tag{3.62}$$

Just for the case of edge ground state overlaps discussed in Chap. 2, this inner product can be expressed as contour integrals of correlation functions of this perturbed field theory, with the partition function of Eq. 3.61, where these contours are *outside* the droplet.

Thus, to understand these edge-state inner products we need to understand the structure of correlation functions of this field theory with the action $\tilde{S}_{FQH}$, where all field insertions are outside the droplet. To this end, one can, in principle, "integrate out" the droplet. We are then left with a field theory that lives on the complex plane with a disk of radius R cut out of it. Assuming short-range correlations inside the droplet, the action of this new field theory $\hat{S}_{FQH}$ can be written as $\hat{S}_{FQH} = S_{\mathrm{CFT}_{\mathcal{A}}} + S_b(R)$,

where $S_{\mathrm{CFT}_{\mathcal{A}}}$ is the action of $\mathrm{CFT}_{\mathcal{A}}$ outside the droplet and $S_b(N)$ is a *boundary action* that is localised on the edge of the droplet (i.e. an integral of local operators along the droplet). We note that as the perturbation in the partition function of Eq. 3.61 has explicit radial dependence one would expect that the boundary action $S_b(N)$ has some dependence on the number of particles in the droplet (as $R \propto \sqrt{N}$).

If the radius of the droplet R is large, then, in principle, we can perform an RG transformation of $\hat{S}_{FQH}$. Such an RG procedure would shrink the radius of the droplet edge. If R is large enough then one can perform a sufficient amount of RG flow whilst keeping the radius of the droplet edge much larger than the magnetic length. One expects that under RG flow the action outside the droplet, S_{CFT_A}, will remain invariant, as this is the action of a CFT, and only the boundary action (on the edge of the droplet), $S_b(N)$, will change. After a sufficient amount of RG flow, one would expect $S_b(N)$ to be close to some *fixed point* boundary action $S_b^*(N)$, $S_b(N) \to S_b^*(N)$. As $S_b(N)$ may have some N dependence the fixed point boundary action that it flows towards $S_b^*(N)$ may also have some N dependence. Thus, edge-state inner products which correspond to long wavelength modes of a correlation function of $\hat{S}_{FQH}$ should be accurately described by $S_b^*(N)$.

As in Chap. 2, we expect these fixed point boundary actions are described by *fixed point boundary conditions*[101, 102, 134, 135] that take the form where some field of $\mathcal{A}$ inserted at the boundary, with a scaling dimension h, can be replaced by some linear combination of fields of $\overline{\mathcal{A}}$ with the same scaling dimension h (inside correlation functions). Thus, one would expect $S_b^*(N)$ to be described by a boundary condition (on the edge of the droplet) of the form,

$$\phi_l^\dagger(z) = \left(\frac{\bar{z}}{z}\right)^h \sum_{l'} M(N)_{ll'} \bar{\phi}_{l'}(\bar{z}) \tag{3.63}$$

where, by $U(1)$ charge conservation, the $\phi_l^\dagger(z)$ can only be replaced with $\bar{\phi}_{l'}(\bar{z})$, h is the scaling dimension of $\phi_l^\dagger(z)$ and $M(N)$ is a matrix that may depend on the number of

particles in the droplet. The $(\bar{z}/z)^h$ factor appears as $\phi_l^\dagger(z)$ has the opposite conformal spin of $\bar{\phi}_{l'}(\bar{z})$

It can be argued, although not rigorously, that this boundary condition should occur. As we discussed in Sec. 3.1, the $\overline{\tilde{\Omega}}(z,\bar{z})\tilde{\Omega}(z,\bar{z})$ insertions behave analogously to a screening plasma. Let the "electric" charge of $\overline{\tilde{\Omega}}(z,\bar{z})\tilde{\Omega}(z,\bar{z})$ be one, which then gives the electric charge of $\phi_l(z)$ and $\phi_l^\dagger(z)$ to be $1/2$ and $-1/2$ respectively. Now consider a correlation function with $\phi_l^\dagger(z)$ inserted very close (i.e. on the order of a magnetic length) to the droplet edge with all other field insertions of the correlation function outside the droplet. By the screening property, the configuration of the $\overline{\tilde{\Omega}}(z,\bar{z})\tilde{\Omega}(z,\bar{z})$ insertions that are the dominant contributions to the correlation function, are such that their density profile is uniform over the droplet except near $\phi_l^\dagger(z)$ where there must be a $1/2$ charge excess to screen the charge of $\phi_l^\dagger(z)$. One then expects that the correlation function can be recast by "fusing" $\phi_l^\dagger(z)$ with this charge excess which leaves some linear combination of the $\bar{\phi}_l(\bar{z})$, on long length scales. Thus, we expect that on long length scales a $\phi_l^\dagger(z)$ insertion at the droplet edge can be replaced with some linear combination of $\bar{\phi}_{l'}(\bar{z})$ insertions at the same location which gives the boundary condition of Eq. 3.63.

Amongst these possible boundary conditions is one that takes the form,

$$\phi_l^\dagger(z) = \left(\frac{\bar{z}}{z}\right)^h \bar{\phi}_l(\bar{z}) \tag{3.64}$$

on the droplet edge. Let $\langle \ldots \rangle_1$ denote the correlation function of $\mathrm{CFT}_{\mathcal{A}}$ with this boundary condition at the edge of the disk. These can be expressed using the CFT_A on the full complex plane as, $\langle \prod_i \phi_i(z_i) \prod_j \bar{\phi}_j(\bar{z}_j) \rangle_1 = \langle 0| \overline{\langle 0|} \prod_i \phi_i(z_i) \prod_j \bar{\phi}_j(\bar{z}_j) R^{L_0+\bar{L}_0} |B\rangle$, for some state $|B\rangle$. We have included a factor of $R^{L_0+\bar{L}_0}$ so that $|B\rangle$ is a state that satisfies the condition $[\phi_l^\dagger(z) - (\bar{z}/z)^h \bar{\phi}_l(\bar{z})] |B\rangle = 0$ where $|z| = 1$ (which enforces the required boundary condition for the $\langle \ldots \rangle_1$ correlation functions). Written in terms of the modes of the fields this reads,

$$[\phi^\dagger_{l,n} - \bar{\phi}_{l,-n}]\,|B\rangle = 0 \tag{3.65}$$

That is $|B\rangle$ is an Ishibashi state. Furthermore, as we are only interested in correlation functions of fields of $\mathcal{A}$ and $\overline{\mathcal{A}}$, one can take $|B\rangle \in \mathcal{H}_0 \otimes \overline{\mathcal{H}}_0$. This implies, that the state $|B\rangle$ is completely determined by the condition of Eq. 3.65 with the property $\langle v|\,\overline{\langle w|}\,|B\rangle \propto \langle v|w\rangle$. Finally, as every field of $\mathcal{A}$ is generated by repeated OPEs of $\phi_l(z)$ and $\phi^\dagger_l(z)$, the boundary condition of Eq. 3.64 implies that any field of $\mathcal{A}$ inserted at the boundary can be replaced by some linear combination of insertions of fields of $\overline{\mathcal{A}}$ at the same point. We can then take $\mathcal{A}$ as the set of *boundary operators*.

We now conjecture some restrictions on possible corresponding boundary conditions of Eq. 3.63 that encodes the fixed point $S^*_b(N)$. Let $\langle\ldots\rangle_{2,N}$ denote the correlation functions of $\mathrm{CFT}_{\mathcal{A}}$ with the $S^*_b(N)$ boundary perturbation on the edge of the disk. By the locality of this boundary action, one may expect $S^*_b(N)$ to be described by local, exactly marginal, perturbation of the boundary action that enforces the boundary condition of Eq. 3.64. We do not have a rigorous justification for this and it should be taken as conjecture. More explicitly, we expect $\langle\prod_i \phi_i(z_i)\prod_j \bar{\phi}_j(\bar{z}_j)\rangle_{2,N} = \langle\prod_i \phi_i(z_i)\prod_j \bar{\phi}_j(\bar{z}_j)e^{\delta S^*_b(N)}\rangle_1$, where $\delta S^*_b(N)$ is an integral along the disk boundary of local boundary operators of the $\langle\ldots\rangle_1$ theory. Thus, these correlation functions can also be expressed as $\langle\prod_i \phi_i(z_i)\prod_j \bar{\phi}_j(\bar{z}_j)\rangle_{2,N} = \langle 0|\,\overline{\langle 0|}\prod_i \phi_i(z_i)\prod_j \bar{\phi}_j(\bar{z}_j)e^{\delta S^*_b(N)}R^{L_0+\bar{L}_0}$ $\times\,|B\rangle$. The boundary operators in $\delta S^*_b(N)$ must be $U(1)$ neutral, by $U(1)$ charge conservation, must have scaling dimension one, for this to be a marginal *boundary* perturbation, and can be taken to be fields from $\mathcal{A}$ by the discussion of the above paragraph. Thus, $\delta S^*_b(N) = \sum_a \oint_{|z|=R}\frac{dz}{2\pi i}f_a(N;\theta)J^a(z)$, where $J^a(z)$ form a basis of $U(1)$ neutral fields of $\mathcal{A}$ with scaling dimension one, θ is the usual polar coordinate around the edge of the disk and $f_a(N;\theta)$ are some complex-valued functions. Assuming rotational invariance[11], however, $f_a(N;\theta)$ must take the form $f_a(N;\theta) = f_a(N)$.

[11]This holds so long as the angular momentum operator maps to the CFT as a linear combination of L_0 and a_0, which is the case for all the Parton states with a unique lowest angular momentum state.

Hence, we are left with $\delta S_b^*(N) = \sum_a f_a(N) \oint_{|z|=R} \frac{dz}{2\pi i} J^a(z) = \sum_a f_a(N) J_0^a$. As $\delta S_b^*(N)$ is a sum of zero modes of $U(1)$ neutral scaling dimension one fields (belonging to $\mathcal{A}$), the commutation relation $[\delta S_b^*(N), \phi_l^\dagger(z)]$ will be expressable as a sum of fields, at z, with the same scaling dimension and $U(1)$ charge of $\phi_l^\dagger(z)$. By passing the $\phi_l^\dagger(z)$ field through $e^{\delta S_b^*(N)}$, one can show the boundary condition for the $\langle \ldots \rangle_{2,N}$ theory will take the form of Eq. 3.63.

Thus, assuming generalised screening and the above conjecture, one expects the inner products corresponding to long wavelength modes of correlation functions, for large N, to take the form,

$$\frac{\langle\langle \Psi_{\langle w|} | \Psi_{\langle v|} \rangle\rangle}{Z_N} \approx \langle v| \overline{\langle w|} e^{\delta S_b^*(N)} R^{L_0 + \bar{L}_0} |B\rangle = \langle v| R^{2L_0} e^{\delta S_b^*(N)} |w\rangle \tag{3.66}$$

This is consistent with the results of Sec. 3.2. By modifying the edge state map by the replacement $\langle v| \to \langle v| e^{-\frac{\delta S_b^*(N)}{2}} R^{-L_0}$ then we have, for large N,

$$\frac{\langle\langle \Psi_{\langle w| e^{-\delta S_b^*(N)/2} R^{-L_0}} | \Psi_{\langle v| e^{-\delta S_b^*(N)/2} R^{-L_0}} \rangle\rangle}{Z_N} \approx \langle v|w\rangle \tag{3.67}$$

Hence, given generalised screening and the above conjecture, there exists a simple modification of the edge state map which becomes an isometric isomorphism in the thermodynamic limit. Even without the conjecture that the $\langle \ldots \rangle_{2,N}$ theory is an exact marginal perturbation of $\langle \ldots \rangle_1$, one can still obtain an isometric isomorphism with the generic fixed point boundary condition of Eq. 3.63, provided the matrix $M_{ll'}(N)$ is invertible. We will assume this conjecture to be true for the remainder of this section.

For intermediate system sizes N, one must consider the RG irrelevant terms in the boundary action $S_b(N)$. This can also be described as a perturbation of the boundary action enforcing the Eq. 3.64, which we denote $\delta S_b(N)$, that includes the exactly marginal $\delta S_b^*(N)$ term and boundary RG irrelevant terms. This can be expressed in the form, $\delta S_b(N) = \delta S_b^*(N) + \sum_{h_j > 1} \alpha_j(N) (2\pi)^{-1} \int_{|z|=R} |dz| e^{i h_j \theta} \phi_j(z)$, where $\phi_j(z)$ are fields of $\mathcal{A}$ with corresponding scaling dimension h_j, $\alpha(N)$ are numbers, and the $e^{i h_j \theta}$ is

required by rotational invarience. In principle, the $\alpha_j(N)$ can depend on the number of particles in the droplet, because of the explicit radial dependence in the perturbation in the partition function of Eq. 3.61. This then gives the following form for edge-state inner products at intermediate system sizes,

$$\frac{\langle\langle \Psi_{\langle w|} | \Psi_{\langle v|} \rangle\rangle}{Z_N} = \langle v| \, R^{2L_0} e^{\delta S_b(N)} \, |w\rangle \tag{3.68}$$

with,

$$\delta S_b(N) = \sum_a f_a(N) J_0^a + \sum_{h_j>1} \frac{\alpha_j(N)}{R^{h_j-1}} \oint \frac{dz}{2\pi i} z^{h_j-1} \phi_j(z) \tag{3.69}$$

where we have used $|dz| e^{h_j\theta} = \frac{dz}{iR^{h_j-1}} z^{h_j-1}$ (at $|z| = R$). Despite the possible N dependence of the α_j, we still expect, by these RG arguments, that for large, but finite N, the edge-state inner products are accurately described by a small number of the most RG relevant terms.

3.4.2 Real-space entanglement spectra

We now will briefly discuss the structure of the real-space entanglement spectrum (RSES). This is a rather straightforward extension of the calculation in DRR's work. We merely wish to point out that DRR's result can be extended to more general CFT constructions.

We take a circular real-space cut centred at the origin with radius $R_c = R/\sqrt{2}$, so that the average number of particles inside the cut is $N/2$ (with R again being the radius of the droplet). We have chosen this particular radius merely for simplicity of exposition and is of no conceptual significance. Let the region inside the real-space cut be A and the region outside be B.

We now define two edge state maps for these two subsystems. For subsystem A we have,

$$|\Psi^A_{\langle v|}\rangle\rangle \equiv \langle v|\, R_c^{-2L_0} C(N/2) e^{\int_A d^2z e^{-\frac{|z|^2}{4}} \Omega(z,\bar{z}) \otimes c^\dagger(z)} \,|0\rangle \otimes |0\rangle\rangle \tag{3.70}$$

and for subsystem B we have,

$$|\Psi^B_{|v\rangle}\rangle\rangle \equiv \langle 0|\, C(N) e^{\int_B d^2z e^{-\frac{|z|^2}{4}} \Omega(z,\bar{z}) \otimes c^\dagger(z)} C^\dagger(N/2) R_c^{2L_0} \,|v\rangle \otimes |0\rangle\rangle \tag{3.71}$$

For subsystems A and B the edge state inner products can be expressed in the form, $\langle\langle \Psi^A_{\langle w|} | \Psi^A_{\langle v|} \rangle\rangle = \langle v|\, e^{\delta S_b^A(N/2)} \,|w\rangle$ and $\langle\langle \Psi^B_{|w\rangle} | \Psi^B_{|v\rangle} \rangle\rangle = \langle w|\, e^{\delta S_b^B(N/2)} \,|v\rangle$ respectively. We absorbed the Z_N^A and Z_N^B factors into $\delta S_b^A(N)$ and $\delta S_b^B(N)$ respectively (for simplicity of notation). Assuming generalised screening holds, along with the additional conjecture, then we expect $\delta S_b^A(N)$ and $\delta S_b^B(N)$ to take the local form of Eq. 3.69.

Now define the entanglement action, S_{ES}, by $e^{-\frac{S_{ES}}{2}} = e^{\frac{\delta S_b^B(N)}{2}} e^{\frac{\delta S_b^A(N)}{2}}$. We write the singular value decompositon $e^{-\frac{S_{ES}}{2}} = \sum_i e^{-\xi_i} \,|u_i\rangle \langle v_i|$, where $|v_i\rangle$ form an orthonormal basis and $|u_i\rangle$ form another orthonormal basis. We can then perform the following resolution of the identity,

$$\begin{aligned} \mathbf{1} =& C^\dagger(N/2) R_c^{2L_0} e^{-\frac{\delta S_b^B(N)}{2}} e^{-\frac{S_{ES}}{2}} e^{-\frac{\delta S_b^A(N)}{2}} R_c^{-2L_0} C(N/2) \\ =& \sum_i e^{-\xi_i} C^\dagger(N/2) R_c^{2L_0} e^{-\frac{\delta S_b^B(N)}{2}} \,|u_i\rangle \langle v_i|\, e^{-\frac{\delta S_b^A(N)}{2}} R_c^{-2L_0} C(N/2) \end{aligned} \tag{3.72}$$

We can then express the ground state trial wave function in the following form,

$$\begin{aligned} |\Psi_{\langle 0|}\rangle\rangle &= \langle 0|\, C(N) e^{\int d^2z e^{-\frac{|z|^2}{4}} \Omega(z,\bar{z}) \otimes c^\dagger(z)} \,|0\rangle \otimes |0\rangle\rangle \\ &= \langle 0|\, C(N) e^{\int_B d^2z e^{-\frac{|z|^2}{4}} \Omega(z,\bar{z}) \otimes c^\dagger(z)} e^{\int_A d^2z e^{-\frac{|z|^2}{4}} \Omega(z,\bar{z}) \otimes c^\dagger(z)} \,|0\rangle \otimes |0\rangle\rangle \end{aligned} \tag{3.73}$$

Then inserting the resolution of the identity in the middle, we have,

$$|\Psi_{\langle 0|}\rangle\rangle = \sum_i e^{-\frac{\xi_i}{2}} \left| \Psi^B_{\;\; e^{-\frac{\delta S_b^B(N)}{2}} |u_i\rangle} \right\rangle\rangle \left| \Psi^A_{\;\; \langle v_i| e^{-\frac{\delta S_b^A(N)}{2}}} \right\rangle\rangle \tag{3.74}$$

This then provides a Schmidt decomposition, which implies that the set of ξ_i, which are the eigenvalues of S_{ES}, forms the entanglement spectrum.

Even if it is not known if generalised screening holds, one can use the above expression to give upper bounds for entanglement level counting in terms of the state counting of $\mathcal{A}$, provided the mapping of the angular momentum operator to the CFT is known.

If the generalised screening hypothesis holds along with the extra conjecture, then from $e^{-\frac{S_{ES}}{2}} = e^{\frac{\delta S_b^B(N)}{2}} e^{\frac{\delta S_b^A(N)}{2}}$ and through the Baker-Cambell-Housdorf formula one can show S_{ES} will take the form of Eq. 3.69. This form of S_{ES} then implies that for large N and for states within the scaling region, the entanglement level state counting will match the state counting of the vacuum representation of $\mathcal{A}$.

In principle then, one can use this result to explain some of the observations of Ref. [136] regarding the RSES of Parton wave functions. However, this will not be discussed here.

3.5 Numerical tests

We will now present our numerical tests of whether Eqs. 3.68 and 3.69 hold in the case of the *unprojected* $\nu = 2/5$ CF state and the *unprojected* ϕ_2^2 Parton state, which is at filling fraction $\nu = 1$. In Sec. 3.5.1 the model inner product action in each case will be discussed, along with how these models were fit to Monte Carlo estimated inner-products in Sec. 3.5.2. Finally, in Sec. 3.5.3 the result these tests are presented, which are found to be consistent with generalised screening.

3.5.1 The models

The following models for the inner product action only contain terms up to scaling dimension two, for simplicity. In principle, there are many fields from the corresponding chiral algebra at scaling dimension two that could appear. However, we *empirically* find that only a small number of these terms are needed to model the inner products with

sufficient accuracy. It may be possible to constrain the inner product action using translation symmetry [35, 105], however, this will not be pursued here.

For the $\nu = 2/5$ CF case the model inner product action is given by,

$$\delta\hat{S}_b = \alpha J_0^3 + \beta J_0^1 + \oint \frac{dz}{2\pi i} z[\gamma : (J^3(z))^2 : +\sqrt{2}\delta J^3(z) i\partial\Phi(z)] \tag{3.75}$$

where $J^3(z) \equiv \frac{i\partial\varphi^{(2)}(z) - i\partial\varphi^{(1)}(z)}{2}$ and $J^1(z) \equiv \frac{:V_1(z)V_2^\dagger(z): + :V_2(z)V_1^\dagger(z):}{\sqrt{2}}$ are the $\widehat{\mathfrak{su}}(2)_1$ currents corresponding to this state (i.e. a special case of Eq. 3.51), and α, β, γ and δ are model parameters that require fitting. The zero mode of $i\partial\Phi(z)$, a_0, is not included as we only fit the inner product action using states with a fixed number of particles and so this term would not be detectable. It should be stressed that Eq.3.69 does not predict the N dependence of α and β. However, by analogy with the result for $\nu = 2$ in Eq. 3.39, one can make an educated guess that $\alpha \sim \ln N$ and $\beta \sim (\ln N)/N$. Furthermore, from previous works [35, 105] we expect $\gamma, \delta \sim 1/\sqrt{N}$ (i.e. under the assumption that the $\alpha_i(N)$ of Eq. 3.69 do not depend on N).

For the ϕ_2^2 state the model inner product action is,

$$\delta\hat{S}_b = \alpha J_0^3 + \beta J_0^1 + \oint \frac{dz}{2\pi i} z\left[\frac{\gamma}{2} : (J^3(z))^2 : +\delta J^3(z) i\partial\Phi(z) + \frac{\epsilon}{2}[: (J^1(z))^2 : + : (J^2(z))^2 :]\right] \tag{3.76}$$

where the $J^a(z)$ and $\Phi(z)$ fields are the $\hat{\mathfrak{u}}(1)\oplus\widehat{\mathfrak{su}}(2)_2$ currents corresponding to this state, where the corresponding generators of J^a are $T^a_{ij} = \sigma_{p(i)p(j)}/2$ with the permutation $p(1) = 2, p(2) = 1$ (i.e. they are proportional to "spin-flipped" Pauli matrices)[12]. As for the CF case, we do not include the zeroth mode of $i\partial\Phi(z)$ and we expect $\alpha \sim \ln N$, $\beta \sim (\ln N)/N$ and $\gamma, \delta, \epsilon \sim 1/\sqrt{N}$.

[12]This is just a convention to be consistent with the choice made for the $\nu = 2/5$.

3.5.2 Fitting procedure

The general procedure is as follows. Let $|M;i\rangle$ be an orthonormal basis of states in the given CFT which have L_0 eigenvalue M and are all $U(1)$ neutral (i.e. $a_0 |M;i\rangle = 0$) so that they map to neutral edge excitations. We assume that the background charge operator, $C(N)$, has been chosen such that these wave functions $|\Psi_{\langle M;i|}\rangle\rangle$ all have angular momentum M *relative* to the ground state trial wave function $|\Psi_{\langle 0|}\rangle\rangle$. This then gives $\langle\langle\Psi_{\langle M;i|}|\Psi_{\langle M';j|}\rangle\rangle = \langle M';j| R^{2L_0} e^{\delta S_b} |M;i\rangle = 0$ for $M \neq M'$. Thus, $\langle M';j| \delta S_b |M;i\rangle = 0$ for $M \neq M'$, which means the operator δS_b must be a block diagonal matrix relative to the $|M;j\rangle$ basis. We then define the series of matrices $G(M)_{ij} \equiv \langle\langle\Psi_{\langle M;j|}|\Psi_{\langle M;i|}\rangle\rangle / R^{2M} = \langle M;i| e^{\delta S_b} |M;j\rangle$. After taking the log of these matrices we have, $[\ln G(M)]_{ij} = \langle M;i| \delta S_b |M;j\rangle$.

To fit the model entanglement action we first compute the $G(M)_{ij}$ using Monte Carlo integration and then the log of these matrices is taken to give estimates for the matrix elements of δS_b. The parameters of the model inner product action are then determined by minimising the sum of squared differences between the model and estimated matrix elements of δS_b, over the $M = 1$ subspace for the $\nu = \frac{2}{5}$ case and the $M = 1, 2$ subspaces for the ϕ_2^2 case, where each matrix element is equally weighted.

For the $\nu = 2/5$ CF state the chosen basis takes the form $|\lambda_1;\lambda_2;p\rangle \equiv \prod_{n_1\in\lambda_1} a_{-n_1} \prod_{n_2\in\lambda_2} J^3_{n_2} (F_2 F_1^\dagger)^p |0\rangle / \sqrt{\mathcal{N}}$, where λ_i are partitions and $\mathcal{N}$ is a normalisation factor. From the gauge invarience of the edge state map the $|\lambda_1;\lambda_2;p\rangle$ state will map to the same edge state as $\prod_{n_1\in\lambda_1} \sqrt{5/2}(\tilde{a}^{(1)}_{-n_1} + \tilde{a}^{(2)}_{-n_1}) \prod_{n_2\in\lambda_2} \sqrt{2}^{-1}(\tilde{a}^{(2)}_{n_2} - \tilde{a}^{(1)}_{n_2})(F_2 F_1^\dagger)^p |0\rangle / \sqrt{\mathcal{N}}$. Using the usual bosonisation relations, such states can be expressed as polynomials in the modes of the $\tilde{V}_j(z)$ fields applied on the vacuum, which then allows for the $\Psi_{\langle\lambda_1;\lambda_2;p|}(\mathbf{z})$ wave functions to be expressed as a sum of Slater determinants of the z^m and $\bar{z}z^m$ orbitals, times the flux attaching Jastrow factor. By expressing the $\Psi_{\langle\lambda_1;\lambda_2;p|}(\mathbf{z})$ wave function in this form the $G(M)$ matrices can then be computed using Monte Carlo integration. To find the matrix elements of the model δS_b we first note that J^3_0 and

$([J^3]^2)_0 \equiv \oint \frac{dz}{2\pi i} z : (J^3(z))^2 :$ are diagonal in the $|\lambda_1;\lambda_2;p\rangle$ basis with $J_0^3 |\lambda_1;\lambda_2;p\rangle = p\,|\lambda_1;\lambda_2;p\rangle$ and $([J^3]^2)_0 |\lambda_1;\lambda_2;p\rangle = [p^2 + (\sum_{n\in\lambda_2} n)]\,|\lambda_1;\lambda_2;p\rangle$. The matrix elements of J_0^1 can be computed by first noting that $J_0^1 = (J_0^+ + J_0^-)/2$. Then define the chiral boson field $\eta(z) \equiv -i\sqrt{2}\ln z J_0^3 + i\sum_n J_n^3 \frac{z^{-n}}{n}$, which can be used to express the $J^{\pm}(z)$ fields as $J^{\pm}(z) = (F_2 F_1^{\dagger})^{\pm 1} : e^{\pm i\sqrt{2}\eta(z)} :$ (i.e. the free field representation of $\widehat{\mathfrak{su}}(2)_1$ [20]). The matrix elements of $J_0^{\pm}$ operators are then equivalent to the matrix elements of modes of chiral vertex operators of a chiral boson which can be computed by a generating function method.

For the ϕ_2^2 Parton case the space of states in the vacuum representation of $\mathcal{A}(2)_2$ that are $U(1)$ charge neutral form the vacuum representation of $\hat{\mathfrak{u}}(1) \oplus \widehat{\mathfrak{su}}(2)_2$. The $\mathfrak{u}(1)$ part is generated by the modes of $i\partial\Phi(z)$ and the $\widehat{\mathfrak{su}}(2)_2$ part can be *represented* using a Majorana field $\psi(z)$ and a chiral boson $\varphi(z)$ with compactification radius one and corresponding Klein factor denoted by F_φ (where this Klein factor should anti-commute with the Majorana field) [137]. We discuss this in more detail in Appendix 3.B and will give a summary here. We denote the chosen basis for the system containing the $\Phi(z)$, $\psi(z)$ and $\varphi(z)$ as $|\lambda_1;\mu,\lambda_2;p\rangle = \prod_{n_1\in\lambda_1} a_{n_1} \prod_{n_3\in\lambda_3} a_{-n_3}^{(\varphi)} F_\varphi^p \prod_{-n_2\in\mu} \psi_{-\frac{n_2}{2}} |0\rangle / \sqrt{\mathcal{N}}$, where $a_n^{(\varphi)}$ are the modes of $\varphi(z)$, λ_i are partitions, μ is a partition with no repeated elements and where all elements are odd, $p \in \mathbb{Z}$, and $\mathcal{N}$ is used to normalise the state. The vacuum representation of $\hat{\mathfrak{u}}(1) \oplus \widehat{\mathfrak{su}}(2)_2$ is spanned by the basis elements $|\lambda_1;\mu;\lambda_2;p\rangle$, such that the parities of the number of elements in μ and p are equal. We further detail how this basis of the $\hat{\mathfrak{u}}(1) \oplus \widehat{\mathfrak{su}}(2)_2$ can be mapped back to states of $\mathcal{H}_L$ with the given states being expressed as modes of the $\tilde{V}_{ij}(z)$ and $\tilde{V}_{ij}^{\dagger}(z)$ fields applied on the vacuum. Expressing the basis this way allows $|\Psi_{\langle\lambda_1;\mu;\lambda_2;p|}\rangle\rangle$ to be expressed as a sum of products of Slater determinants of the z^m and $\bar{z}z^m$ orbitals using the IQH edge state map, which allows for the $G(M)$ matrices to be estimated. The computation of the matrix elements of the model inner product action is also discussed in Appendix 3.B.

3.5.3 Results

3.5.3.1 $\nu = 2/5$ CF

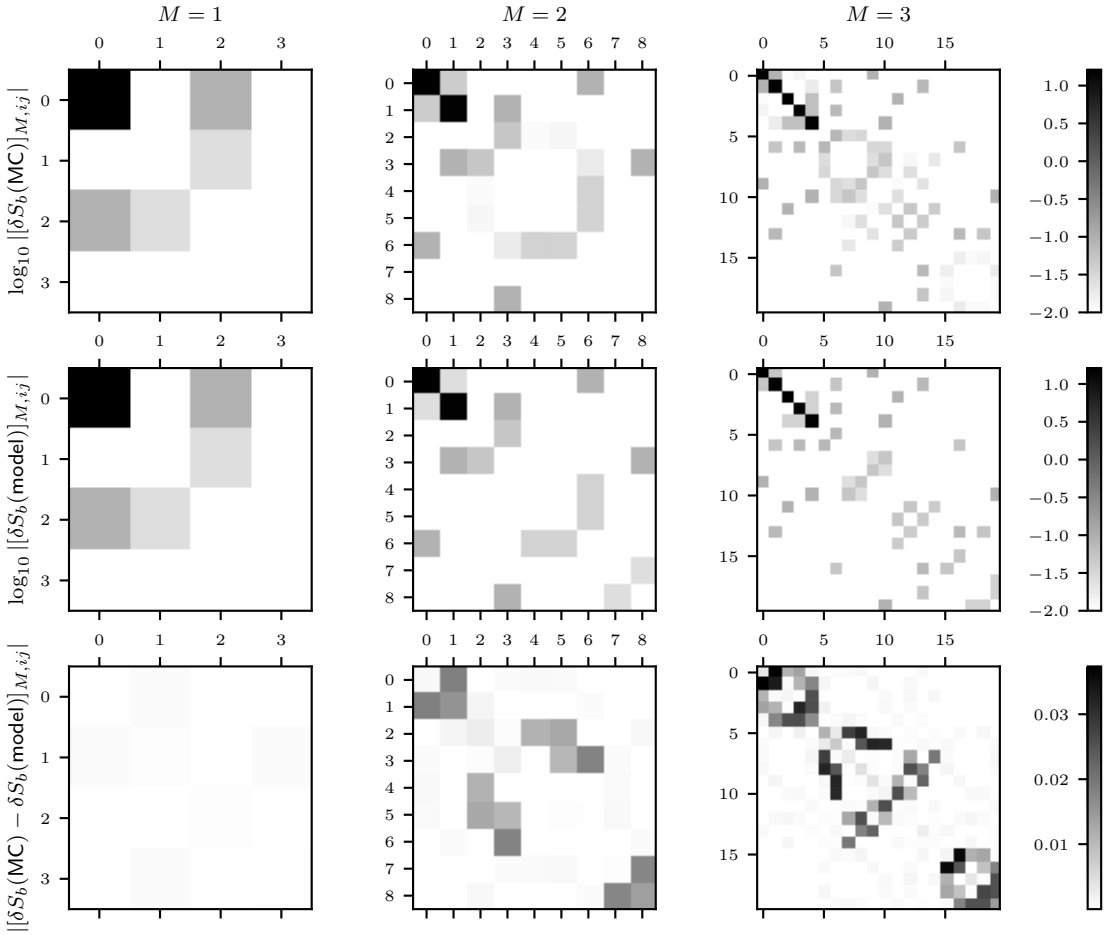

Figure 3.1: Comparison between the Monte Carlo (MC) estimated and model (Model) inner product action matrix elements, for the case of $\nu = 2/5$ CF state where the ground state wave function contains $N = 55$ fermions. We use the shorthand notation $[\delta S_b]_{M,ij} \equiv \langle M; i| \, \delta S_b \, |M; j\rangle$, where the basis reference for the index i can be found in Appendix 3.C. Note that when presenting the $\log_{10}$ of the absolute value of the matrix elements, we have used a cutoff where any matrix elements whose absolute value is below 10^{-2} have been replaced by 10^{-2}, for clarity. No cuttof has been used for the matrix element errors, $|[\delta S_b(\mathrm{MC}) - \delta S_b(\mathrm{Model})]_{M,ij}|$.

Fig. 3.1 shows a comparison of the resulting fitted model (Model) inner product action matrix elements and the Monte Carlo (MC) estimated inner product action matrix elements for the $U(1)$ neutral CFT states with L_0 eigenvalues $M = 1, 2, 3$, in

the case where the ground state trial wave function contains $N = 55$ fermions. We use the shorthand notation $[\delta S_b]_{M,ij} \equiv \langle M; i| \, \delta S_b \, |M; j\rangle$ for the inner product action matrix elements, where the basis reference for the index i is given in Table 3.1 in Appendix 3.C. The first two rows show a colour map of the $\log_{10}$ of the absolute value of the MC estimated matrix elements and fitted model matrix elements, where we have introduced a cutoff such that any matrix element with an absolute value below 10^{-2} is replaced with 10^{-2}, for clarity. The third row shows a colour map of the absolute values of the errors of the matrix elements (i.e. the difference between the MC and model matrix elements), where no cutoff is used. We find the model matrix elements to be in good agreement with the MC matrix elements with errors $\lessapprox 3 \times 10^{-2}$.

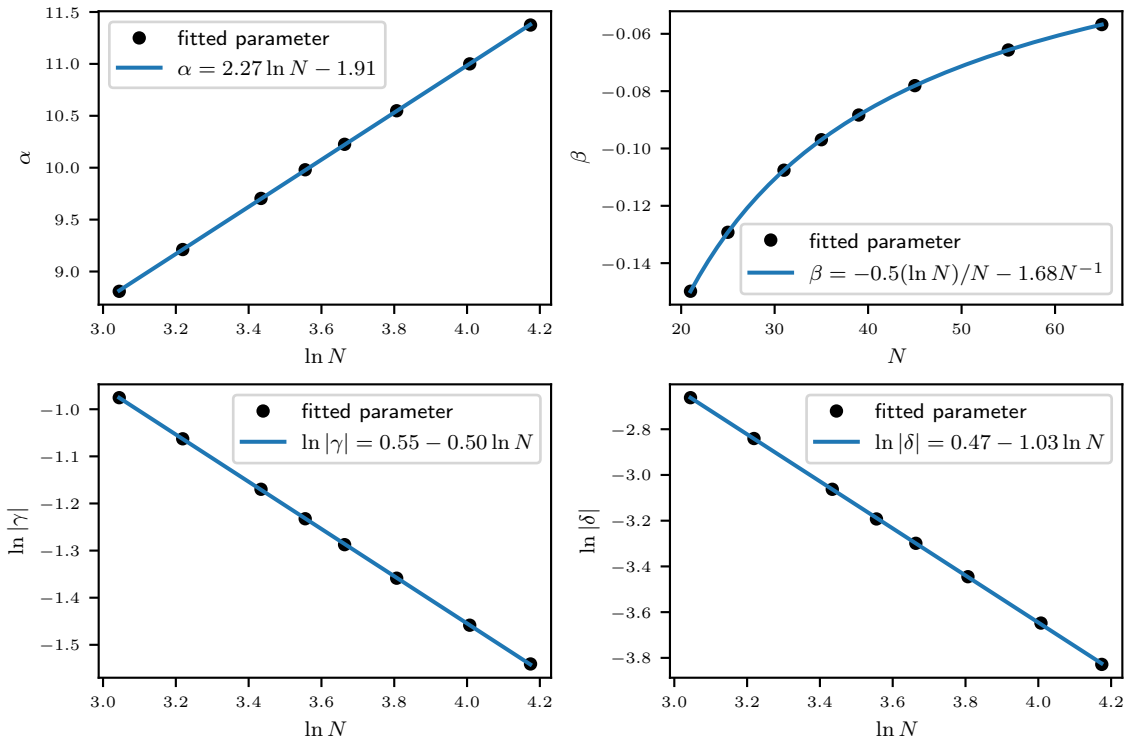

Figure 3.2: Shows the fitted $\nu = 2/5$ CF inner product action model parameters α, β γ and δ, of Eq. 3.75, for various system sizes N, along with a fit to a particular functional form for the N dependence of each parameter.

Fig. 3.2 shows the fitted α, β, γ and δ model parameters of Eq. 3.75, for various system sizes N, along with a fit to a particular functional form for the N dependence

of each parameter. By extrapolating the fitted functions from Fig. 3.2, we see that for large N $\alpha \approx 2.3 \ln N$ and $\beta \approx -0.5(\ln N)/N$. This is in agreement with the "educated guess" of the N dependence of α and β based on the result of $\nu = 2$ in Eq. 3.39. We can then see that γ can be fit very well to the form $\gamma \sim \frac{1}{\sqrt{N}}$, as expected. The δ parameter, however, has a fitted N dependence of the form $\delta \sim \frac{1}{N}$. In Eq. 3.75 δ is the coefficient of the term $\oint \frac{dz}{2\pi i} z J^3(z) i\partial\Phi(z)$. This can also be expressed, by integration by parts, as an integral of a scaling dimension 3 term, where one would expect the $1/N$ dependence, just as was seen in Chap. 2.

3.5.3.2 ϕ_2^2 Parton

Fig. 3.3 shows the same comparison between the MC estimated and model inner product action matrix elements that was done for the CF case, but now for the ϕ_2^2 Parton case where the ground state trial wave function contains $N = 31$ bosons. We find the MC estimated matrix elements to be in good agreement with the fitted model matrix elements with errors $\lessapprox 8 \times 10^{-2}$.

Fig. 3.4 shows the fitted α, β, γ, δ and ϵ parameters, for the model of Eq. 3.76, for various system sizes N, along with a fit to a particular functional form for the N dependence of each parameter. One can see that for large N $\alpha \approx 3 \ln N$ and $\beta \approx -3.2(\ln N)/N$. This is again in agreement with our "educated guess" based on the result of $\nu = 2$, in Eq. 3.39. Despite significant noise compared with the CF case, we can then see that both γ and ϵ roughly have an N dependence of the form $\gamma, \epsilon \sim \frac{1}{\sqrt{N}}$, as expected. The δ parameter has an N dependence of the form $\delta \sim \frac{1}{N}$, which is the same N dependence for the corresponding term in the CF case. As discussed above for the CF case, this is consistent with interpreting ϵ as the coefficient of an integral of a scaling dimension 3 operator.

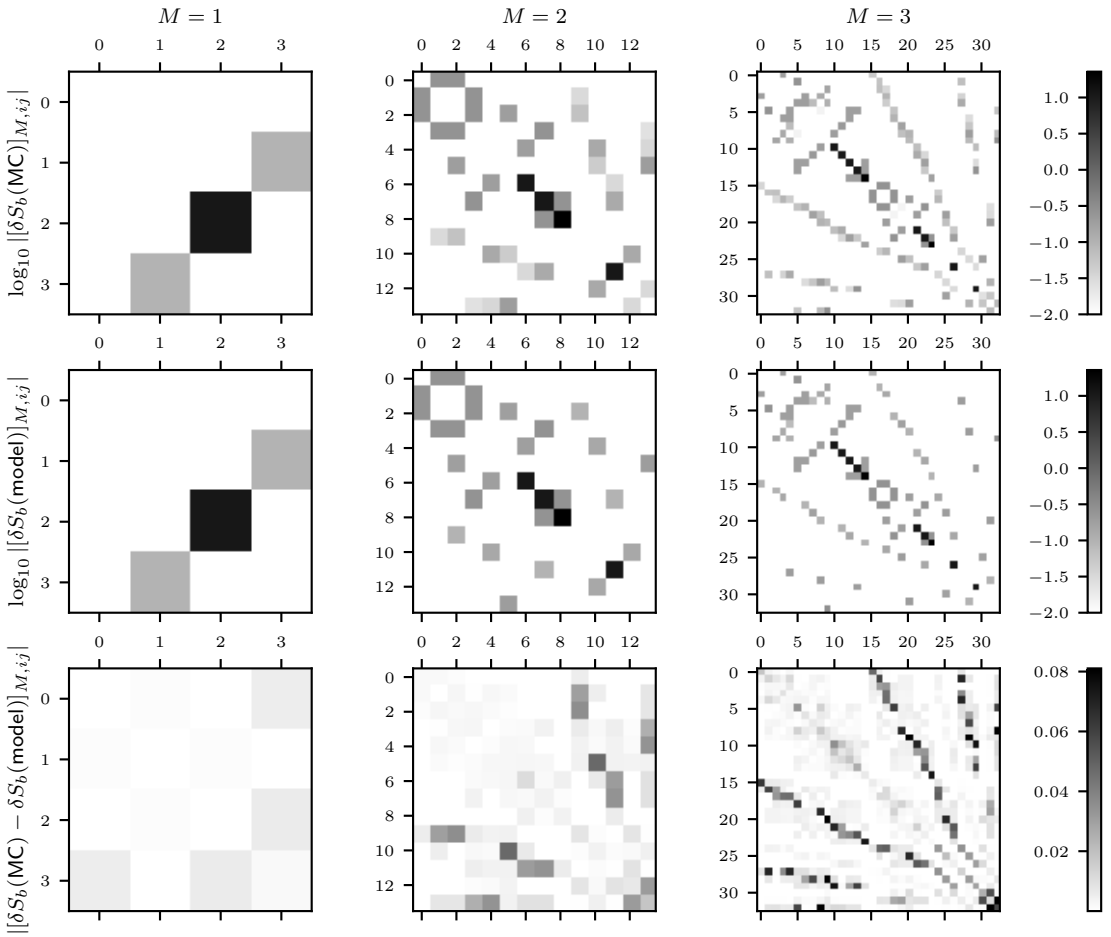

Figure 3.3: Comparison between the Monte Carlo (MC) estimated and model (Model) inner product action matrix elements, for the case of ϕ_2^2 Parton state where the ground state wave function contains $N = 31$ bosons. We use the shorthand notation $[\delta S_b]_{M,ij} \equiv \langle M; i| \, \delta S_b \, |M; j\rangle$, where the basis reference for the index i can be found in Appendix 3.C. Note that when presenting the $\log_{10}$ of the absolute value of the matrix elements, we have used a cutoff where any matrix elements whose absolute value is below 10^{-2} have been replaced by 10^{-2}, for clarity. No cuttof has been used for the matrix element errors, $|[\delta S_b(\mathrm{MC}) - \delta S_b(\mathrm{Model})]_{M,ij}|$.

3.6 Summary and outlook

In this chapter, we have extended the CFT constructions of FQHE trial wave functions to the broad class of chiral Parton-type trial wave functions in the planar geometry. More specifically, we have shown that all chiral Parton ground and edge state trial wave functions can be expressed as CFT correlation functions, where for each Parton state we

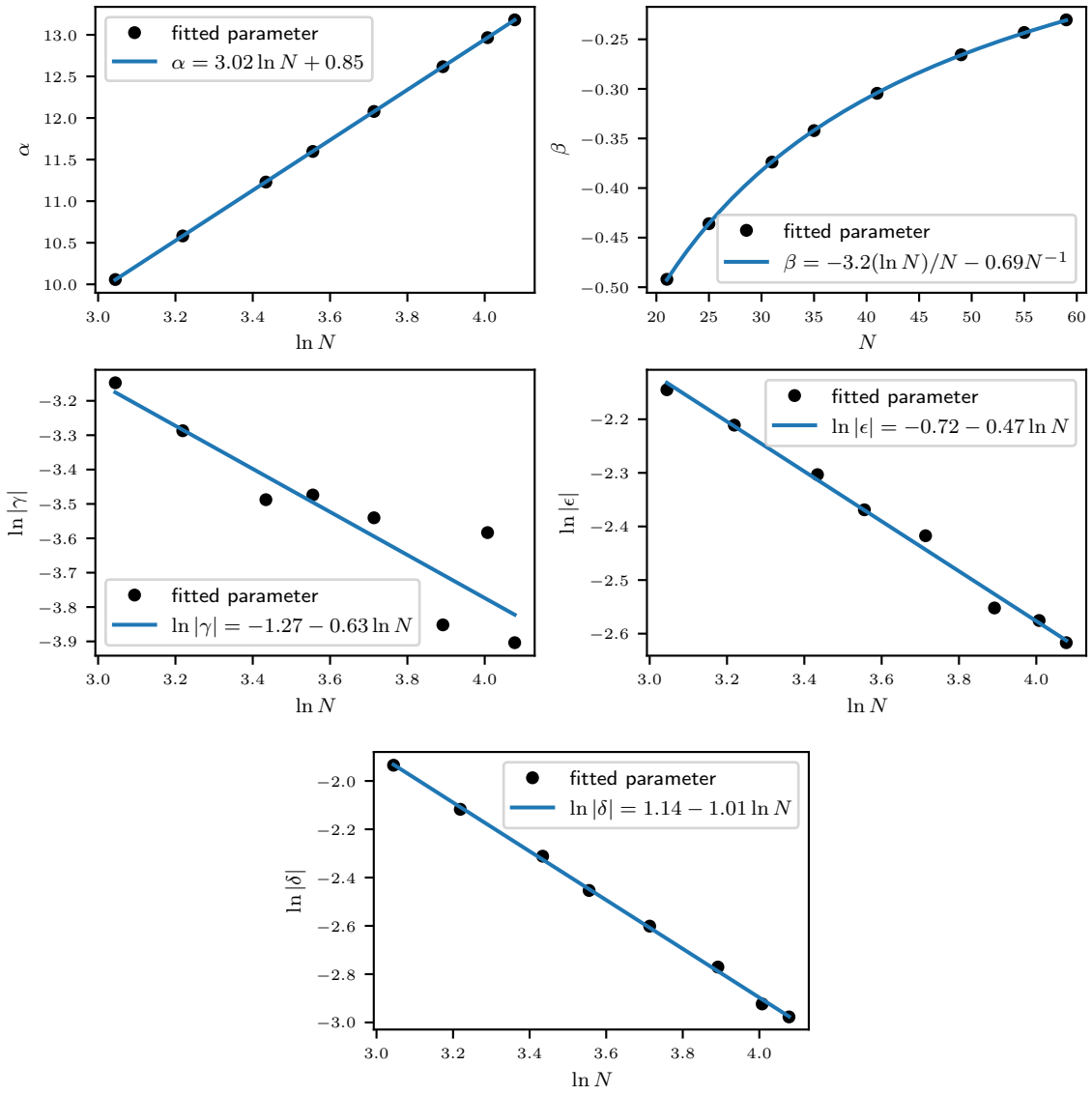

Figure 3.4: Shows the fitted ϕ_2^2 Parton inner product action model parameters α, β, γ, δ and ϵ of Eq. 3.76, for various system sizes N, along with a fit to a particular functional form for the N dependence of each parameter.

have shown how one can identify a chiral algebra $\mathcal{A}$ such that $\text{CFT}_{\mathcal{A}}$, roughly speaking, is the "smallest" CFT that can generate the ground and edge trial wave functions. From this construction, we were then able to show that all chiral CF wave functions could be expressed using CFT correlation functions without any explicit symmetrisation or anti-symmetrisation and that the symmetric Parton states, ϕ_n^m, could be expressed using the $\hat{\mathfrak{u}}(1) \oplus \widehat{\mathfrak{su}}(n)_m$ WZW model. A generalised screening hypothesis for general

chiral Parton states was then formulated, where we discussed how this can be used to generalise DRR's results for edge state inner products and the RSES for these states, which implied, assuming generalised screening and an additional conjecture, that the edge state and entanglement level counting should be the same as the state counting for chiral algebra $\mathcal{A}$ corresponding to the given Parton wave function. Finally, these implications for the edge state inner products were directly tested for the unprojected $\nu = 2/5$ CF state and the ϕ_2^2 Parton state, where no contradictions with generalised screening were found.

The identification of each Parton state with a chiral algebra $\mathcal{A}$, which one expects to describe the wave function's topological order, could in principle allow for a mathematical classification of all the possible topological orders Parton states could describe by precisely understanding which $\mathcal{A}$ correspond to which Parton wave functions. It would also be useful to explore how these CFT constructions can be extended to other geometries, such as the sphere, torus and cylinder, for completeness. Furthermore, if this can be well understood for the cylindrical geometry then one could in principle construct analytically computable arbitrarily precise MPS representations for Parton wave functions using their corresponding CFTs by using and extending the methods of Refs. [117–119]. Finally, it would also be interesting to understand if these CFT methods can be used to describe Parton wave functions with mixed chirality, which may require more general mathematical constructions than chiral algebras. Some progress has already been made in this direction for non-chiral hierarchy states [51, 52, 138].

3.A Further details for symmetric Parton wave functions

We will now show that $i\partial\Phi(z) \in \mathcal{A}(r)_m$ and $J^a(z) \in \mathcal{A}(r)_m$. To simplify the following calculation we introduce yet another set of fields $\mathtt{J}^{ij}(z) = \sum_k :\tilde{V}_{ki}\tilde{V}_{kj}^\dagger:$, which can be

expressed as linear combinations of $i\partial\Phi(z)$ and $J^a(z)$, and vice-versa. Let $p(n)_m$ be the number of ordered sets of m positive integers whose sum is n. We then have the following OPEs for $l < r$,

$$V_l(z)V_l^\dagger(w) \sim \frac{p(l+m)_m}{(z-w)^m} + \frac{\sum_{i=1}^{l+1} p(l+m-i)_{m-1}\mathtt{J}^{ii}(w)}{(z-w)^{m-1}} + \dots \tag{3.77}$$

These OPEs show that all $\mathtt{J}^{ii}(z) \in \mathcal{A}(r)_m$. The OPEs,

$$\begin{aligned} V_0(z)V_{i-1}^\dagger(w) \sim & \frac{\mathtt{J}^{1i}(w)}{(z-w)^{m-1}} + \dots \\ V_{i-1}(z)V_0^\dagger(w) \sim & \frac{\mathtt{J}^{i1}(w)}{(z-w)^{m-1}} + \dots \end{aligned} \tag{3.78}$$

imply that $\mathtt{J}^{1i}(z), \mathtt{J}^{i1}(z) \in \mathcal{A}(r)_m$. For $i \neq j \neq k$ $\mathtt{J}^{ik}(z)\mathtt{J}^{kj}(w) \sim (z-w)^{-1}\mathtt{J}^{ij}(w)$, which then implies all $\mathtt{J}^{ij}(z) \in \mathcal{A}(r)_m$. Hence, $i\partial\Phi(z), J^a(z) \in \mathcal{A}(r)_m$.

3.B Free field representation of $\widehat{\mathfrak{su}}(2)_2$ currents and Parton mapping

We will first detail how a combination of a Majorana field $\psi(z)$ and a free chiral boson $\varphi(z)$, with compactification radius one and corresponding Klein factor F_φ, can be used to generate the vacuum representation of the $\widehat{\mathfrak{su}}(2)_2$ Kac-Moody algebra.

The $\psi(z)$ field has conformal dimension of 1/2 and has the following OPE,

$$\psi(z)\psi(w) = \frac{1}{z-w} + 2(z-w)T^\psi(w) + \dots \tag{3.79}$$

where $T^\psi(z)$ is the energy-momentum tensor of this Majorana degree of freedom given by $T^\psi(z) = -\frac{1}{2} :\psi(z)\partial\psi(z):$. The above OPE implies the following anti-commutation relations $\{\psi_n, \psi_m\} = \delta_{n+m,0}$, where n and m are half-integral $n, m \in \mathbb{Z} + \frac{1}{2}$.

We then define the usual vertex operator for $\varphi(z)$ as $V_\varphi(z) \equiv F_\varphi :e^{i\varphi(z)}:$. Let the Hilbert space of this combined system of $\psi(z)$ and $\varphi(z)$ be $\mathcal{H}_{\psi,\varphi}$. This Hilbert space can

be spanned by an orthonormal basis of the form $|\mu;\lambda;p\rangle = \prod_{n_2\in\lambda} a^{(\varphi)}_{-n_2} F^p_\varphi \prod_{n_1\in\mu} \psi_{-\frac{n_1}{2}} \times |0\rangle / \sqrt{\mathcal{N}}$, where λ is a partition, μ is a partition with no repeated elements and with all elements being odd, $p \in \mathbb{Z}$, $a^{(\varphi)}_n$ are the modes of $i\partial\varphi(z)$, and $\mathcal{N}$ is used to normalise the state.

Now consider the following currents,

$$J^+(z) \equiv \sqrt{2}\psi(z)V_\varphi(z) \quad J^-(z) \equiv \sqrt{2}V^\dagger_\varphi(z)\psi(z) \quad J^3(z) \equiv i\partial\varphi(z) \tag{3.80}$$

It can be easily shown that the $J^3(z)$ and $J^\pm(z)$ currents have the OPEs corresponding to the $\widehat{\mathfrak{su}}(2)_2$ Kac-Moody algebra.

Let $\mathcal{H}_{\widehat{\mathfrak{su}}(2)_2} \subset \mathcal{H}_{\psi,\varphi}$ be the Hilbert space generated by polynomials in the modes of the $J^3(z)$ and $J^\pm(z)$ fields applied on the vacuum, $|0\rangle$. By definition $\mathcal{H}_{\widehat{\mathfrak{su}}(2)_2}$ will form the vacuum representation of $\widehat{\mathfrak{su}}(2)_2$. In fact, $\mathcal{H}_{\widehat{\mathfrak{su}}(2)_2}$ is equivalent to the space of states with even fermion parity, where F_φ has odd parity.

We first note that the Hilbert space of just the Majorana field can be split up into two irreducible representations of the Virasoro algebra formed by the modes, L^ψ_n, of $T^\psi(z)$ with central charge $c = 1/2$, with conformal dimensions 0 and 1/2. By matching the L_0 eigenvalues, both of the 0 and 1/2 representations occur with multiplicity one with corresponding primary states $|0\rangle$ and $\psi_{-\frac{1}{2}}|0\rangle$ respectively. We can then use the following *overcomplete* basis for $\mathcal{H}_{\psi,\varphi}$, with the basis elements $|0;\lambda_1;\lambda_2;p\rangle = \prod_{n_1\in\lambda_1} L^\psi_{-n_1} \prod_{n_2\in\lambda_2} a^{(\varphi)}_{-n_2} F^p_\varphi |0\rangle$ and $|1/2;\lambda_1;\lambda_2;p\rangle = (-1)^p \psi_{-\frac{1}{2}}|0;\lambda_1;\lambda_2;p\rangle$[13], where λ_i are partitions and $p \in \mathbb{Z}$. The space of states with even fermion parity is spanned by the basis elements $|0;\lambda_1;\lambda_2;p\rangle$ with p even and $|1/2;\lambda_1;\lambda_2;p\rangle$ with p odd.

Note the OPEs,

$$J^+(z)J^+(w) = -2F^2_\varphi : e^{2i\varphi(w)} : + \ldots \quad J^-(z)J^-(w) = -2F^{-2}_\varphi : e^{-2i\varphi(w)} : + \ldots \tag{3.81}$$

and,

[13]Note that ψ_k and F_φ anticommute.

$$J^+(z)J^-(w) = \frac{2}{(z-w)^2} + \frac{2J^3(w)}{z-w} + 4T^\psi(w) + (\partial J^3(w) + :(J^3(w))^2:) + \dots \quad (3.82)$$

Now let $\mathcal{H}_{\Phi,\psi,\varphi}$ be the Hilbert space of the combination of a chiral boson $\Phi(z)$, and the $\psi(z)$ and $\varphi(z)$ system we discussed above. Let $\mathcal{H}_{\hat{\mathfrak{u}}(1)\oplus\widehat{\mathfrak{su}}(2)_2} \subset \mathcal{H}_{\Phi,\psi,\varphi}$ be the space of states that are $U(1)$ charge neutral relative to $\Phi(z)$ and have even fermion parity, which forms the vacuum representation of the $\hat{\mathfrak{u}}(1) \oplus \widehat{\mathfrak{su}}(2)_2$. A basis for this space, written as $|\lambda_1;\mu;\lambda_2;p\rangle$, was given in Sec. 3.5.2. We then define the extension of the overcomplete $|0;\lambda_2;\lambda_2;p\rangle$ and $|1/2;\lambda_1;\lambda_2;p\rangle$ basis for the $\mathcal{H}_{\psi,\varphi}$ system to the $\mathcal{H}_{\Phi,\psi,\varphi}$ as,

$$\begin{aligned} |\lambda_1 : 0;\lambda_2;\lambda_3;p\rangle &\equiv \prod_{n_1\in\lambda_1} a_{-n_1} \prod_{n_2\in\lambda_2} L^\psi_{-n_2} \prod_{n_3\in\lambda_3} a^{(\varphi)}_{-n_3} F^p_\varphi |0\rangle \\ |\lambda_1 : 1/2;\lambda_2;\lambda_3;p\rangle &\equiv (-1)^p \psi_{-\frac{1}{2}} |\lambda_1 : 0;\lambda_2;\lambda;p\rangle \end{aligned} \quad (3.83)$$

Before moving on, we will now briefly discuss how the matrix elements of the model inner product action of Eq. 3.76 can be computed using this representation of $\hat{\mathfrak{u}}(1) \oplus \widehat{\mathfrak{su}}(2)_2$. We first note that $\frac{1}{2}[:(J^1(z))^2: + :(J^2(z))^2:] = T^\psi(z)$. Now let $L^\varphi_0 \equiv \frac{1}{2}\oint \frac{dz}{2\pi i} z : (J^3(z))^2 := \frac{1}{2}\oint \frac{dz}{2\pi i} z : (i\partial\varphi(z))^2 :$. In the $|\lambda_1;\mu;\lambda_2;p\rangle$ basis the operators L^ψ_0, L^φ_0 and J^3_0 are diagonal with $L^\psi_0 |\lambda_1;\mu;\lambda_2;p\rangle = [\sum_{n\in\mu} n/2] |\lambda_1;\mu;\lambda_2;p\rangle$, $L^\varphi_0 |\lambda_1;\mu;\lambda_2;p\rangle = [p^2/2 + (\sum_{n\in\lambda_2} n)] |\lambda_1;\mu;\lambda_2;p\rangle$ and $J^3_0 |\lambda_1;\mu;\lambda_2;p\rangle = p |\lambda_1;\mu;\lambda_2;p\rangle$. The matrix elements, in this basis, of the operator $(J^3 i\partial\Phi)_0 \equiv \oint \frac{dz}{2\pi i} z J^3(z) i\partial\Phi(z)$ can be computed by expressing it as $(J^3 i\partial\Phi)_0 = \sum_n a^{(\varphi)}_{-n} a_n$. Finally, the matrix elements of J^1_0 can be computed by noting that $J^1_0 = [J^+_0 + J^-_0]/2$ with $J^+_0 = \sqrt{2}\sum_k \psi_{-k} V_{\varphi,k}$ and $J^-_0 = \sqrt{2}\sum_k V^\dagger_{\varphi,-k}\psi_k$, where the matrix elements of the $V_{\varphi,k}$ and $V^\dagger_{\varphi,k}$ modes can be computed using a generating function method.

Now consider the system of four chiral bosons $\tilde{\varphi}^{(ij)}(z)$ with the Hilbert space $\mathcal{H}_L$. Within this system we have the $\hat{\mathfrak{u}}(1) \oplus \widehat{\mathfrak{su}}(2)_2$ currents,

$$
\begin{aligned}
i\partial\hat{\Phi}(z) =& \frac{1}{2}[i\partial\tilde{\varphi}^{(11)}(z) + i\partial\tilde{\varphi}^{(12)}(z) + i\partial\tilde{\varphi}^{(21)}(z) + i\partial\tilde{\varphi}^{(22)}(z)] \\
\hat{J}^{\pm}(z) =& V_1^{\pm}(z) + V_2^{\pm}(z) \\
\hat{J}^3(z) =& \frac{1}{2}[i\partial\tilde{\varphi}^{(12)}(z) - i\partial\tilde{\varphi}^{(11)}(z) + i\partial\tilde{\varphi}^{(22)}(z) - i\partial\tilde{\varphi}^{(21)}(z)]
\end{aligned}
\tag{3.84}
$$

where $V_j^{\pm}(z) = (\tilde{F}_{j2}\tilde{F}_{j1}^{\dagger})^{\pm 1} : e^{\pm i(\tilde{\varphi}^{(j2)}(z) - \tilde{\varphi}^{(j1)}(z))} :$. We will denote the vacuum representation formed by these currents in $\mathcal{H}_L$ as $\hat{\mathcal{H}}_{\hat{\mathfrak{u}}(1)\oplus\hat{\mathfrak{su}}(2)_2}$.

We will now construct the isomorphism between $\mathcal{H}_{\hat{\mathfrak{u}}(1)\oplus\hat{\mathfrak{su}}(2)_2}$ and $\hat{\mathcal{H}}_{\hat{\mathfrak{u}}(1)\oplus\hat{\mathfrak{su}}(2)_2}$, where we will write this linear map as $\mathtt{M} : \mathcal{H}_{\hat{\mathfrak{u}}(1)\oplus\hat{\mathfrak{su}}(2)_2} \to \hat{\mathcal{H}}_{\hat{\mathfrak{u}}(1)\oplus\hat{\mathfrak{su}}(2)_2}$. This is the *unique* linear map with the property,

$$
\mathtt{M}a_n\,|v\rangle = \hat{a}_n\mathtt{M}\,|v\rangle \quad \mathtt{M}J_n^3\,|v\rangle = \hat{J}_n^3\mathtt{M}\,|v\rangle \quad \mathtt{M}J_n^{\pm}\,|v\rangle = \hat{J}_n^{\pm}\mathtt{M}\,|v\rangle \quad \mathtt{M}\,|0\rangle = |\hat{0}\rangle \tag{3.85}
$$

where $|v\rangle \in \mathcal{H}_{\hat{\mathfrak{u}}(1)\oplus\hat{\mathfrak{su}}(2)_2}$ and $|\hat{0}\rangle$ is the vacuum state of $\hat{\mathcal{H}}_{\hat{\mathfrak{u}}(1)\oplus\hat{\mathfrak{su}}(2)_2}$.

By its defining property, we can immediately see that $\mathtt{M}$ must have the property,

$$
\mathtt{M}a_n^{(\varphi)}\,|v\rangle = \frac{1}{2}[\tilde{a}_n^{(12)} - \tilde{a}_n^{(11)} + \tilde{a}_n^{(22)} - \tilde{a}_n^{(21)}]\mathtt{M}\,|v\rangle = \hat{J}_n^3\mathtt{M}\,|v\rangle \tag{3.86}
$$

We also have the OPEs $\hat{J}^{\pm}(z)\hat{J}^{\pm}(w) = 2V_1^{\pm}(w)V_2^{\pm}(w) + \ldots$, By matching these with the OPEs of Eq. 3.81, it follows that,

$$
\mathtt{M}F_{\varphi}^{2p}\,|v\rangle = [-\tilde{F}_{12}\tilde{F}_{11}^{\dagger}\tilde{F}_{22}\tilde{F}_{21}^{\dagger}]^p\mathtt{M}\,|v\rangle \tag{3.87}
$$

where $p \in \mathbb{Z}$. Let $\phi^{(j)}(z) \equiv \frac{i}{\sqrt{2}}[\partial\tilde{\varphi}^{(j2)} - \partial\tilde{\varphi}^{(j1)}]$ for $j = 1, 2$. Now consider the OPE,

$$
\begin{aligned}
\hat{J}^+(z)\hat{J}^-(w) =& \frac{2}{(z-w)^2} + \frac{2\hat{J}^3(w)}{z-w} + V_1^+(w)V_2^-(w) + V_1^-(w)V_2^+(w) \\
&+ \frac{1}{2} : (\phi^{(2)}(w) - \phi^{(1)}(w))^2 : + \partial\hat{J}^3(w) + : (\hat{J}^3(w))^2 : + \ldots
\end{aligned}
\tag{3.88}
$$

By comparing this with the OPE of Eq. 3.82, one can then see that the Majorana energy-momentum tensor, $T^{\psi}(z)$, must map over to $\hat{\mathcal{H}}_{\hat{\mathfrak{u}}(1)\oplus\hat{\mathfrak{su}}(2)_2}$ as,

$$\hat{T}^{\psi}(z) = \frac{1}{4}\left[V_1^+(w)V_2^-(w) + V_1^-(w)V_2^+(w) + \frac{1}{2} : (\phi^{(2)}(w) - \phi^{(1)}(w))^2 :\right] \tag{3.89}$$

Let the modes of $\hat{T}^{\psi}(z)$ be $\hat{L}_n^{\psi}$. We can then write,

$$\mathtt{M} L_n^{\psi} |v\rangle = \hat{L}_n^{\psi} \mathtt{M} |v\rangle \tag{3.90}$$

Finally, we also have,

$$\begin{aligned}
\mathtt{M}\psi_{-\frac{1}{2}} F_{\varphi} |0\rangle =& \mathtt{M}\frac{1}{\sqrt{2}} J_{-1}^{+} |0\rangle = \frac{1}{\sqrt{2}} \hat{J}_{-1}^{+} |\hat{0}\rangle = \frac{1}{\sqrt{2}} [\tilde{V}_{12,-\frac{1}{2}} \tilde{V}^{\dagger}_{11,-\frac{1}{2}} + \tilde{V}_{22,-\frac{1}{2}} \tilde{V}^{\dagger}_{21,-\frac{1}{2}}] |\hat{0}\rangle \\
\mathtt{M}\psi_{-\frac{1}{2}} F^{\dagger}_{\varphi} |0\rangle =& \mathtt{M}\frac{-1}{\sqrt{2}} J_{-1}^{-} |0\rangle = \frac{-1}{\sqrt{2}} \hat{J}_{-1}^{-} |\hat{0}\rangle = \frac{-1}{\sqrt{2}} [\tilde{V}_{11,-\frac{1}{2}} \tilde{V}^{\dagger}_{12,-\frac{1}{2}} + \tilde{V}_{21,-\frac{1}{2}} \tilde{V}^{\dagger}_{22,-\frac{1}{2}}] |\hat{0}\rangle
\end{aligned} \tag{3.91}$$

By combining Eqs. 3.85, 3.86, 3.90 and 3.91, one can map the basis of Eq. 3.83 over to $\hat{\mathcal{H}}_{\hat{\mathfrak{u}}(1)\oplus\hat{\mathfrak{su}}(2)_2}$, in such a way that they can be expressed as modes of the $\tilde{V}_{ij}(z)$ and $\tilde{V}^{\dagger}_{ij}(z)$ acting on the vacuum[14], which then allows one to express the edge states they map to as a sum of products of Slater determinants of z^m and $\bar{z}z^m$ using the results of Sec. 3.2.

Finally, we can then map over the $|\lambda_1; \mu; \lambda_2; p\rangle$ basis by understanding how this can be expressed as linear combintations of the overlcomplete $|\lambda_1 : 0; \lambda_2; \lambda_3; p\rangle$ and $|\lambda_1 : 1/2; \lambda_2; \lambda_3; p\rangle$ basis. This can be done level by level (in L_0 eigenvalues), where $|\lambda_1 : 0; \lambda_2; \lambda_3; p\rangle$ and $|\lambda_1 : 1/2; \lambda_2; \lambda_3; p\rangle$ can be expressed in terms of $|\lambda_1; \mu; \lambda_2; p\rangle$ using $L_n^{\psi} = (1/2)\sum_k (k+1/2) : \psi_{n-k}\psi_k :$ and then finding a solution to the underdetermined set of linear equations. The wave functions that $|\lambda_1; \mu; \lambda_2; p\rangle$ map to can then also be expressed as a sum of products of Slater determinants of the orbitals z^m and $\bar{z}z^m$.

[14]This can be achieved recursively using a computer.

M	Basis reference $\|\lambda_1;\lambda_2;p\rangle$			
1	$0:\ \|\emptyset;\emptyset;1\rangle$	$1:\ \|1;\emptyset;0\rangle$	$2:\ \|\emptyset;1;0\rangle$	$3:\ \|\emptyset;\emptyset;-1\rangle$
2	$0:\ \|1;\emptyset;1\rangle$ $4:\ \|11;\emptyset;0\rangle$ $8:\ \|\emptyset;1;-1\rangle$	$1:\ \|\emptyset;1;1\rangle$ $5:\ \|\emptyset;11;0\rangle$	$2:\ \|2;\emptyset;0\rangle$ $6:\ \|1;1;0\rangle$	$3:\ \|\emptyset;2;0\rangle$ $7:\ \|1;\emptyset;-1\rangle$
3	$0:\ \|2;\emptyset;1\rangle$ $4:\ \|1;1;1\rangle$ $8:\ \|\emptyset;12;0\rangle$ $12:\ \|1;11;0\rangle$ $16:\ \|\emptyset;2;-1\rangle$	$1:\ \|\emptyset;2;1\rangle$ $5:\ \|3;\emptyset;0\rangle$ $9:\ \|2;1;0\rangle$ $13:\ \|\emptyset;111;0\rangle$ $17:\ \|11;\emptyset;-1\rangle$	$2:\ \|11;\emptyset;1\rangle$ $6:\ \|\emptyset;3;0\rangle$ $10:\ \|1;2;0\rangle$ $14:\ \|111;\emptyset;0\rangle$ $18:\ \|\emptyset;11;-1\rangle$	$3:\ \|\emptyset;11;1\rangle$ $7:\ \|12;\emptyset;0\rangle$ $11:\ \|11;1;0\rangle$ $15:\ \|2;\emptyset;-1\rangle$ $19:\ \|1;1;-1\rangle$

Table 3.1: Basis reference, used in Fig. 3.1, for the $\nu = 2/5$ CF CFT $U(1)$ neutral states with L_0 eigenvalue $M = 1, 2, 3$ (i.e. states that map to trial edge state wave functions with the same particle number as the ground state trial wave function and with angular momentum $M = 1, 2, 3$ relative to the ground state trial wave function). The corresponding basis elements are defined in Sec. 3.5.2. Here each basis element is $|\lambda_1;\lambda_2;p\rangle$ with λ_i partitions and p an integer.

3.C Basis reference

For the $\nu = 2/5$ CF case the basis references used in Fig. 3.1 can be found in Table 3.1. For the ϕ_2^2 Parton case the basis references used in Fig. 3.3 can be found in Table 3.2.

M	Basis reference $\|\lambda_1;\mu;\lambda_2;p\rangle$			
1	$0:\ \|\emptyset;1;\emptyset;-1\rangle$	$1:\ \|\emptyset;\emptyset;1;0\rangle$	$2:\ \|\emptyset;1;\emptyset;1\rangle$	$3:\ \|1;\emptyset;\emptyset;0\rangle$
2	$0:\ \|\emptyset;\emptyset;\emptyset;-2\rangle$ $4:\ \|\emptyset;\emptyset;11;0\rangle$ $8:\ \|\emptyset;\emptyset;\emptyset;2\rangle$ $12:\ \|11;\emptyset;\emptyset;0\rangle$	$1:\ \|\emptyset;3;\emptyset;-1\rangle$ $5:\ \|\emptyset;\emptyset;2;0\rangle$ $9:\ \|1;1;\emptyset;-1\rangle$ $13:\ \|2;\emptyset;\emptyset;0\rangle$	$2:\ \|\emptyset;1;1;-1\rangle$ $6:\ \|\emptyset;3;\emptyset;1\rangle$ $10:\ \|1;\emptyset;1;0\rangle$	$3:\ \|\emptyset;31;\emptyset;0\rangle$ $7:\ \|\emptyset;1;1;1\rangle$ $11:\ \|1;1;\emptyset;1\rangle$
3	$0:\ \|\emptyset;\emptyset;1;-2\rangle$ $4:\ \|\emptyset;1;2;-1\rangle$ $8:\ \|\emptyset;\emptyset;12;0\rangle$ $12:\ \|\emptyset;1;11;1\rangle$ $16:\ \|1;3;\emptyset;-1\rangle$ $20:\ \|1;\emptyset;2;0\rangle$ $24:\ \|11;1;\emptyset;-1\rangle$ $28:\ \|2;\emptyset;1;0\rangle$ $32:\ \|3;\emptyset;\emptyset;0\rangle$	$1:\ \|\emptyset;5;\emptyset;-1\rangle$ $5:\ \|\emptyset;51;\emptyset;0\rangle$ $9:\ \|\emptyset;\emptyset;3;0\rangle$ $13:\ \|\emptyset;1;2;1\rangle$ $17:\ \|1;1;1;-1\rangle$ $21:\ \|1;3;\emptyset;1\rangle$ $25:\ \|11;\emptyset;1;0\rangle$ $29:\ \|2;1;\emptyset;1\rangle$	$2:\ \|\emptyset;3;1;-1\rangle$ $6:\ \|\emptyset;31;1;0\rangle$ $10:\ \|\emptyset;5;\emptyset;1\rangle$ $14:\ \|\emptyset;\emptyset;1;2\rangle$ $18:\ \|1;31;\emptyset;0\rangle$ $22:\ \|1;1;1;1\rangle$ $26:\ \|11;1;\emptyset;1\rangle$ $30:\ \|111;\emptyset;\emptyset;0\rangle$	$3:\ \|\emptyset;1;11;-1\rangle$ $7:\ \|\emptyset;\emptyset;111;0\rangle$ $11:\ \|\emptyset;3;1;1\rangle$ $15:\ \|1;\emptyset;\emptyset;-2\rangle$ $19:\ \|1;\emptyset;11;0\rangle$ $23:\ \|1;\emptyset;\emptyset;2\rangle$ $27:\ \|2;1;\emptyset;-1\rangle$ $31:\ \|12;\emptyset;\emptyset;0\rangle$

Table 3.2: Basis reference, used in Fig. 3.3, for the ϕ_2^2 Parton CFT $U(1)$ neutral states with L_0 eigenvalue $M = 1, 2, 3$ (i.e. states that map to trial edge state wave functions with the same particle number as the ground state trial wave function and with angular momentum $M = 1, 2, 3$ relative to the ground state trial wave function). The corresponding basis elements are defined in Sec. 3.5.2. Each basis is element is $|\lambda_1;\mu;\lambda_2;p\rangle$ with λ_i partitions, μ a partition with only odd non-repeating elements and p an integer.

Chapter 4

Energy Minimisation of Paired Composite Fermions

At $\nu = \frac{5}{2}$ in GaAs heterostructures the LLL is completely full for both the spin up and spin down electron orbitals and the second LL is *half* full where the magnetic field is strong enough that the electrons are spin-polarised in the second LL. To model the bulk of this system numerical studies typically consider the half-full second LL in the *spherical* geometry. This problem is then mapped to an effective description where the electrons are in the LLL by mapping the electron orbitals as $Y_{Q(Q+1)m}(\mathbf{\Omega}) \rightarrow Y_{(Q+1)(Q+1)m}(\mathbf{\Omega})$, where $2Q$ is the magnetic flux through the sphere.

With this effective description in mind, the first candidate trial wave function for this problem was the Moore-Read (MR) wave function [14, 60, 61], which can be expressed on the sphere as,

$$\Psi_{\mathrm{MR}} = \mathrm{Pf}\left[\frac{1}{u_i v_j - v_i u_j}\right] \prod_{i<j}^{N} (u_i v_j - v_i u_j)^2 \tag{4.1}$$

where $\mathrm{Pf}[G_{ij}]$ denotes the Pfaffian of a matrix $G_{ij} = \frac{1}{u_i v_j - v_i u_j}$ which is given by,

$$\mathrm{Pf}[G_{ij}] = \frac{1}{(N/2)! 2^{N/2}} \sum_{\sigma \in S_N} \mathrm{sgn}\sigma \prod_{i=1}^{N/2} G_{\sigma(2i-1)\sigma(2i)} \tag{4.2}$$

where S_N is the set of permutations of N elements. The phase of matter this wave function represents is generally referred to as the Pfaffian state. It was realised early on

that the MR wave function could be interpreted as a paired state of CFs [69, 139, 140] with pairing channel $\ell = -1$ (p-wave pairing), which is in contrast to the half-filled LLL where CFs form the *gapless* CF Fermi-liquid state [141, 142].

It was later realised that, in the absence of LL mixing, the particle-hole transformed MR wave function, which we denote $\overline{\text{MR}}$, could also be a possible candidate wave function [63, 64] as these two wave function would have the same energy in the thermodynamic limit. It has been argued that the $\overline{\text{MR}}$ wave function represents a different phase of matter[63], which we will refer to as the anti-Pfaffian state and can also be understood as paired CFs with pairing channel $\ell = 3$. The other candidate phase, proposed by Son [65], is the particle-hole Pfaffian (PH-Pfaffian) which has a corresponding trial wave function that can be interpreted as paired CFs in the $\ell = 1$ pairing channel [70, 71, 143]. As mentioned in Chap. 1, numerical studies point towards the Pfaffian or anti-Pfaffian phases as being far more energetically favourable than the PH-Pfaffian phase, with the anti-Pfaffian being the most energetically favourable after taking into account LL mixing [67, 71, 144–146]. However, experimental measurements of the heat conductivity along the edges of these systems [68] and measurements of noise along interfaces of these systems with other quantum Hall states [147] are more consistent with the PH-Pfaffian state. Whilst some suggestions have been made to attempt to resolve this issue [23, 148–153], the precise phase of matter that occurs at $\nu = \frac{5}{2}$ in GaAs is still unknown.

Numerical investigations into these candidate phases of matter are limited by the lack of accurate trial wave functions for the PH-Pfaffian and anti-Pfaffian phases which are numerically tractable at larger system sizes. The paired CF wave functions proposed by Möller and Simon (MS) [72] denoted MS_ℓ, and their fixed parameter versions proposed by Yutushui and Mross (YM) [73], denoted YM_ℓ, where ℓ is the pairing channel, may then offer the required numerically tractable wave functions. It has been argued by MS and YM that these wave functions at $\ell = -1$ and $\ell = 3$ belong to the

Pfaffian and anti-Pfaffian phases respectively. However, YM, in studying their version of PH-Pfaffian trial wave functions YM_1, and other numerical studies, investigating the "ideal" PH-Pfaffian wave function, have also cast doubt on whether PH-Pfaffian wave functions represent a gapped phase of matter [70, 154, 155]. To reiterate from Chap. 1, the energetics of these MS_ℓ and YM_ℓ wave functions have not yet been studied, and it is not known if the MS_ℓ wave functions with their energy minimised can offer significantly better approximations to the corresponding ground states at $\ell = 1, 3$. In particular, minimising the energy of the MS_1 wave functions could, in principle, produce PH-Pfaffian trial wave functions with energies significantly closer to the $\ell = -1, 3$ trial wave functions. YM actually propose two versions of this set of wave functions called "single-particle projected" and "pair-projected". We will only be concerned with the "single-particle" projected versions here as they are more numerically tractable.

There has also been some recent interest in understanding if the effective CF pairing in these phases can be approximated by some weak pairing BCS-type description, where the BCS gap parameter can be estimated [156]. As well as offering some physical insight into these phases of matter, it also has some practical use, by allowing, for example, to observe when the system is transitioning from CF pairing to the CF Fermi liquid [72]. The precise BCS weak pairing description has only so far been studied for the $\ell = -1$ pairing on the torus and it is not known if such a description is accurate for the $\ell = 3, 1$ cases.

In this chapter, we will discuss how the energy of the MS_ℓ wave functions can be minimised at larger system sizes, in the spherical geometry, where we will present the results of this optimisation for the case of the Coulomb interaction in the second LL in the absence of LL mixing. At small system sizes we find that the minimised energies of the MS_{-1} wave functions are comparable with those from exact diagonalisation and from density matrix renormalisation group (DMRG) methods for the pure Coulomb interaction in the second LL. However, we find that, the energies of the optimised

MS_ℓ, YM_ℓ, for $\ell = -1, 3$, MR and $\overline{\mathrm{MS}}$ wave functions all converge to the same value in the thermodynamic limit and so one cannot obtain an improved thermodynamic energy estimate from optimisation. We also find the YM_3 wave functions to be a very good approximation, in energy, to the $\overline{\mathrm{MR}}$ wave function, and that the optimised MS_3 wave functions offer considerably less energy reduction over the corresponding zero-parameter trial wave functions in comparison to the MS_{-1} wave functions. Furthermore, the amount by which the energy of the MS_1 wave functions can be minimised compared with the YM_1 wave functions is negligible where we find both wave functions to be energetically unfavourable. We demonstrate that the effective CF pairing in the optimised MS_ℓ and YM_ℓ wave functions, for $\ell = -1, 3$, can be well approximated by a weak pairing BCS type description, where, for finite size systems, the MS_ℓ wave function show stronger pairing than the corresponding YM_ℓ wave function. Finally, further pathologies of the MS_1 wave functions are found.

The MS_ℓ and YM_ℓ wave functions are introduced in Sec. 4.1. Then in Sec. 4.2 we discuss how the Coulomb interaction in the second LL is modelled in this LLL description and then in Sec. 4.3 we discuss the chosen algorithm that allows for energy minimisation at larger system sizes. Finally, in Sec. 4.4 the results of these energy minimisations are presented in the case of the Coulomb interaction in the second LL, where it is also shown how the effective weak-pairing BCS description can be extracted from these wave functions.

4.1 Paired CF wave functions on the Haldane sphere

In the BCS theory of superconductivity [157] one typically starts with the *mean-field* Hamiltonian for a system of fermions, which we will take to be in two spatial dimensions, which takes the form

$$H_{\mathrm{BCS}} = \sum_{\mathbf{k}} \left[\varepsilon_{\mathbf{k}} c^\dagger_{\mathbf{k}} c_{\mathbf{k}} + \frac{1}{2}(\overline{\Delta}_{\mathbf{k}} c_{-\mathbf{k}} c_{\mathbf{k}} + \Delta_{\mathbf{k}} c^\dagger_{\mathbf{k}} c^\dagger_{-\mathbf{k}}) \right] \tag{4.3}$$

and is assumed to be a reasonable approximation to the actual Hamiltonian of the system at low energies, where $\Delta_{\mathbf{k}}$ is known as the *gap function* and $\varepsilon_{\mathbf{k}}$ is the kinetic energy relative to the Fermi level of a single particle state labelled by $\mathbf{k}$ (i.e. $\varepsilon_{\mathbf{k}} = E_{\mathbf{k}} - E_{\mathbf{k}_F}$). The unnormalised ground state of this Hamiltonian is given by,

$$|\Psi_{\mathrm{BCS}}\rangle = \exp\left(\frac{1}{2}\sum_{\mathbf{k}} g_{\mathbf{k}} c^{\dagger}_{-\mathbf{k}} c^{\dagger}_{\mathbf{k}}\right)|0\rangle \tag{4.4}$$

where $g_{\mathbf{k}} = (\varepsilon_{\mathbf{k}} - \sqrt{\varepsilon^2_{\mathbf{k}} + |\Delta_{\mathbf{k}}|^2})/\overline{\Delta}_{\mathbf{k}}$. Note that for this case of spinless fermions $g_{\mathbf{k}}$ must be an odd function of $\mathbf{k}$, $g_{-\mathbf{k}} = -g_{\mathbf{k}}$. In real-space this can be expressed as $|\Psi_{\mathrm{BCS}}\rangle = \exp\left(\frac{1}{2}\int d^2\mathbf{r}_2 d^2\mathbf{r}_2 g(\mathbf{r}_1 - \mathbf{r}_2) c^{\dagger}(\mathbf{r}_1) c^{\dagger}(\mathbf{r}_2)\right)|0\rangle$. $|\Psi_{\mathrm{BCS}}\rangle$ is physically interpreted as a *paired state*, where particles near the Fermi level become bound into pairs with $g(\mathbf{r})$ being referred to as the *pairing function*.

The average occupation of the orbital labelled by $\mathbf{k}$, $n_{\mathbf{k}}$, can be expressed as $n_{\mathbf{k}} = \langle\Psi_{\mathrm{BCS}}|\Psi_{\mathrm{BCS}}\rangle^{-1} \langle\Psi_{\mathrm{BCS}}| c^{\dagger}_{\mathbf{k}} c_{\mathbf{k}} |\Psi_{\mathrm{BCS}}\rangle = \langle\Psi_{\mathrm{BCS}}|\Psi_{\mathrm{BCS}}\rangle^{-1} (g_{\mathbf{k}} - g_{-\mathbf{k}}) \langle\Psi_{\mathrm{BCS}}| \partial_{g_{\mathbf{k}}} |\Psi_{\mathrm{BCS}}\rangle = \langle\Psi_{\mathrm{BCS}}|\Psi_{\mathrm{BCS}}\rangle^{-1} 2(g_{\mathbf{k}}) \langle\Psi_{\mathrm{BCS}}| \partial_{g_{\mathbf{k}}} |\Psi_{\mathrm{BCS}}\rangle = |g_{\mathbf{k}}|^2/(1 + |g_{\mathbf{k}}|^2)$. This can be expressed in terms of $\varepsilon_{\mathbf{k}}$ and $\Delta_{\mathbf{k}}$ as $n_{\mathbf{k}} = \frac{1}{2}\left(1 - \frac{\varepsilon_{\mathbf{k}}}{\sqrt{\varepsilon^2_{\mathbf{k}} + |\Delta_{\mathbf{k}}|^2}}\right)$.

For a rotationally symmetric microscopic Hamiltonian, the gap function is some eigenstate of the rotation operator. In two dimensions this would mean that under a rotation by angle ϑ the gap function transforms as $\Delta_{\mathbf{k}} \to e^{i\ell\vartheta}\Delta_{\mathbf{k}}$, where ℓ is known as the *pairing channel*. For spinless fermion cases we are considering here $\Delta_{\mathbf{k}}$ is an odd function of $\mathbf{k}$, as $g_{\mathbf{k}}$ is, and a typical ansatz for $\Delta_{\mathbf{k}}$ is $\Delta_{\mathbf{k}} = \Delta|k|e^{i\ell\theta}$, where θ is the angle from the x-axis in $\mathbf{k}$-space. For $|\mathbf{r}| \gg \Delta/E_{k_F}$ the pairing function corresponding to this gap function is $g(\mathbf{r}) \propto \frac{e^{i\ell\theta}}{|\mathbf{r}|}$ (see Appendix A of Ref. [73]). When this long-distance form of g occurs the fermions are said to be in a weak-pairing phase[69].

This BCS mean-field wave function can be used to create a trial wave function for a fixed number of fermions N, by projecting it to the space of states with N particles, with the projector written as P_N. We then define $|\Psi_N\rangle \equiv P_N |\Psi_{\mathrm{BCS}}\rangle$. The wave function of $|\Psi_N\rangle$ is given by $\Psi_N(\mathbf{r}_1, \mathbf{r}_2, \ldots, \mathbf{r}_N) = \mathrm{Pf}[g(\mathbf{r}_i - \mathbf{r}_j)]$. Note that as $[c^{\dagger}_{\mathbf{k}} c_{\mathbf{k}}, P_N] = 0$,

we still have the property that $c^\dagger_{\mathbf{k}} c_{\mathbf{k}} |\Psi_N\rangle = 2g_{\mathbf{k}} \partial_{g_{\mathbf{k}}} |\Psi_N\rangle$. Hence, the average orbital occupations are given by $n_{\mathbf{k}} = \langle\Psi_N|\Psi_N\rangle^{-1} 2g_{\mathbf{k}} \langle\Psi_N| \partial_{g_{\mathbf{k}}} |\Psi_N\rangle$.

Now we move to a system of N spinless fermions moving on a sphere with $N_\phi = 2Q = 2(N-1+q)$ flux quanta passing through its surface, where q is on the order of one (i.e. does not scale with N) and it is presumed that the magnetic field is strong enough that the fermions are confined to the LLL. Thus, in the thermodynamic limit, this system is at filling fraction $\nu = \lim_{N\to\infty} \frac{N}{N_\phi} = \frac{1}{2}$. Let us then assume they form CFs with each fermion being bound to 2 wave function vortices. The effective flux that the CFs experience is then $N^*_\phi = 2q$. As the effective magnetic field is negligible in the thermodynamic limit, if the effective interaction between the CFs is weakly attractive we then expect them to form some weakly paired BCS state. Let u_i, v_i be the spinor coordinates for i^{th} fermion. On the sphere, the flux attaching Jastrow factor is $\prod_{i<j}^N (u_i v_j - v_i u_j)^2$. From standard CF theory we then write the "ideal" trial wave function as $\Psi = P_{LLL}\text{Pf}[g(\mathbf{r}_i - \mathbf{r}_j)] \prod_{i<j}^N (u_i v_j - v_i u_j)^2$, where, by imposing rotational invariance, the pairing function takes the general form $g(\mathbf{r}_i - \mathbf{r}_j) = \sum_{lm} (-1)^{m+|q|} g_l Y_{qlm}(\mathbf{\Omega}_i) Y_{ql(-m)}(\mathbf{\Omega}_j)$ for some unspecified $g_l \in \mathbb{C}$. In principle, one can then extract the pairing physics of the CFs by finding the g_l that minimizes the energy of this wave function.

This is, however, numerically intractable for $N \gtrapprox 10$ due to the projection to the LLL. To create a numerically tractable trial wave function MS proposed using the Jain-Kamila [108] procedure where we can produce a LLL wave function simply by replacing the single-particle orbitals $Y_{qlm}(\mathbf{\Omega}_i)$ by the corresponding CF "orbitals" defined by,

$$\tilde{Y}_{qlm}(\mathbf{\Omega}_i) \equiv J_i^{-1}[P_{LLL} Y_{qlm}(\mathbf{\Omega}_i) J_i] \tag{4.5}$$

where $J_i = \prod_{j\neq i}^N (u_i v_j - v_i u_j)$ and P_{LLL} projects particle i to the LLL with magnetic flux $2q + N - 1$. The resulting family of pairing wave functions then defines MS paired CF wave functions [72],

$$\Psi_{\mathrm{MS}} = \mathrm{Pf}\Big[\sum_{lm}(-1)^{m+|q|}g_l\tilde{Y}_{qlm}(\mathbf{\Omega}_i)\tilde{Y}_{ql(-m)}(\mathbf{\Omega}_j)\Big]\prod_{i<j}^{N}(u_iv_j - v_iu_j)^2 \tag{4.6}$$

In particular, we denote the MS family of wave functions at effective flux q by MS_{2q}. One can then vary the g_l to minimize the energy. The YM wave function at effective flux $2q$, denoted YM_{2q}, is defined to be the MS_{2q} wave function with $g_l = \frac{1}{2l+1}$. Note that as the interaction potential $V(\mathbf{r})$ is real-valued, we must have that $\langle\Psi_{\mathrm{MS}}|\, V\,|\Psi_{\mathrm{MS}}\rangle$ is invariant under time reversal where we simply replace the wave function by its complex conjugate. Furthermore, by expressing $\langle\Psi_{\mathrm{MS}}|\, V\,|\Psi_{\mathrm{MS}}\rangle$ as an integral one can perform a change of variable where we change the azimuthal angle $\phi \to -\phi$ which is the same as the transformation $u \to u^*$ and $v \to v^*$. Combining these two transformations we must have that $\langle\Psi_{\mathrm{MS}}|\, V\,|\Psi_{\mathrm{MS}}\rangle$ is invariant under $g_l \to g_l^*$. Assuming that the minimum energy solution is unique up to multiplying all g_l by the same complex number, it then follows that the minimum energy wave function can be expressed with g_l all being real numbers. We will take $g_l \in \mathbb{R}$ from now on.

From the usual CF theory, we expect that this can be physically interpreted as being analogous to a BCS state, of the CFs, of the form $|\Psi_{\mathrm{BCS}}\rangle = \exp\left(\frac{1}{2}\sum_{lm} g_l(-1)^{m+|q|} c^\dagger_{qlm}c^\dagger_{ql(-m)}\right)|0\rangle$, where $c^\dagger_{qlm}$ is the creation operator for the orbital $Y_{qlm}(\mathbf{\Omega})$. The pairing wave function of this BCS state is $g(\mathbf{r}_i - \mathbf{r}_j) = \sum_{lm} g_l(-1)^{m+|q|}Y_{qlm}(\mathbf{\Omega}_i)Y_{ql(-m)}(\mathbf{\Omega}_j)$. Using Eq. B4 of Ref. [73] this can be expressed as $g(\mathbf{r}_i - \mathbf{r}_j) = \sum_l \frac{g_l(-1)^{|q|-q}(2l+1)}{4\pi}(u_iv_j - v_iu_j)^{2q}P^{(2q,0)}_{l-q}(\cos\theta)$, where θ is the angle between particle i and particle j and $P^{(2q,0)}_n$ are the Jacobi polynomials, where it should be noted that if $q < 0$ then one should replace $(u, v) \to (u^*, v^*)$. From the $(u_iv_j - v_iu_j)^{2q}$ factor we can read off the pairing channel to be $\ell = 2q$[1]. Also from Eq. B6b of Ref. [73] we have $\frac{(u_iv_j - v_iu_j)^{q-1/2}}{(u_i^*v_j^* - v_i^*u_j^*)^{q+1/2}} = \sum_{l=q}^{\infty}(-1)^{q+m}\frac{4\pi}{2l+l}Y_{qlm}(\mathbf{\Omega}_i)Y_{ql(-m)}(\mathbf{\Omega}_j)$, where again negative q requires complex conjugation. This pairing function scales with the distance between particle i and particle

[1]This can be seen using stereographic coordinates with $z_i = u_i/v_i$ which then gives $(u_iv_j - v_iu_j)^2q = v_i^{2q}v_j^{2q}(z_i - z_j)^{2q}$. Hence, as we bring particle i around particle j the phase of the wave function will wind $2q$ times in the anti-clockwise direction.

j as $g \sim 1/r$. Thus the analogous weak pairing on the sphere is given by $g_l \sim \frac{1}{2l+1}$ at small l. Now let $\varepsilon_l = \frac{\hbar^2}{2m_{CF}R^2}(l(l+1) - l_F(l_F+1))$ where R is the radius of the sphere, m_{CF} the the CF effective mass and l_F is the Fermi "shell". We can express $g_l = (\varepsilon_l - \sqrt{\varepsilon_l^2 + \Delta_l^2})/\Delta_l^*$ where Δ_l is the gap function on the sphere. We can then make the analogous weak pairing ansatz for the gap function $\Delta_l = \Delta\frac{l+1/2}{R}$. By matching the kinetic energy for $l \gg 1$ one can see that the correspondence between l and the wave vector k is $k = \frac{l}{R}$ for large l. This then reproduces the previous ansatz for the gap function in terms of k for large l, $\Delta_l \approx \Delta k$. By symmetry, the occupation of all orbitals in the l shell must be the same n_l, which can then be expressed as $n_l = \frac{2g_l}{2l+1}\langle\Psi_{\mathrm{BCS}}|\Psi_{\mathrm{BCS}}\rangle^{-1}\langle\Psi_{\mathrm{BCS}}|\,\partial_{g_l}\,|\Psi_{\mathrm{BCS}}\rangle$. For the weak pairing ansatz, this gives,

$$n_l = \frac{1}{2}\left(1 - \frac{\varepsilon_l}{\sqrt{\varepsilon_l^2 + \left(\frac{\Delta(l+1/2)}{R}\right)^2}}\right) \tag{4.7}$$

Whilst this is perhaps an appealing way to physically interpret the MS wave function, it is not obvious if the CF orbitals are "normalised" in such a way that the g_l of the MS wave function should be the same as the g_l of the effective BCS state. As discussed by MS in Ref. [72], one can get around this issue by defining the effective CF occupations as $n_l^{\mathrm{CF}} \equiv \frac{2g_l}{2l+1}\langle\Psi_{\mathrm{MS}}|\Psi_{\mathrm{MS}}\rangle^{-1}\langle\Psi_{\mathrm{MS}}|\,\partial_{g_l}\,|\Psi_{\mathrm{MS}}\rangle$. This can also be expressed as,

$$n_l^{\mathrm{CF}} = \frac{2g_l}{2l+1}\left\langle\frac{\partial_{g_l}\Psi_{\mathrm{MS}}}{\Psi_{\mathrm{MS}}}\right\rangle \tag{4.8}$$

where the expectation value is taken with respect to $|\Psi_{\mathrm{MS}}\rangle$. From their definition, these clearly do not depend on the normalisation of g_l. These effective occupation probabilities for the minimum energy g_l were empirically found by MS to behave as the occupation probabilities of an actual fermion system. We will then use these n_l^{CF} in this work to relate optimised MS wave functions to their effective CF-BCS description.

As the pairing channel is given by $\ell = 2q$, we expect that the MS wave functions MS_{-1}, MS_3 and MS_1 to be in the Pfaffian, anti-Pfaffian and PH-Pfaffian phases respec-

tively. In what follows we will also use yet another variational wave function for the Pfaffian phase which we will denote MR* and can be expressed as,

$$\Psi_{\mathrm{MR}^*} = \mathrm{Pf}\left[\frac{1}{u_i v_j - v_i u_j} + \sum_{lm} (-1)^{m+1/2} g_l \tilde{Y}_{(-1/2)lm}(\mathbf{\Omega}_i)\tilde{Y}_{(-1/2)l(-m)}(\mathbf{\Omega}_j)\right] \prod_{i<j}^{N} (u_i v_j - v_i u_j)^2 \tag{4.9}$$

Roughly speaking, the MR* wave function allows us to "perturb" around the MR wave function. By varying the g_l parameters, one may expect that an MR* wave function can always be found with lower energy than the corresponding MR wave function (at the same system size). We will thus use the MR* wave function as a benchmark for the optimisation of the standard MS_{-1} wave function.

4.2 Effective interactions

As discussed at the start of this chapter, we are interested in understanding the physics of spin-polarised electrons in the half-filled second LL, by mapping this to a problem in the LLL. The effective interaction is defined by

$$\langle Q+1, Q+1, m_1, m_2 | \, V^{\mathrm{eff}} \, | Q+1, Q+1, m_3 m_4 \rangle \equiv \langle Q, Q+1, m_1 m_2 | \, V \, | Q, Q+1, m_3 m_4 \rangle \tag{4.10}$$

where $|Q, l, m_1 m_2\rangle$ is a two-particle state (with the particles not identical) with particle 1 and 2 in the Y_{Qlm_1} and Y_{Qlm_2} orbitals respectively and V is the interaction of the original problem. Note that for the second LL system, we will take the radius of the sphere to be $R = l_B\sqrt{Q}$ and for the LLL system we will take $R^* = l_B\sqrt{Q+1}$. We will now discuss how V^{eff} can be modelled in the case where V is the Coulomb interaction in the second LL.

The space of states spanned by $|Qlm_1m_2\rangle$ can also be spanned by $|LM\rangle$ which are the eigenstates of the total angular momentum $\hat{L}^2$ and L_z operators. For any

rotationally symmetric interaction V we must then have $\langle L'M'|\, V\, |LM\rangle = \delta_{LL'}\delta_{MM'}V_L$ where V_L is s real number. Thus, any V which is projected to one LL can be expressed as $V = \sum_{LM} V_L\, |LM\rangle\, \langle LM|$, where the $\sum_M |LM\rangle\, \langle LM|$ are how the Haldane pseudo-potentials are expressed on the sphere. The pseudo-potential coefficient V_L is related to the pseudo-potential coefficient on the planar geometry V_m by $V_m = V_{L=2l-m}$. One can then write $\langle Qlm_1m_2|\, V\, |Qlm_3m_4\rangle = \sum_L V_L\, \langle Qlm_1m_2|L(m_1+m_2)\rangle$
$\langle L(m_1+m_2)|Qlm_3m_4\rangle$.

As the Clebsch-Gordon coefficients $\langle Qlm_1m_2|LM\rangle$ do not depend on Q, the pseudo-potential coefficients for V^{eff} must be the same as those of the actual potential V. Hence, to model V^{eff} we simply need to find some interaction potential in the LLL which has the same V_L as the interaction in the second LLL. The Coulomb interaction in the second LL has been shown in previous works [140, 156] to be accurately modelled in the LLL by,

$$V^{\text{eff}}(r) = \frac{a_0}{r} + a_1 e^{-\alpha_1 r^2} + a_2 r^2 e^{-\alpha_2 r^2} \tag{4.11}$$

In this work, we allow for the parameters a_i, α_i to vary with the system size, where the parameters are determined by minimising the sum of squared differences between the pseudo-potential of this interaction in the LLL and those of the Coulomb interaction in the second LL for $L = 0, 1, 2, \ldots, 2Q+2$ (with $2Q$ being the magnetic flux for the system in the second LL).

To fit the effective interaction, we compute the V_L's using Eq. 2.37 of Ref. [158], where the pseudo-potential coefficients are expressed in terms of Wigner 3-j and 6-j symbols, and V_k which are the coefficients in the expansion of $V(r)$ in terms of Legendre polynomials, $V(r) = \sum_k V_k P_k(\cos\theta)$ (with θ being the angle between the two particles on the sphere). The results of this fitting procedure for the $2Q = 35$ case can be seen in Fig. 4.1, where it can be seen V^{eff} can accurately reproduce the Haldane pseudo-potential coefficients for the Coulomb interaction in the 2nd LL with only slight

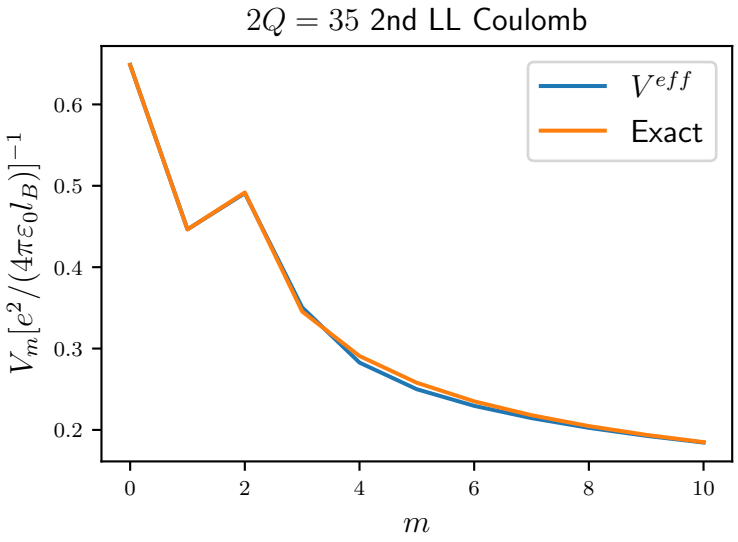

Figure 4.1: Showing the Haldane pseudo-potential coefficients, V_m, of both the Coulomb interaction in the second LL along with the V_m of the fitted LLL V^{eff}, where the total number of magnetic flux quanta is $2Q = 35$ for the system in the second LL. Note that $V_L = V_{m=2Q+2-L}$.

deviations at intermediate m. The parameters used for V^{eff} for the Coulomb in the second LL for the system sizes used in this study are given in Appendix 4.A.

4.3 Optimisation algorithm

One possible way of minimising the energy of an MS wave function at a given system size would be to use a standard optimisation algorithm where the energy for a given set of parameters is computed *exactly*. This is, however, computationally expensive and would restrict one to only working with smaller system sizes. For the energy minimisation of wave functions of large systems, there exists a large class of algorithms under the name *variational quantum Monte Carlo* [159], where Monte Carlo methods are used to estimate the energy and energy gradients. Whilst there are many specific algorithms to choose from, for the problem at hand we have used a combination of the *Stochastic Reconfiguration* algorithm [160] and the Adam optimiser [161], which we will now describe.

First, let us describe the Adam optimiser. Let $E(\mathbf{g})$ be the expectation value of the Energy as a function of the wave function parameters $\mathbf{g}$. We will then impose a yet unspecified geometry on this parameter space defined by some metric tensor S which can vary over the parameter space. At each iteration t of the optimisation, we have three vectors, $\mathbf{f}_t \equiv \frac{\partial E}{\partial \mathbf{g}_t}$ (gradient vector), $\mathbf{m}_t$ (momentum) and $\hat{\mathbf{m}}_t$ (bias-corrected momentum). We also have the real numbers v_t and $\hat{v}_t$ the bias-corrected version. The algorithm has four hyper parameters: γ (learning rate), β_1, β_2 and ϵ. At each iteration, everything is updated by,

$$\begin{aligned}
\mathbf{m}_{t+1} =& \beta_1 \mathbf{m}_t + (1-\beta_1) S^{-1} \mathbf{f}_t \\
\hat{\mathbf{m}}_{t+1} =& m_{t+1}/(1-\beta_1^{t+1}) \\
v_{t+1} =& \beta_2 v_t + (1-\beta_2) \mathbf{f}_t^T S^{-1} \mathbf{f}_t \\
\hat{v}_{t+1} =& v_{t+1}/(1-\beta_2^{t+1}) \\
\mathbf{g}_{t+1} =& \mathbf{g}_t - \gamma \hat{\mathbf{m}}_{t+1}/(\sqrt{\hat{v}_{t+1}} + \epsilon)
\end{aligned} \tag{4.12}$$

Let O_l be an operator which is diagonal in the position space representation, which is defined by $O_l \equiv \frac{\partial_{g_l} \Psi_{\mathrm{MS}}}{\Psi_{\mathrm{MS}}}$. The energy gradients can then be expressed as,

$$\frac{\partial E}{\partial g_l} = 2\Re \left\langle V^{\mathrm{eff}} O_l \right\rangle - 2 \left\langle V^{\mathrm{eff}} \right\rangle \Re \left\langle O_l \right\rangle \tag{4.13}$$

where $\Re$ denotes the real part. We compute these expectation values using the Hastings-Metropolis Monte Carlo algorithm, which introduces stochastic noise into the optimisation.

Using the momentum $\mathbf{m}_t$ allows the algorithm to smooth out the noise in estimating gradients and v_t ensures we move roughly the same distance in parameter space at every iteration. One can view this algorithm as a particle moving in parameter space with friction and noise in the potential given by E. β_1 can then be thought of as setting our inertia. β_2 sets the time scale over which we average the sizes of $S^{-1} g_t$. The ϵ parameter is simply a distance cut-off.

The SR algorithm can be interpreted as a standard gradient descent algorithm where

one uses the Fubini-Study metric to define the geometry of the parameter space of the wave function. To combine this with the Adam optimiser we simply take S to be the Fubini-Study metric. This metric is given by defining the distance between two nearby points in parameter space to be the Hilbert space norm of the difference between the *normalised* states at the two coordinate points. This can be straightforwardly shown to be given by,

$$S_{l_1 l_2} = \Re \langle O_{l_1}^* O_{l_2} \rangle - \Re \langle O_{l_1} \rangle \Re \langle O_{l_2} \rangle \tag{4.14}$$

Using this metric has the advantage that it removes the ambiguity over how the parameters are normalised. At each iteration of the algorithm, we again use the Hastings-Metropolis Monte Carlo algorithm to estimate S.

Both the gradients $\mathbf{f}$ and S are estimated using $\sim 10^6$ Monte Carlo samples, with the actual number of samples used increasing with the system size. To lessen the computation time sampling at each iteration was run in parallel using around 10^2 computing nodes. To ensure the sampling on each computing node is statistically independent we used the cryptographic counter-based pseudo-random number generators of Ref. [162].

In practice, we regularise this metric as the Ψ_{MS} is invariant under multiplying all the g_l by a constant which will mean S will always have determinant zero. We regularise by, $S_{l_1 l_2} \to (1 + \varepsilon \delta_{l_1 l_2}) S_{l_1 l_2}$, for some small ε which is kept constant throughout the optimisation.

Throughout the optimisations performed in this study we use the recommended hyperparameters from Ref. [161] of $\beta_1 = 0.9$, $\beta_2 = 0.999$ and $\epsilon = 10^{-5}$. We found that a suitable learning rate for this optimisation problem is around $\gamma \sim 0.005$ and we use the same ε to regulate S as given in Ref. [163] with $\varepsilon = 10^{-3}$.

The issue of how to pick the number of g_l to use is addressed as follows. For the MS_{-1} case, we ran the optimisation at $N = 12$ with the first 7 g_l, where it was found that the broadening of the Fermi surface, as seen through the n_l^{CF}, was around 2 in l

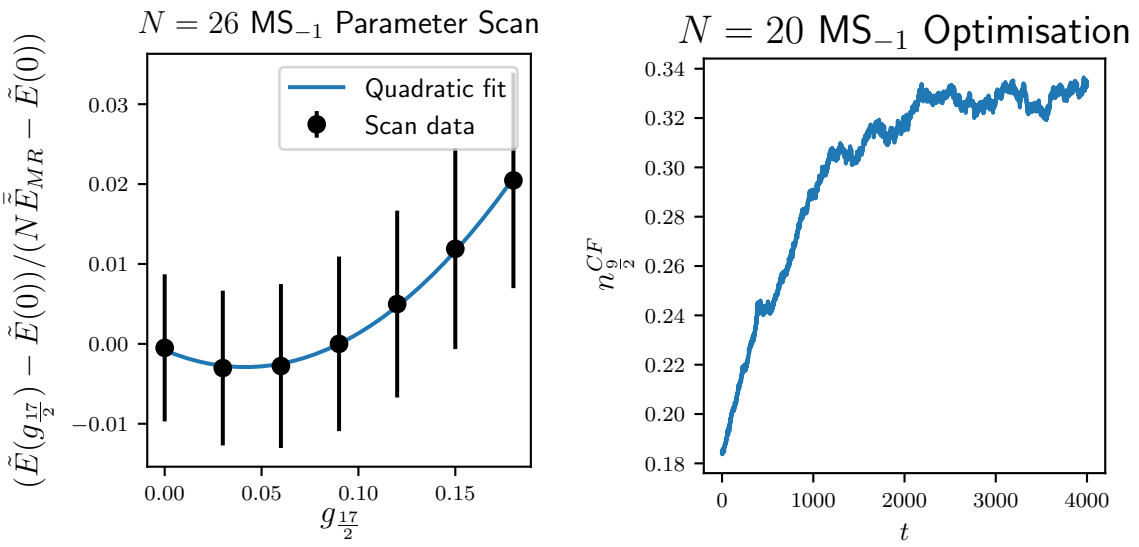

Figure 4.2: Left - adjusted energy $\tilde{E}$ (see Eq. 4.15) as a function of the 9th g_l, around the optimum solution for the first 8 g_l for the $N = 26$ MS$_{-1}$ wave function with the 2nd LL Coulomb interaction, where $\tilde{\tilde{E}}_{MR}$ is the thermodynamic $\tilde{E}/N$ of the MR wave function (see Tab. 4.1). Right - showing $n^{\mathrm{CF}}_{\frac{9}{2}}$ (see Eq. 4.8) at each iteration t of the optimisation of the $N = 20$ MS$_{-1}$ wave function with the 2nd LL Coulomb interaction.

space (i.e. n_l^{CF} were found to be sufficiently close to zero for $l > l_f + 2$). We expect this broadening in l space to scale as $\sqrt{N}$ as $l \sim kR$. Thus, for system sizes from 12-20 particles, we used the first 7 g_l to optimise the MS$_{-1}$ wave functions and at 26 particles we used the first 8. To demonstrate this number of parameters is sufficient we estimated the energy as a function of the 9^{th} g_l around the optimum set when using the first 8 g_l for the $N = 26$ MS$_{-1}$ optimisation with the Coulomb interaction in the second LL. The result of this parameter scan can be seen in the left plot of Fig. 4.2, where it can be seen that the possible energy reduction per particle that can be achieved by varying this parameter is small in comparison to the difference between the previous optimum energy per particle and the thermodynamic energy per particle of the Moore-Read wave function (see Fig. 4.3 and Tab. 4.1 for details of thermodynamic estimates). Similarly, for both the MR* and the MS$_1$ wave functions we used the first 7 g_l for 12-20 particles and used the first 8 for 26 particles. By the same method, we found that using the first 6 and 7 g_l was sufficient to optimise the MS$_3$ wave functions

for 10-18 and 24 particles respectively.

When optimising a given MS_ℓ wave function we start the algorithm with $g_l = \frac{1}{2l+1}$ for the parameters that are actually varied and all other g_l are set to zero, $g_l = 0$. This is the approximate YM_ℓ wave function which we expect to be close to the minimum energy.

The right plot of Fig. 4.2 shows the $n^{\mathrm{CF}}_{\frac{9}{2}}$ occupation probability at each iteration t for the optimisation of the $N = 20$ MS_{-1} wave function with the 2nd LL Coulomb interaction (note that $l = \frac{9}{2}$ is just at the Fermi level). Initially, the algorithm moves sharply towards a minimum where it plateaus near the minimum energy at around $t = 4000$. We found that this algorithm converged after around $t \sim 4000$ iterations for all cases considered using the hyperparameters given above. One can also see that the apparent noise in the $n^{\mathrm{CF}}_{\frac{9}{2}}(t)$ path increases as we approach the minimum. At larger system sizes this sometimes required a fine-tuning stage with around 100 iterations where the number of samples and the learning rate are increased to obtain the minimum energy solution with the desired accuracy.

4.4 Results and discussion

4.4.1 Energetics

Fig. 4.3 shows the *adjusted* energy, $\tilde{E}$, per particle of the optimised MR* and MS_ℓ wave functions with $\ell = -1, 1, 3$, as well as the $\tilde{E}/N$ of the MR, YM_ℓ, with $\ell = -1, 1, 3$, $\overline{\mathrm{MR}}$ and $\overline{\mathrm{MS}}_\ell$, with $\ell = -1, 3$, wave functions as a function of $1/N$ for the Coulomb interaction in the 2nd LL, where a bar denotes the particle-hole conjugate of a wave function and the adjusted energy is defined by,

$$\tilde{E} = \sqrt{\frac{Q}{N}}\left(E - \frac{N^2 e^2}{8\pi\varepsilon_0 l_B \sqrt{Q}}\right) \tag{4.15}$$

In the case of the Coulomb interaction, the multiplicative factor adjusts the energies

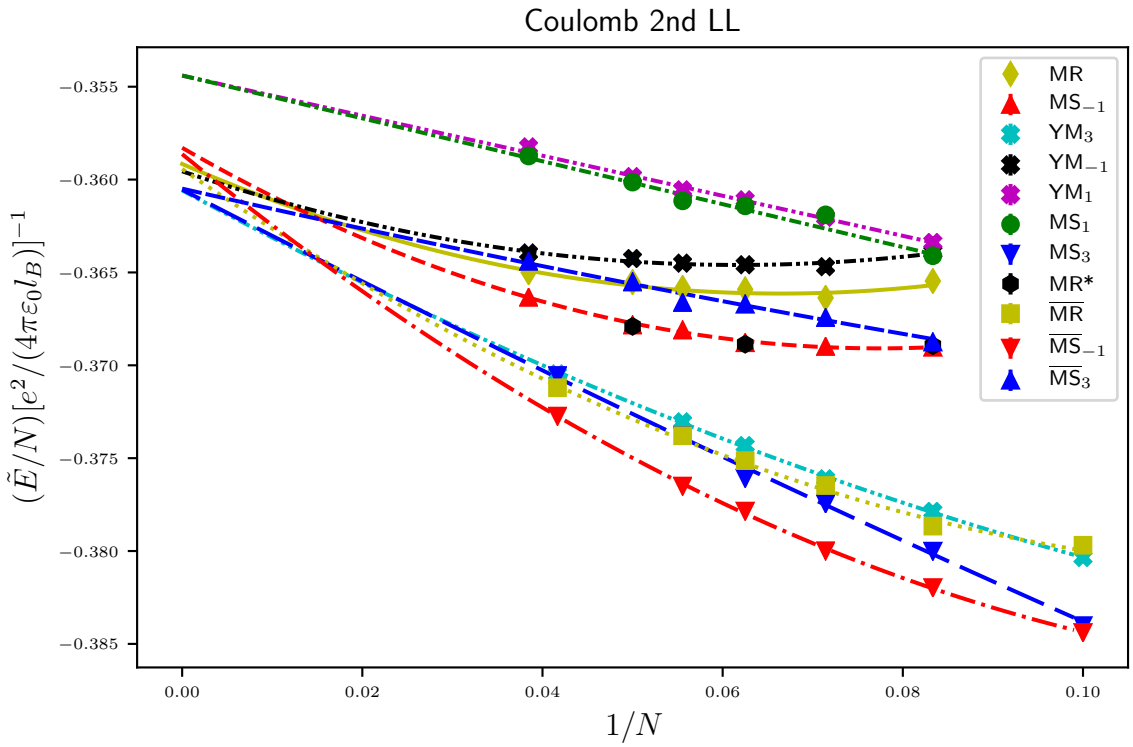

Figure 4.3: Shows the $\tilde{E}/N$ (see Eq. 4.15) for the optimised wave functions as well for the MR and particle-hole conjugated wave functions of these, denoted with a bar, for Coulomb interaction in the 2nd LL. Lines show the resulting polynomial fits in $1/N$ (see main text for full details). Whilst error bars are included for the Monte Carlo estimated energies their sizes are similar to those of the markers.

so that the particle density is kept constant, by rescaling the radius of the sphere $R = l_B\sqrt{Q} \to l_B\sqrt{N}$, and the $\frac{N^2}{8\pi\varepsilon_0 l_B\sqrt{Q}}$ term is the electrostatic energy of a uniformly charged sphere of radius $l_B\sqrt{Q}$ with total charge Ne. As discussed in Ref. [164] this is used to improve the estimates of the thermodynamic energy per particle, which we achieve by fitting a quadratic polynomial in $1/N$ to the $\tilde{E}/N$ of the MR, YM$_\ell$, MS$_\ell$ and $\overline{\text{MS}}_\ell$, with $\ell = -1, 3$, wave functions and a linear function of $1/N$ for the $\tilde{E}/N$ of the YM$_1$ and MS$_1$ wave functions. The resulting estimated thermodynamic energies per particle can be found in Tab. 4.1. For those wave functions whose real-space form is known exactly, the energies at each system size have been estimated using $\sim 5 \times 10^9$ Monte Carlo samples. The energies of the particle-hole conjugated wave functions have been calculated using the result Ref. [165], where for a rotationally symmetric interaction

state	$(\tilde{E}/N)[e^2/(4\pi\varepsilon_0 l_B)]^{-1}$	state	$(\tilde{E}/N)[e^2/(4\pi\varepsilon_0 l_B)]^{-1}$
MS_{-1}	-0.358 ± 0.001	MR	-0.359 ± 0.001
$\overline{\mathrm{MS}}_{-1}$	-0.359 ± 0.001	$\overline{\mathrm{MR}}$	-0.359 ± 0.001
MS_3	-0.361 ± 0.002	YM_{-1}	-0.360 ± 0.001
$\overline{\mathrm{MS}}_3$	-0.360 ± 0.002	YM_3	-0.361 ± 0.001
MS_1	-0.354 ± 0.000	YM_1	-0.354 ± 0.000

Table 4.1: Showing the thermodynamic energies per particle $\tilde{E}/N$ for Coulomb interaction in the second LL, which are estimated by fitting polynomials to the adjusted energy per particle as a function of $1/N$ (see Fig. 4.3), for the various wave functions. Errors have been estimated using the square root of the corresponding diagonal element of the estimated covariance matrix of the polynomial parameters that is outputted by the scipy curve fitting function.

under a particle-hole transform the energy transforms as $E \to \big(1 - \frac{2N}{2Q+1}\big)E_{\text{filled}} + E$, where E_{filled} is the energy of the corresponding filled Landau level.

As can be immediately seen from Fig. 4.3 despite allowing for some optimisation, the MS_1 wave functions, which are expected to be in the PH-Pfaffian phase, are energetically unfavourable in comparison with all other wave functions tested here in the case of the Coulomb interaction in the 2nd LL. In fact, the amount by which one can reduce the energy of these $\ell = 1$ wave functions is negligible in comparison with the energy scales in Fig. 4.3.

Another immediate observation from Fig. 4.3 is that the YM_3 wave function appears to have energy very close to the $\overline{\mathrm{MR}}$ wave function (the "ideal" anti-Pfaffian trial wave unction) on the energy scales considered at the tested system sizes. In other words, the YM_3 is already an excellent approximation, energetically, to the $\overline{\mathrm{MR}}$ wave function. The YM_{-1} wave function, on the other hand, appears to offer a comparatively worse energetic approximation to the MR wave function at finite system sizes.

If we roughly[2] compare the energies of the MS_{-1} wave functions at $N = 12$ and $N = 18$, with energies $(\tilde{E}/N)[e^2/(4\pi\varepsilon_0 l_B)]^{-1} \approx -0.369$ and $(\tilde{E}/N)[e^2/(4\pi\varepsilon_0 l_B)]^{-1} \approx -0.368$ respectively, with those obtained by exact diagonalisation in Ref. [60], with

[2]One should be very cautious about making direct comparisons between our numerical energies and those obtained by more exact methods as one can see from Fig. 4.1 the effective interaction does not perfectly reproduce the Haldane pseudo-potential coefficients at intermediate m.

energies $(\tilde{E}/N)[e^2/(4\pi\varepsilon_0 l_B)]^{-1} \approx -0.369$ and $(\tilde{E}/N)[e^2/(4\pi\varepsilon_0 l_B)]^{-1} \approx -0.368$ respectively, we find them to be almost identical (to three significant figures). Furthermore, if we compare the optimised energy of the MS_{-1} wave function at $N = 20$, with energy $(\tilde{E}/N)[e^2/(4\pi\varepsilon_0 l_B)]^{-1} \approx -0.367$, with the energy estimate obtained by the DMRG study of Ref. [66] at the same system size on the sphere, with energy $(\tilde{E}/N)[e^2/(4\pi\varepsilon_0 l_B)]^{-1} \approx -0.367$, we also find them to be almost identical. The fact that the optimised energies of the MS_{-1} wave functions are so close to those obtained by ED and DMRG, at these intermediate system sizes, then explains why the energies of the optimised MR* wave functions, used the benchmark the MS_{-1} optimisations, are not discernable from those of the MS_{-1} at $N = 12, 16, 20$, where we then find no advantage of using the MR* wave functions over the MS_{-1}. On the other hand, we can clearly see that the amount by which the energies of MS_3 wave functions can be minimised is comparatively less, with the $\overline{\mathrm{MS}_{-1}}$ wave functions offering clearly better estimates of the corresponding exact ground state energies.

Furthermore, as can be seen from Fig. 4.3 and Tab. 4.1 the energies of the MR, $\overline{\mathrm{MR}}$, YM_ℓ, with $\ell = -1, 3$, and the optimised MS_ℓ, along with their particle-hole conjugates $\overline{\mathrm{MS}}_\ell$, wave functions all converge in the thermodynamic limit. This is perhaps surprising as one would typically expect that allowing for some energy minimisation away from the zero-parameter trial wave functions would allow for an improved estimate of the energy of the actual ground state in the thermodynamic limit.

There are several possibilities at this point. Firstly, it may, in fact, be the case that the amount by which the energy can be reduced by optimising the MS_{-1} and MS_3 wave functions compared with the MR and YM_3 wave functions falls to zero in the thermodynamic limit. In short, these wave functions may just not offer enough variational freedom at larger system sizes. One may expect, however, that the MS_{-1} wave functions should offer better thermodynamic estimates given that at smaller system sizes their energies are comparable with more exact methods. On the contrary,

it should be noted that the polynomial used to extrapolate MS_{-1} has a noticeable curvature, which implies even slight differences between the exact energies and the MS_{-1} can result in a large difference between their thermodynamic extrapolations [3]. Of course, one could object to the extrapolation method used here. Whilst it can never be definitively known if the extrapolation method is correct, we can at least verify it is a "reasonable" method by the fact that the thermodynamic energy extrapolations of each wave function converge precisely with its corresponding particle-hole conjugate, when the conjugate wave function has been included.

Another possibility is that the optimisation algorithm is getting stuck at a local minimum. This could be alleviated by starting the optimisation at randomized g_l, however, this would come at an increased computational cost as the algorithm must explore a larger area of parameter space to find a minimum. Indeed, the computational cost of optimising these wave functions using the procedure outlined in this chapter should be emphasised. For example, at $N = 26$ particles the optimisation of a wave function with 8 g_l using 300 computing nodes can take around a week, at current computer standards, from the beginning of the optimisation to obtaining an accurate estimate of the energy of the optimised wave function. In the worst case, if several fine-tuning phases are required, obtaining the optimum energy at the desired level of accuracy can take on the order of a month. As can be seen from Fig. 4.3 this is partly due to the fact that many Monte Carlo samples are required at each iteration of the optimisation in order to resolve the rather small differences in the energies of the various wave functions. Thus, although the algorithm could be started from randomized g_l this would come at an increased cost which would render this procedure impractical for most interesting use cases. Whilst, we have checked in Fig. 4.2 if using extra g_l in the optimisations performed makes very little difference in the energies, it is possible that adding these extra g_l could make a difference to the thermodynamic extrapolation,

[3] i.e. fitting quadratic polynomials can be much less stable than fitting a linear function

particularly for the MS_{-1} where the extrapolating polynomial has noticeable curvature. However, with each new g_l the computational cost increases as many more CF orbitals need to be computed. In short, this is perhaps not a practical method for obtaining better thermodynamic estimates in comparison with other numerical methods.

4.4.2 Effective CF pairing

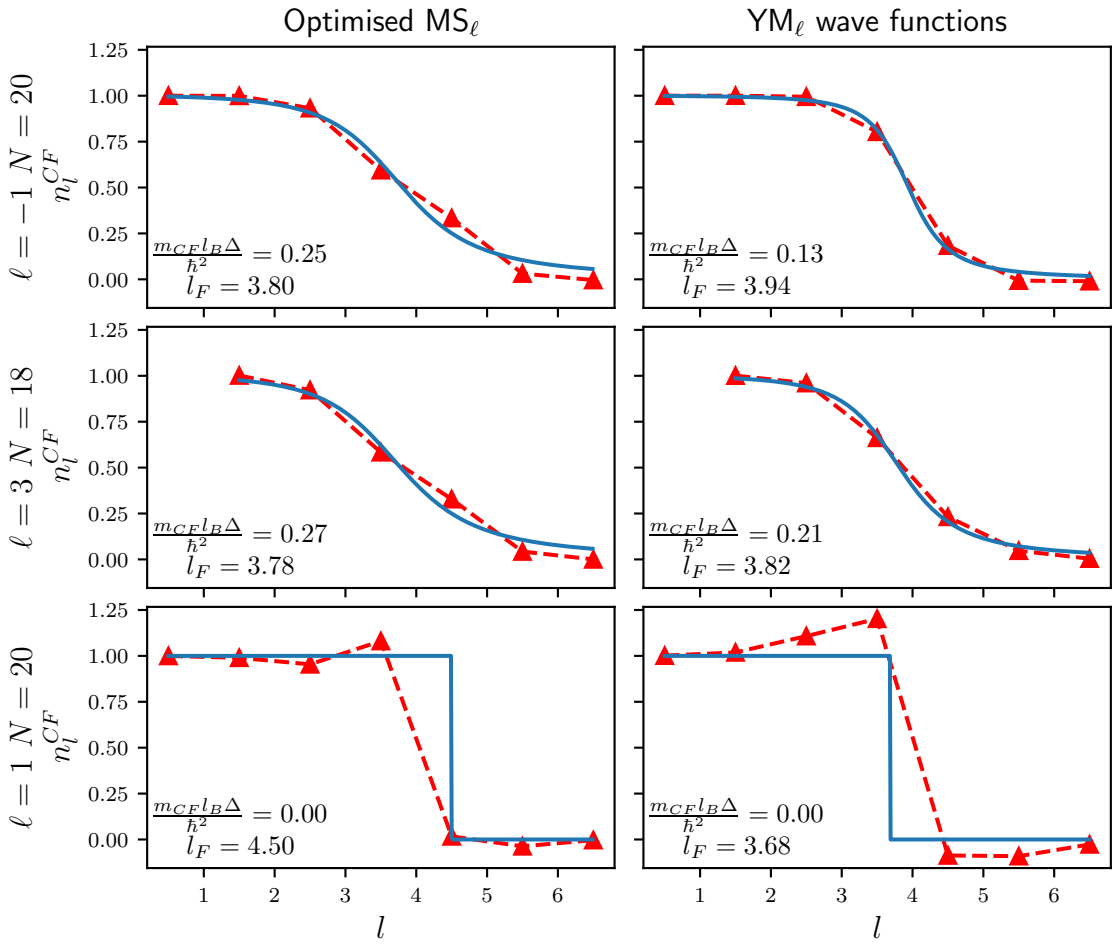

Figure 4.4: Showing the CF orbital occupation probabilities n_l^{CF} (see Eq. 4.8) for various YM_ℓ and optimised MS_ℓ wave functions (dashed lines) along with a corresponding fit to the weak-pairing ansatz of Eq. 4.7 (solid lines), where l_F is taken to be an adjustable parameter. The fitted parameters are indicated in the bottom left corner of the corresponding plot, where m_{CF} is the (unknown) effective CF mass. Note that $m_{\mathrm{CF}} l_B \Delta / \hbar^2$ parameter has been estimated where we take the radius of the sphere to be $R = l_B \sqrt{N}$, which keeps the particle density constant.

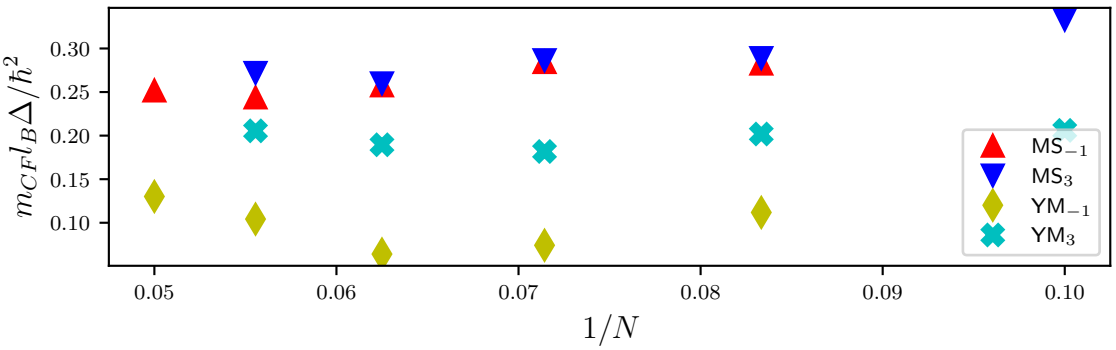

Figure 4.5: Showing the fitted $m_{\rm CF} l_B \Delta/\hbar^2$ of the weak pairing ansatz, Eq. 4.7, for the effective CF occupations n_l^{CF} for the optimised MS$_\ell$ and the fixed parameter YM$_\ell$ wave functions for $\ell = -1, 3$ over a variety of system sizes, where m_{CF} is the unknown effective CF mass. Note that $m_{\rm CF} l_B \Delta/\hbar^2$ parameter has been estimated where we take the radius of the sphere to be $R = l_B\sqrt{N}$, which keeps the particle density constant.

Whilst the optimised MS$_\ell$ wave functions do not appear to offer any better thermodynamic energy estimates compared with the YM$_\ell$, they do offer more insight at finite-size systems through the effective paired CF description. We have estimated, using Monte Carlo, the effective CF occupation probabilities $n_l^{\rm CF}$ (Eq. 4.8) for the optimised MS$_\ell$ wave functions and for the corresponding YM$_\ell$. We have then fitted the BCS type weak pairing ansatz (WPA) of Eq. 4.7 for the various estimated $n_l^{\rm CF}$, where we allow for the Fermi-level, l_F, to be a parameter that can be varied in the fit and we take the radius of the sphere used in Eq. 4.7 to be $R = l_B\sqrt{N}$ so as to keep the particle density constant. This then allows us to give an estimate for the dimensionless parameter $\frac{m_{\rm CF} l_B \Delta}{\hbar^2}$, where $m_{\rm CF}$ is the effective CF mass which we will assume to be constant so that we can take $\frac{m_{\rm CF} l_B \Delta}{\hbar^2}$ as a measure of the effective CF pairing strength.

Fig. 4.4 shows the estimated $n_l^{\rm CF}$ and corresponding fitted WPA for the optimised MS$_\ell$ and fixed parameter YM$_\ell$ wave functions at $\ell = -1, 3, 1$ for $N = 20, 18, 20$ respectively. The $n_l^{\rm CF}$ of the MS$_\ell$ and YM$_\ell$ for $\ell = -1, 3$ can be fit reasonably well to the WPA.

In Fig. 4.5 shows the fitted $m_{\rm CF} l_B \Delta/\hbar^2$ parameter of the optimised MS$_\ell$ and YM$_\ell$ wave functions for $\ell = -1, 3$ as a function of $1/N$, where it can generally be seen that

the effective CF pairing in the optimised MS_ℓ wave functions is higher than that of the YM_ℓ. Interestingly we find the effective pairing strength for the optimised MS_ℓ for $\ell = -1, 3$ wave functions to be roughly the same at the same number of particles N, where it should be emphasised that at the same N the MS_{-1} and MS_3 wave functions occur at different total magnetic flux through the sphere (i.e. have different shifts $\mathcal{S}$).

The data from Fig. 4.5 can also offer more insight into some of the observations one can make from Fig. 4.3. One can see that from Fig. 4.3 that the amount by which the energy of the MS_{-1} wave functions can be lowered compared with the corresponding MR wave functions is generally larger than the amount by which the energy of the MS_3 wave function can be lowered in comparison with the YM_3 wave functions. Taking the YM_{-1} wave function as an approximation of the MR wave function, this has a simple interpretation in the effective pairing description in that the effective pairing strength of the YM_{-1} wave function is generally lower than that of the YM_3 wave functions. Thus the YM_3 wave functions have an effective pairing closer to the optimum compared with the YM_{-1} wave functions which gives some explanation as to why the energy of the YM_3 wave functions are already close to optimal MS_3 wave functions, whereas at intermediate system sizes the optimum MS_{-1} wave functions have energy noticeably lower than the corresponding MR wave function.

Finally, as can also be seen in Fig. 4.4 the n_l^{CF} of the optimised MS_1 and YM_1 wave functions are noticeably larger than one in some cases and are negative in some other cases, which is clearly inconsistent with interpreting these n_l^{CF} as occupation *probabilites*. This was found to occur at all other tested system sizes. This interpretation of the n_l^{CF} is based on the assumption that the Jastrow factor of the wave function can be approximated in some "mean-field" way, which is usually assumed when interpreting generic CF wave functions. Combining this with the observations of YM, that the YM_1 wave function shows no sign of emergent pairing in the pair correlation function, and with the evidence that the "ideal" PH-Pfaffian wave function may, in

fact, represent a gapless phase of matter [155], indicates the possibility that this usual "mean-field" interpretation of the Jastrow factor might break down for the current candidate PH-Pfaffian wave functions and so may in fact not be a representative for the phase of matter predicted by Son [65]. It has also recently been argued by Haldane [166], based on a conjecture that FQH states must have a non-zero so-called "guiding centre quadrupole moment", that particle-hole symmetric states can never be FQH states, which may give an explanation for these observed pathologies. Despite this, we can still see that the n_l^{CF} of the optimised MS_1 wave functions can still be roughly fit to the WPA with $\Delta = 0$, which would correspond to the gapless CF Fermi-liquid. If the actual ground state occurs at a shift of $\mathcal{S} = -3$ or $\mathcal{S} = 1$ (i.e. those of the Pfaffian and anti-Pfaffian states), then the system being at the shift of the PH-Pfaffian wave functions would correspond to some quasi-particle excitation, which in the absence of disorder would then be a gapless sector. This may then give some explanation as to why the optimised MS_1 wave functions, roughly, resemble the *gapless* CF liquid. In summary, however, even after some optimisation we see no evidence of an effective paired CF description for the PH-Pfaffian wave functions.

4.5 Summary and outlook

The main goal of this chapter was to understand if minimising the energy of the MS_ℓ wave functions could offer more accurate approximations to the ground state, for the Coulomb interaction in the second LL, in comparison to the YM_ℓ wave functions and if this would dramatically change the energetics of the $\ell = 1$ wave functions, which were expected to represent the PH-Pfaffian phase. In the end, we found that the energies of the optimised MS_ℓ, YM_ℓ, for $\ell = -1, 3$, MR and $\overline{\mathrm{MR}}$ wave functions all converge in the thermodynamic limit where we found the YM_3 wave function to be an excellent approximation, in energy, to the $\overline{\mathrm{MR}}$ wave function. This then, obviously, did not allow for improved thermodynamic energy estimates of the actual ground state. Furthermore,

we found that the energy of the MS_1 wave functions could only be minimised by a negligible amount in comparison to the corresponding YM_1 wave function, where both these wave functions remain energetically unfavourable. However, we did find that the energies of the optimised MS_{-1} wave functions are comparable to those obtained by exact diagonalisation and DMRG at small system sizes, with this not being the case for the MS_3 wave functions. By considering the effective CF orbital occupation probabilities, n_l^{CF}, we found that the CF pairing of the MS_ℓ and YM_ℓ wave functions, at $\ell = -1, 3$, can be well approximated by a BCS weak pairing type ansatz, where the optimised MS_ℓ showed stronger pairing than the YM_ℓ wave functions. We also found further pathologies in the MS_1 and YM_1 wave functions in that their n_l^{CF} could not be consistently interpreted as probabilities.

It is not obvious if the convergence of the thermodynamic energies of the wave functions in the Pfaffian and anti-Pfaffian phases is unique to the Coulomb interaction in the second LL. It would be interesting to perform these optimisations at slightly different interactions. Although one should be cautious of the observed charge density wave phase in the vicinity of the Coulomb interaction in the second LL [61]. In particular, it may be useful to carry out these optimisations for the two body interactions found in Ref. [155] to approximately stabilise the "ideal" PH-Pfaffian trial wave function, where it would be interesting to see if the pathologies of the MS_1 wave functions can be removed. Finally, given that the YM_3 wave functions are excellent energetic approximations to the $\overline{\mathrm{MR}}$ wave functions it could be possible to use these wave functions to better understand the effects LL mixing has at larger system sizes, using Monte Carlo methods, in separating the energies of the MR and $\overline{\mathrm{MR}}$ wave functions.

4.A Effective interaction parameters

See Table 4.2 for the V^{eff} parameters used in this study for the Coulomb interaction in the second LL.

$2Q$	a_0	a_1	α_1	a_2	α_2
19	1.120	115.660	1.357	-757.200	2.964
21	1.111	140.458	1.458	-973.385	3.164
23	1.102	115.604	1.353	-755.689	2.959
25	1.096	115.688	1.351	-755.678	2.956
27	1.090	115.754	1.350	-755.670	2.954
29	1.085	116.224	1.350	-758.751	2.954
31	1.080	120.041	1.329	-755.159	2.876
33	1.077	115.913	1.347	-755.650	2.949
35	1.073	115.957	1.346	-755.645	2.948
37	1.070	115.995	1.345	-755.640	2.947
47	1.059	116.095	1.342	-755.259	2.942
49	1.057	116.178	1.342	-755.617	2.941

Table 4.2: Fitted V^{eff} parameters for the 2nd LL Coulomb interaction at all $2Q$ (of the second LL system) considered in this study.

Chapter 5

Conclusions

In this thesis, we have investigated how various CFT and numerical methods can be applied to the analysis of FQHE trial wave functions to understand various physical properties of some of the possible phases of matter that can occur in the FQHE setting. In particular, we have seen how one can use CFT to understand and model the finer structure of the real-space entanglement spectra of chiral FQHE ground states and how we can understand the topological properties of Parton-type trial wave functions by expressing them as CFT correlation functions. Furthermore, we have seen how the energy minimisation of paired CF trial wave functions can potentially shed new light on the physics of the half-filled second Landau levels of electrons in GaAs heterostructures.

In Chapter 2, it was argued using QKL's cut-and-glue approach that the real-space entanglement spectra (RSES) of chiral FQHE ground states have a scaling property, where a given RSES could be reproduced by the spectrum of an effective "Hamiltonian", also called an entanglement action, of the system's edge degrees of freedom that takes the form of an integral of local operators at the edge that can be expanded in negative powers of the real-space cut length. This was then directly tested in the case of $\nu = 2/3$ bosonic CF wave function on the sphere, by fitting a model truncated entanglement action to the numerically computed RSES, where we found the numerical and model RSES to be in excellent agreement, with the scaling of the model parameters being consistent with the scaling property.

In Chapter 3 it was shown that all chiral Parton ground and edge state trial wave functions, in the planar geometry, can be expressed as CFT correlation functions, where we can associate a chiral algebra $\mathcal{A}$ to each Parton state such that one expects $\mathcal{A}$ to describe the topological properties of the corresponding state. As a specific example, we demonstrated that the symmetric Parton states ϕ_n^m could be expressed using the $\hat{\mathfrak{u}}(1)\oplus\widehat{\mathfrak{su}}(n)_m$ WZW model, which is consistent with the effective field theories derived by Wen [92]. We then extended the generalised screening hypothesis to these states, where it was argued that if this and an additional conjecture holds the inner products between edge state trial wave functions can be expressed as matrix elements of an exponentiated local action operator in the CFT, extending DRR's result, which implied the existence of an isometric isomporphism from CFT states to edge state wave functions in the thermodynamic limit. This was then numerically tested for unprojected the $\nu = 2/5$ CF edge states and the ϕ_2^2 Parton edge states, where we found no contradiction with generalised screening.

Finally, in Chapter 4 we investigated the possibility of minimising the energy of paired CF trial wave functions, at pairing channels $\ell = -1, 1, 3$ corresponding to the Pfaffian PH-Pfaffian and anti-Pfaffian topological orders respectively, to gain further insights into the physics at $\nu = 5/2$. At small system sizes, with the Coulomb interaction in the absence of LL mixing, we found the energy reduction at $\ell = -1$ to be comparable with exact diagonalization, and that the optimised $\ell = 3$ wave functions were energetically similar to their corresponding zero-parameter trial wave functions. The optimised $\ell = 1$ wave functions were found to still be noticeably unfavourable energetically compared with the $\ell = -1, 3$ pairing channels with further pathologies of the $\ell = 1$ wave functions being found. Finally, we found the pairing function of the optimised $\ell = -1, 3$ wave functions could be well approximated by weak-pairing BCS type descriptions with both pairing channels showing near equal pairing strengths at the same system size.

The CFT and numerical methods presented in this thesis could still be further developed with wider applicability. For example, it would be interesting to see if the machinery of chapters 2 and 3 can be extended to non-chiral FQHE ground and edge states which are less well understood in comparison with many chiral FQHE states. Furthermore, the CFT constructions of chapter 3 could be applied more generally to construct trial wave functions from chiral algebras which are generated by more than one field and its conjugate, and it would be perhaps interesting to understand exactly what topological orders can, in principle, be described by these constructions. Finally, the numerical methods presented in Chapter 4 could potentially be used to study other systems with evidence of Composite Fermion pairing such as bilayer graphene [167, 168].

References

[1] G. J. Henderson, G. J. Sreejith, and S. H. Simon, Entanglement action for the real-space entanglement spectra of chiral Abelian quantum Hall wave functions, Phys. Rev. B **104**, 195434 (2021).

[2] P. W. Anderson, More is different: broken symmetry and the nature of the hierarchical structure of science. Science **177**, 393 (1972).

[3] L. D. Landau, On the theory of phase transitions. I. Phys. Z. Sowjet. **11**, 26 (1937).

[4] K. V. Klitzing, G. Dorda, and M. Pepper, New method for high-accuracy determination of the fine-structure constant based on quantized hall resistance, Phys. Rev. Lett. **45**, 494 (1980).

[5] D. C. Tsui, H. L. Stormer, and A. C. Gossard, Two-Dimensional Magnetotransport in the Extreme Quantum Limit, Phys. Rev. Lett. **48**, 1559 (1982).

[6] X. G. Wen and Q. Niu, Ground-state degeneracy of the fractional quantum Hall states in the presence of a random potential and on high-genus Riemann surfaces, Phys. Rev. B **41**, 9377 (1990).

[7] X. G. Wen, *Colloquium* : Zoo of quantum-topological phases of matter, Rev. Mod. Phys. **89**, 041004 (2017).

[8] F. D. M. Haldane, Nobel Lecture: Topological quantum matter *, Rev. Mod. Phys. **89**, 040502 (2017).

[9] C. Nayak, S. H. Simon, A. Stern, M. Freedman, and S. Das Sarma, Non-Abelian anyons and topological quantum computation, Rev. Mod. Phys. **80**, 1083 (2008).

[10] R. B. Laughlin, Anomalous quantum Hall effect: An incompressible quantum fluid with fractionally charged excitations, Phys. Rev. Lett. **50**, 1395 (1983).

[11] D. Arovas, J. R. Schrieffer, and F. Wilczek, Fractional Statistics and the Quantum Hall Effect, Phys. Rev. Lett. **53**, 722 (1984).

[12] N. Read, Excitation structure of the hierarchy scheme in the fractional quantum Hall effect, Phys. Rev. Lett. **65**, 1502 (1990).

[13] X. G. Wen and A. Zee, Classification of Abelian quantum Hall states and matrix formulation of topological fluids, Phys. Rev. B **46**, 2290 (1992).

[14] G. Moore and N. Read, Nonabelions in the fractional quantum hall effect, Nuc. Phys. B **360**, 362 (1991).

[15] A. Stern, Anyons and the quantum Hall effect—A pedagogical review, Ann. Phys., January Special Issue 2008 **323**, 204 (2008).

[16] A. Kitaev, Anyons in an exactly solved model and beyond, Ann. Phys. **321**, 2 (2006).

[17] X. G. Wen, Chiral Luttinger liquid and the edge excitations in the fractional quantum Hall states, Phys. Rev. B **41**, 12838 (1990).

[18] N. Read, Conformal invariance of chiral edge theories, Phys. Rev. B **79**, 245304 (2009).

[19] X. G. Wen, Topological orders and Edge excitations in FQH states, Adv. Phys. **44**, 405 (1995).

[20] P. Di Francesco, P. Mathieu, and D. Sénéchal, *Conformal Field Theory* (Springer New York, New York, NY, 1997).

[21] E. Witten, Topological quantum field theory, Commun. Math. Phys. **117**, 353 (1988).

[22] Y. Zhang, T. Grover, A. Turner, M. Oshikawa, and A. Vishwanath, Quasiparticle statistics and braiding from ground-state entanglement, Phys. Rev. B **85**, 235151 (2012).

[23] C. Wang, A. Vishwanath, and B. I. Halperin, Topological order from disorder and the quantized Hall thermal metal: Possible applications to the $\nu = 5/2$ state, Phys. Rev. B **98**, 045112 (2018).

[24] Z. Wang, *Topological Quantum Computation* (Am. Math. Soc., 2010).

[25] X. Chen, Z. C. Gu, and X. G. Wen, Local unitary transformation, long-range quantum entanglement, wave function renormalization, and topological order, Phys. Rev. B **82**, 155138 (2010).

[26] J. M. Leinaas and J. Myrheim, On the theory of identical particles, Nuovo. Cim. B **37**, 1 (1977).

[27] F. Wilczek, Magnetic Flux, Angular Momentum, and Statistics, Phys. Rev. Lett. **48**, 1144 (1982).

[28] S. H. Simon, *Wavefunctionology: The Special Structure of Certain Fractional Quantum Hall Wavefunctions* (2020).

[29] N. Laflorencie, Quantum Entanglement in Condensed Matter Systems, Physics Reports **646**, 1 (2016).

[30] H. Li and F. D. Haldane, Entanglement spectrum as a generalization of entanglement entropy: Identification of topological order in non-Abelian fractional quantum hall effect states, Phys. Rev. Lett. **101**, 1 (2008).

[31] A. Sterdyniak, A. Chandran, N. Regnault, B. A. Bernevig, and P. Bonderson, Real-space entanglement spectrum of quantum Hall states, Phys. Rev. B **85**, 125308 (2012).

[32] I. D. Rodríguez, S. H. Simon, and J. K. Slingerland, Evaluation of Ranks of Real Space and Particle Entanglement Spectra for Large Systems, Phys. Rev. Lett. **108**, 256806 (2012).

[33] R. Thomale, A. Sterdyniak, N. Regnault, and B. A. Bernevig, Entanglement Gap and a New Principle of Adiabatic Continuity, Phys. Rev. Lett. **104**, 180502 (2010).

[34] J. Dubail, N. Read, and E. H. Rezayi, Real-space entanglement spectrum of quantum Hall systems, Phys. Rev. B **85**, 115321 (2012).

[35] J. Dubail, N. Read, and E. H. Rezayi, Edge-state inner products and real-space entanglement spectrum of trial quantum Hall states, Phys. Rev. B **86**, 1 (2012).

[36] X. L. Qi, H. Katsura, and A. W. Ludwig, General relationship between the entanglement spectrum and the edge state spectrum of topological quantum states, Phys. Rev. Lett. **108**, 1 (2012).

[37] B. Swingle and T. Senthil, Geometric proof of the equality between entanglement and edge spectra, Phys. Rev. B **86**, 45117 (2012).

[38] A. A. Belavin, A. M. Polyakov, and A. B. Zamolodchikov, Infinite conformal symmetry of critical fluctuations in two dimensions, J. Stat. Phys. **34**, 763 (1984).

[39] A. A. Belavin, A. M. Polyakov, and A. B. Zamolodchikov, Infinite conformal symmetry in two-dimensional quantum field theory, Nuc. Phys. B **241**, 333 (1984).

[40] A. Tsuchiya and Y. Kanie, Vertex operators in the conformal field theory on P1 and monodromy representations of the braid group, Lett. Math. Phys. **13**, 303 (1987).

[41] G. Moore and N. Seiberg, Polynomial equations for rational conformal field theories, Phys. Lett. B **212**, 451 (1988).

[42] G. Moore and N. Seiberg, Classical and quantum conformal field theory, Commun. Math. Phys. **123**, 177 (1989).

[43] E. Witten, Quantum field theory and the Jones polynomial, Commun. Math. Phys. **121**, 351 (1989).

[44] S. Fubini, Vertex operators and quantum hall effect, Mod. Phys. Lett. A **06**, 347 (1991).

[45] Y. Tserkovnyak and S. H. Simon, Monte Carlo Evaluation of Non-Abelian Statistics, Phys. Rev. Lett. **90**, 016802 (2003).

[46] X. G. Wen, Y. S. Wu, and Y. Hatsugai, Chiral operator product algebra and edge excitations of a fractional quantum Hall droplet, Nuc. Phys. B **422**, 476 (1994).

[47] N. Read, Non-Abelian adiabatic statistics and Hall viscosity in quantum Hall states and px + ipy paired superfluids, Phys. Rev. B **79**, 045308 (2009).

[48] J. K. Jain, Composite-Fermion Approach for the Fractional Quantum Hall Effect, Phys. Rev. Lett. **63**, 199 (1989).

[49] J. Jain, *Composite fermions*, Vol. 9780521862 (Cambridge University Press, Jan. 2007).

[50] T. H. Hansson, C. C. Chang, J. K. Jain, and S. Viefers, Composite-fermion wave functions as correlators in conformal field theory, Phys. Rev. B **76**, 075347 (2007).

[51] T. Kvorning, Quantum Hall hierarchy in a spherical geometry, Phy. Rev. B **87**, 195131 (2013).

[52] T. H. Hansson, M. Hermanns, S. H. Simon, and S. F. Viefers, Quantum Hall Physics-hierarchies and CFT techniques, Rev. Mod. Phys. **89**, 025005 (2017).

[53] A. C. Balram, M. Barkeshli, and M. S. Rudner, Parton construction of particle-hole-conjugate Read-Rezayi parafermion fractional quantum Hall states and beyond, Phys. Rev. B **99**, 241108 (2019).

[54] A. C. Balram, A non-Abelian parton state for the $\nu = 2+3/8$ fractional quantum Hall effect, SciPost Phys. **10**, 083 (2021).

[55] Y. H. Wu, T. Shi, and J. K. Jain, Non-Abelian Parton Fractional Quantum Hall Effect in Multilayer Graphene, Nano Lett. **17**, 4643 (2017).

[56] S. Bandyopadhyay, L. Chen, M. T. Ahari, G. Ortiz, Z. Nussinov, and A. Seidel, Entangled Pauli principles: The DNA of quantum Hall fluids, Phys. Rev. B **98**, 161118 (2018).

[57] M. Tanhayi Ahari, S. Bandyopadhyay, Z. Nussinov, A. Seidel, and G. Ortiz, Partons as unique ground states of quantum hall parent hamiltonians: the case of fibonacci anyons, arXiv preprint arXiv:2204.09684 (2022).

[58] B. Blok and X. G. Wen, Many-body systems with non-abelian statistics, Nuc. Phys. B **374**, 615 (1992).

[59] X. G. Wen, Projective construction of non-Abelian quantum Hall liquids, Phys. Rev. B **60**, 8827 (1999).

[60] R. H. Morf, Transition from quantum hall to compressible states in the second landau level: new light on the $\nu = 5/2$ enigma, Phys. Rev. Lett. **80**, 1505 (1998).

[61] E. H. Rezayi and F. D. M. Haldane, Incompressible Paired Hall State, Stripe Order, and the Composite Fermion Liquid Phase in Half-Filled Landau Levels, Phys. Rev. Lett. **84**, 4685 (2000).

[62] M. Storni, R. H. Morf, and S. Das Sarma, Fractional Quantum Hall State at $\nu = 5/2$ and the Moore-Read Pfaffian, Phys. Rev. Lett. **104**, 076803 (2010).

[63] M. Levin, B. I. Halperin, and B. Rosenow, Particle-Hole Symmetry and the Pfaffian State, Phys. Rev. Lett. **99**, 236806 (2007).

[64] S.-S. Lee, S. Ryu, C. Nayak, and M. P. A. Fisher, Particle-Hole Symmetry and the $\nu = 5/2$ Quantum Hall State, Phys. Rev. Lett. **99**, 236807 (2007).

[65] D. T. Son, Is the composite fermion a dirac particle?, Phys. Rev. X **5** (2015).

[66] A. E. Feiguin, E. Rezayi, C. Nayak, and S. Das Sarma, Density Matrix Renormalization Group Study of Incompressible Fractional Quantum Hall States, Phys. Rev. Lett. **100**, 166803 (2008).

[67] M. P. Zaletel, R. S. Mong, F. Pollmann, and E. H. Rezayi, Infinite density matrix renormalization group for multicomponent quantum Hall systems, Phys. Rev. B **91**, 045115 (2015).

[68] M. Banerjee, M. Heiblum, V. Umansky, D. E. Feldman, Y. Oreg, and A. Stern, Observation of half-integer thermal Hall conductance, Nature **559**, 205 (2018).

[69] N. Read and D. Green, Paired states of fermions in two dimensions with breaking of parity and time-reversal symmetries and the fractional quantum Hall effect, Phys. Rev. B **61**, 10267 (2000).

[70] R. V. Mishmash, D. F. Mross, J. Alicea, and O. I. Motrunich, Numerical exploration of trial wave functions for the particle-hole-symmetric Pfaffian, Phys. Rev. B **98**, 081107 (2018).

[71] E. H. Rezayi, K. Pakrouski, and F. D. M. Haldane, Stability of the particle-hole pfaffian state and the $\frac{5}{2}$-fractional quantum hall effect, Phys. Rev. B **104**, 81407 (2021).

[72] G. Möller and S. H. Simon, Paired composite-fermion wave functions, Phys. Rev. B **77**, 075319 (2008).

[73] M. Yutushui and D. F. Mross, Large-scale simulations of particle-hole-symmetric Pfaffian trial wave functions, Phys. Rev. B **102**, 195153 (2020).

[74] B. Laughlin, Quantized Hall conductivity in two dimensions, Phys. Rev. B **23**, 5632 (1981).

[75] B. I. Halperin, Quantized Hall conductance, current-carrying edge states, and the existence of extended states in a two-dimensional disordered potential, Phys. Rev. B **25**, 2185 (1982).

[76] F. D. Haldane, Fractional quantization of the hall effect: A hierarchy of incompressible quantum fluid states, Phys. Rev. Lett. **51**, 605 (1983).

[77] T. T. Wu and C. N. Yang, Dirac monopole without strings: Monopole harmonics, Nuc. Phys. B **107**, 365 (1976).

[78] T. T. Wu and C. N. Yang, Some properties of monopole harmonics, Phys. Rev. D **16**, 1018 (1977).

[79] F. D. M. Haldane and E. H. Rezayi, Finite-Size Studies of the Incompressible State of the Fractionally Quantized Hall Effect and its Excitations, Phys. Rev. Lett. **54**, 237 (1985).

[80] S. Pu, G. J. Sreejith, and J. K. Jain, Anderson localization in fractional quantum Hall effect, Phys. Rev. Lett. **128**, 116801 (2022).

[81] A. M. Chang, P. Berglund, D. C. Tsui, H. L. Stormer, and J. C. M. Hwang, Higher-Order States in the Multiple-Series, Fractional, Quantum Hall Effect, Phys. Rev. Lett. **53**, 997 (1984).

[82] H. L. Stormer, A. Chang, D. C. Tsui, J. C. M. Hwang, A. C. Gossard, and W. Wiegmann, Fractional Quantization of the Hall Effect, Phys. Rev. Lett. **50**, 1953 (1983).

[83] W. Pan, H. L. Stormer, D. C. Tsui, L. N. Pfeiffer, K. W. Baldwin, and K. W. West, Transition from an Electron Solid to the Sequence of Fractional Quantum Hall States at Very Low Landau Level Filling Factor, Phys. Rev. Lett. **88**, 176802 (2002).

[84] B. I. Halperin, Statistics of quasiparticles and the hierarchy of fractional quantized hall states, Phys. Rev. Lett. **52**, 1583 (1984).

[85] J. Jain, Incompressible quantum Hall states, Phys. Rev. B **40**, 8079 (1989).

[86] J. K. Jain, Theory of the fractional quantum Hall effect, Phys. Rev. B **41**, 7653 (1990).

[87] J. K. Jain, *Thirty Years of Composite Fermions and Beyond* (June 2020).

[88] J. Nakamura, S. Liang, G. C. Gardner, and M. J. Manfra, Direct observation of anyonic braiding statistics, Nat. Phys. **16**, 931 (2020).

[89] J. M. Caillol, D. Levesque, J. J. Weis, and J. P. Hansen, A Monte Carlo study of the classical two-dimensional one-component plasma, J. Stat. Phys. **28**, 325 (1982).

[90] X. G. Wen, Theory of the edge states in fractional quantum hall effects, Int. J. Mod. Phys. B **06**, 1711 (1992).

[91] X. G. Wen, *Quantum Field Theory of Many-Body Systems* (Oxford University Press, 2007).

[92] X. G. Wen, Non-Abelian statistics in the fractional quantum Hall states, Phys. Rev. Lett. **66**, 802 (1991).

[93] V. G. Knizhnik and A. B. Zamolodchikov, Current algebra and Wess-Zumino model in two dimensions, Nuc. Phys. B **247**, 83 (1984).

[94] I. D. Rodríguez and G. Sierra, Entanglement entropy of integer quantum Hall states, Phys. Rev. B **80**, 153303 (2009).

[95] A. M. Turner, Y. Zhang, and A. Vishwanath, Entanglement and inversion symmetry in topological insulators, Phys. Rev. B **82**, 241102 (2010).

[96] P. Calabrese and J. Cardy, Time Dependence of Correlation Functions Following a Quantum Quench, Phys. Rev. Lett. **96**, 136801 (2006).

[97] P. Calabrese and J. Cardy, Quantum quenches in extended systems, J. Stat. Mech. Theory Exp. **2007**, P06008 (2007).

[98] N. Regnault, B. A. Bernevig, and F. D. M. Haldane, Topological Entanglement and Clustering of Jain Hierarchy States, Phys. Rev. Lett. **103**, 016801 (2009).

[99] B. Yan, R. R. Biswas, and C. H. Greene, Bulk-edge correspondence in fractional quantum Hall states, Phys. Rev. B **99**, 035153 (2019).

[100] A. Sterdyniak, B. A. Bernevig, N. Regnault, and F. D. Haldane, The hierarchical structure in the orbital entanglement spectrum of fractional quantum Hall systems, New J. Phys. **13**, 105001 (2011).

[101] N. Ishibashi, The Boundary and Crosscap States in Conformal Field Theories, Mod. Phys. Lett. **04**, 251 (1988).

[102] J. L. Cardy, Boundary conditions, fusion rules and the Verlinde formula, Nuc. Phys. B **324**, 581 (1989).

[103] B. Blok and X. G. Wen, Effective theories of the fractional quantum Hall effect at generic filling fractions, Phys. Rev. B **42**, 8133 (1990).

[104] R. Fern, R. Bondesan, and S. H. Simon, Effective edge state dynamics in the fractional quantum Hall effect, Phys. Rev. B **98**, 1 (2018).

[105] R. Fern, R. Bondesan, and S. H. Simon, Structure of edge-state inner products in the fractional quantum Hall effect, Phys. Rev. B **97**, 155108 (2018).

[106] I. D. Rodríguez, S. C. Davenport, S. H. Simon, and J. K. Slingerland, Entanglement spectrum of composite fermion states in real space, Phys. Rev. B **88**, 3 (2013).

[107] A. Anand and G. Sreejith, Real-space entanglement spectra of lowest landau level projected fractional quantum hall states using monte carlo methods, Phys. Rev. B **107**, 085101 (2023).

[108] J. K. Jain and R. K. Kamilla, Composite fermions in the Hilbert space of the lowest electronic Landau level, Int. J. Mod. Phys. B **11**, 2621 (1997).

[109] M. J. Arildsen, N. Schuch, and A. W. W. Ludwig, Entanglement spectra of non-chiral topological (2+1)-dimensional phases with strong time-reversal breaking, Li-Haldane state counting, and PEPS, arXiv preprint arXiv:2207.03246 (2022).

[110] S. M. Girvin and A. H. MacDonald, Off-diagonal long-range order, oblique confinement, and the fractional quantum Hall effect, Phys. Rev. Lett. **58**, 1252 (1987).

[111] I. Peschel, Calculation of reduced density matrices from correlation functions, J. Phys. A Math. Theor. **36**, 205 (2003).

[112] S. C. Davenport, I. D. Rodríguez, J. K. Slingerland, and S. H. Simon, Composite fermion model for entanglement spectrum of fractional quantum Hall states, Phys. Rev. B **92**, 1 (2015).

[113] N. Read, Order Parameter and Ginzburg-Landau Theory for the Fractional Quantum Hall Effect, Phys. Rev. Lett. **62**, 86 (1989).

[114] S. C. Zhang, T. H. Hansson, and S. Kivelson, Effective-Field-Theory Model for the Fractional Quantum Hall Effect, Phys. Rev. Lett. **62**, 82 (1989).

[115] H. Goldman, R. Sohal, and E. Fradkin, Non-Abelian fermionization and the landscape of quantum Hall phases, Phys. Rev. B **102**, 195151 (2020).

[116] H. Goldman, R. Sohal, and E. Fradkin, Landau-Ginzburg theories of non-Abelian quantum Hall states from non-Abelian bosonization, Phys. Rev. B **100**, 115111 (2019).

[117] M. P. Zaletel and R. S. Mong, Exact matrix product states for quantum Hall wave functions, Phys. Rev. B **86**, 245305 (2012).

[118] B. Estienne, N. Regnault, and B. A. Bernevig, Fractional Quantum Hall Matrix Product States For Interacting Conformal Field Theories, arXiv preprint arXiv:1311.2936 (2013).

[119] B. Estienne, Z. Papić, N. Regnault, and B. A. Bernevig, Matrix product states for trial quantum Hall states, Phys. Rev. B **87**, 161112 (2013).

[120] Y. L. Wu, B. Estienne, N. Regnault, and B. A. Bernevig, Braiding Non-Abelian Quasiholes in Fractional Quantum Hall States, Phys. Rev. Lett. **113**, 116801 (2014).

[121] N. Read and E. Rezayi, Beyond paired quantum Hall states: Parafermions and incompressible states in the first excited Landau level, Phys. Rev. B **59**, 8084 (1999).

[122] P. Bonderson, V. Gurarie, and C. Nayak, Plasma analogy and non-Abelian statistics for Ising-type quantum Hall states, Phys. Rev. B **83**, 075303 (2011).

[123] B. A. Bernevig, P. Bonderson, and N. Regnault, Screening Behavior and Scaling Exponents from Quantum Hall Wavefunctions, arXiv preprint arXiv:1207.3305 (2012).

[124] E. V. Herland, E. Babaev, P. Bonderson, V. Gurarie, C. Nayak, and A. Sudbø, Screening properties and phase transitions in unconventional plasmas for Ising-type quantum Hall states, Phys. Rev. B **85**, 024520 (2012).

[125] A. Kitaev and J. Preskill, Topological Entanglement Entropy, Phys. Rev. Lett. **96**, 110404 (2006).

[126] J. von Delft and H. Schoeller, Bosonization for beginners - refermionization for experts, Ann. Phys. **510**, 225 (1998).

[127] S. Carpi, Y. Kawahigashi, R. Longo, and M. Weiner, *From Vertex Operator Algebras to Conformal Nets and Back*, Vol. 254, Memoirs of the American Mathematical Society (American Mathematical Society, 2018).

[128] E. Witten, Non-abelian bosonization in two dimensions, Commun. Math. Phys. **92**, 455 (1984).

[129] I. Affleck, Exact critical exponents for quantum spin chains, non-linear σ-models at θ=π and the quantum hall effect, Nuc. Phys. B **265**, 409 (1986).

[130] T. Nakanishi and A. Tsuchiya, Level-rank duality of WZW models in conformal field theory, Commun. Math. Phys. **144**, 351 (1992).

[131] S. G. Naculich and H. J. Schnitzer, Duality relations between SU (N)k and SU (k)N WZW models and their braid matrices, Phys. Lett. B **244**, 235 (1990).

[132] S. G. Naculich and H. J. Schnitzer, Duality between SU(N)k and SU(k)N WZW models, Nuc. Phys. B **347**, 687 (1990).

[133] A. N. Schellekens and S. Yankielowicz, Extended chiral algebras and modular invariant partition functions, Nuc. Phys. B **327**, 673 (1989).

[134] R. E. Behrend, P. A. Pearce, V. B. Petkova, and J.-B. Zuber, Boundary conditions in rational conformal field theories, Nuc. Phys. B **579**, 707 (2000).

[135] L. Li, C. T. Hsieh, Y. Yao, and M. Oshikawa, Boundary conditions and anomalies of conformal field theories in 1+1 dimensions, arXiv preprint arXiv:2205.11190 (2022).

[136] A. Anand, R. A. Patil, A. C. Balram, and G. J. Sreejith, Real-space entanglement spectra of parton states in fractional quantum Hall systems, Phys. Rev. B **106**, 085136 (2022).

[137] D. Gepner and Z. Qiu, Modular invariant partition functions for parafermionic field theories, Nuc. Phys. B **285**, 423 (1987).

[138] E. J. Bergholtz, T. H. Hansson, M. Hermanns, A. Karlhede, and S. Viefers, Quantum Hall hierarchy wave functions: From conformal correlators to Tao-Thouless states, Phys. Rev. B **77**, 165325 (2008).

[139] M. Greiter, X. G. Wen, and F. Wilczek, Paired Hall state at half filling, Phys. Rev. Lett. **66**, 3205 (1991).

[140] K. Park, V. Melik-Alaverdian, N. E. Bonesteel, and J. K. Jain, Possibility of p-wave pairing of composite fermions at 1 2, **58** (1998).

[141] B. I. Halperin, P. A. Lee, and N. Read, Theory of the half-filled Landau level, Phys. Rev. B **47**, 7312 (1993).

[142] V. Kalmeyer and S. C. Zhang, Metallic phase of the quantum Hall system at even-denominator filling fractions, Phys. Rev. B **46**, 9889 (1992).

[143] P. T. Zucker and D. E. Feldman, Stabilization of the Particle-Hole Pfaffian Order by Landau-Level Mixing and Impurities That Break Particle-Hole Symmetry, Phys. Rev. Lett. **117**, 096802 (2016).

[144] E. H. Rezayi and S. H. Simon, Breaking of particle-hole symmetry by landau level mixing in the ν=5/2 quantized hall state, Phys. Rev. Lett. **106**, 116801 (2011).

[145] S. H. Simon and E. H. Rezayi, Landau level mixing in the perturbative limit, Phys. Rev. B **87**, 155426 (2013).

[146] E. H. Rezayi, Landau Level Mixing and the Ground State of the $\nu = 5/2$ Quantum Hall Effect, Phys. Rev. Lett. **119**, 026801 (2017).

[147] B. Dutta, W. Yang, R. A. Melcer, H. K. Kundu, M. Heiblum, V. Umansky, Y. Oreg, A. Stern, and D. Mross, Novel method distinguishing between competing topological orders, arXiv preprint arXiv:2101.01419 (2021).

[148] D. F. Mross, Y. Oreg, A. Stern, G. Margalit, and M. Heiblum, Theory of Disorder-Induced Half-Integer Thermal Hall Conductance, Phys. Rev. Lett. **121**, 026801 (2018).

[149] B. Lian and J. Wang, Theory of the disordered $\nu = 5/2$ quantum thermal Hall state: Emergent symmetry and phase diagram, Phys. Rev. B **97**, 165124 (2018).

[150] S. H. Simon, Interpretation of Thermal Conductance of the nu=5/2 Edge, Phys. Rev. B **97**, 121406 (2018).

[151] K. K. W. Ma and D. E. Feldman, Partial equilibration of integer and fractional edge channels in the thermal quantum Hall effect, Phys. Rev. B **99**, 085309 (2019).

[152] S. H. Simon and B. Rosenow, Partial Equilibration of the Anti-Pfaffian edge due to Majorana Disorder, Phys. Rev. Lett. **124**, 126801 (2019).

[153] H. Asasi and M. Mulligan, Partial equilibration of anti-Pfaffian edge modes at $\nu = 5/2$, Phys. Rev. A **102**, 205104 (2020).

[154] A. C. Balram, S. Mukherjee, K. Park, M. Barkeshli, M. S. Rudner, and J. K. Jain, Fractional Quantum Hall Effect at $\nu = 2 + 6 / 13$: The Parton Paradigm for the Second Landau Level, Phys. Rev. Lett. **121**, 186601 (2018).

[155] K. Pakrouski, Approximate two-body generating Hamiltonian for the particle-hole Pfaffian wave function, Phys. Rev. B **104**, 245306 (2021).

[156] A. Sharma, S. Pu, and J. K. Jain, Bardeen-Cooper-Schrieffer pairing of composite fermions, Phys. Rev. B **104**, 205303 (2021).

[157] J. Bardeen, L. N. Cooper, and J. R. Schrieffer, Theory of Superconductivity, Phys. Rev. **108**, 1175 (1957).

[158] R. E. Wooten, "Haldane pseudopotentials and Landau level mixing in the quantum Hall effect", PhD thesis (2013).

[159] W. von der Linden, A quantum Monte Carlo approach to many-body physics, Phys. Rep. **220**, 53 (1992).

[160] S. Sorella, M. Casula, and D. Rocca, Weak binding between two aromatic rings: Feeling the van der Waals attraction by quantum Monte Carlo methods, J. Chem. Phys. **127** (2007).

[161] D. P. Kingma and J. L. Ba, "Adam: A method for stochastic optimization", in 3rd International Conference on Learning Representations, ICLR 2015 - Conference Track Proceedings (Dec. 2015).

[162] J. K. Salmon, M. A. Moraes, R. O. Dror, and D. E. Shaw, "Parallel random numbers: as easy as 1, 2, 3", in Proceedings of 2011 International Conference for High Performance Computing, Networking, Storage and Analysis on - SC '11 (2011), p. 1.

[163] G. Carleo and M. Troyer, Solving the quantum many-body problem with artificial neural networks, Science **355**, 602 (2017).

[164] R. Morf and B. I. Halperin, Monte Carlo evaluation of trial wavefunctions for the fractional quantized Hall effect: Spherical geometry, Z. Physik B **68**, 391 (1987).

[165] G. Möller and S. H. Simon, Composite fermions in a negative effective magnetic field: A Monte Carlo study, Phys. Rev. B **72**, 045344 (2005).

[166] F. Haldane, Incompressible quantum hall fluids as electric quadrupole fluids, arXiv preprint arXiv:2302.12472 (2023).

[167] J. I. A. Li, Q. Shi, Y. Zeng, K. Watanabe, T. Taniguchi, J. Hone, and C. R. Dean, Pairing states of composite fermions in double-layer graphene, Nat. Phys. **15**, 898 (2019).

[168] G. Wagner, D. X. Nguyen, S. H. Simon, and B. I. Halperin, *s*-Wave Paired Electron and Hole Composite Fermion Trial State for Quantum Hall Bilayers with $\nu = 1$, Phys. Rev. Lett. **127**, 246803 (2021).